Hypothalamic gene expression profiling in mouse strains susceptible or resistant to diet-induced obesity

Dissertation

zur
Erlangung des Doktorgrades
der Naturwissenschaften
(Dr. rer. nat.)

dem
Fachbereich Biologie
der Philipps-Universität Marburg
vorgelegt von

Lianxing Yang

aus Hebei, V. R. China

Marburg/Lahn, 2004

Vom Fachbereich Biologie

der Philipps-Universität Marburg als Dissertation am 31. 12. 2004 angenommen.

Erstgutachter HD Dr. Martin Klingenspor

Zweitgutachter Prof. Dr. Renate Renkawitz-Pohl

Tag der mündlichen Prüfung am 13. 01. 2005

Zusammenfassung 1
1 Summary 3
2 Introduction 5
2.1 Epidemiology of obesity 5
2.2 Effects of obesity 6
2.3 Etiology 7
2.3.1 External factors 7
2.3.2 Internal factors 8
2.4 Hypothalamus 9
2.5 Animal model for research 12
2.6 Aim of this study 13
3 Materials and Methods 14
3.1 Diet experiment 14
3.2 RNA manipulations 15
3.2.1 RNA isolation 15
3.2.2 RNA electrophoresis 15
3.2.3 RNA transfer 16
3.2.4 Northern hybridization 16
3.3 DNA manipulations 17
3.3.1 Genomic DNA isolation 17
3.3.2 Plasmid DNA preparation from *E. coli* cells 17
3.3.3 Precipitation of plasmid DNA 18
3.3.4 DNA electrophoresis 18
3.3.5 Digestion of DNA by restriction endonucleases 19
3.3.6 DNA isolation from agarose gel 19
3.3.7 PCR 19
3.3.8 PCR purification 21
3.3.9 DNA ligation 21
3.3.10 Transformation of *E. coli* 21
3.3.11 DNA sequencing 22
3.4 RZPD filter hybridization 22
3.4.1 Quality control of filter 22
3.4.2 Complex hybridization 23
3.4.2.1 Preparation of complex cDNA samples 24
3.4.2.2 Pre-hybridization 25
3.4.2.3 Complex hybridization 26
3.4.2.4 Post-hybridization 26
3.5 Affymetrix GeneChip hybridization 26
3.5.1 RNA isolation 27
3.5.2 cDNA synthesis 27
3.5.2.1 First-strand cDNA synthesis 27
3.5.2.2 Second-strand cDNA synthesis 27
3.5.2.3 Cleanup of double-strand cDNA 28
3.5.3 cRNA synthesis 28
3.5.4 Cleanup and quantification of biotin-labeled cRNA 28
3.5.5 Fragmenting the cRNA for target preparation 29
3.5.6 GeneChip hybridization 29

3.5.7 Post-hybridization 30
3.6 In Situ hybridization 31
3.6.1 Brain sectioning 31
3.6.2 Glass slide preparation – silanization 31
3.6.3 Preparation of the probe 31
3.6.3.1 Linearization of DNA template from section 3.3.3. 31
3.6.3.2 *In Vitro* transcription (IVT) 32
3.6.4 Pre-hybridization 33
3.6.5 Hybridization 33
3.6.6 Post-hybridization 34
3.6.7 Signal detection 34
3.7 Quantitative real-time RT-PCR 35
3.7.1 First-strand cDNA synthesis 35
3.7.2 Primer design 35
3.7.3 Real-time RT-PCR protocol and program 36
3.8 Data analysis 37
3.8.1 Data analysis I 37
3.8.2 Data analysis II 38
3.8.3 Data analysis III 39
3.9 Post analysis 39
3.10 Single nucleotide polymorphism (SNP) analysis 40
4 Results 41
4.1 Diet induced obesity in mice 41
4.1.1 Body mass 41
4.1.2 Energy intake 43
4.1.3 Body fat 44
4.1.4 Tissue mass 46
4.1.5 Litter size 48
4.2 Gene expression study 50
4.2.1 Data analysis I 50
4.2.1.1 Array hybridization 50
4.2.1.2 Visual inspection of the filter array image 53
4.2.1.3 Northern blot analysis 54
4.2.1.4 Sequencing 58
4.2.1.5 In Situ hybridization 59
4.2.2 Data analysis II 59
4.2.2.1 Array hybridization 59
4.2.2.2 Visual inspection of the filter array image 63
4.2.2.3 Northern blot analysis of Glo1 64
4.2.2.4 PCR 65
4.2.2.5 In Situ hybridization 66
4.2.2.6 Alignment of hemoglobin and neuroglobin gene sequences 67
4.2.3 Data analysis III 69
4.2.4 Real-time RT-PCR 72
4.3 SNP analysis of gene Glo1 75
5 Discussion 76
5.1 Diet experiment 76

5.1.1 Body mass and body fat 76
5.1.2 Energy intake 77
5.1.3 Energy expenditure 77
5.1.4 Litter size 78
5.2 Gene expression profiling 78
5.2.1 Normalization 78
5.2.2 Candidate selection criteria 79
5.2.3 RZPD high density cDNA Filters and Affymetrix GeneChips 80
5.2.4 Validation of candidate genes from array analysis 81
5.2.4.1 Transthyretin (TTR) 82
5.2.4.2 Hemoglobin alpha, adult chain 1 (Hba-α1) 83
5.2.4.3 Glyoxalase I 84
5.2.4.4 Tumor necrosis factor alpha-induced protein 1 (endothelial) (TNFAIP1) 85
6 Reference list 87
7 Abbreviations 100
8 Appendix 102
8.1 Appendix 1 102
8.2 Appendix 2 105
9 Erklärung 107
10 Acknowledgements 108
11 Curriculum Vitae 109

Zusammenfassung

Fettleibigkeit hat sich zu einem weltweiten Gesundheitsproblem in der Öffentlichkeit entwickelt. Sie wird durch ein komplexes Ungleichgewicht der Regulation von Appetit und Energiestoffwechsel verursacht, die durch verschiedene Faktoren wie genetische Defekte, Nahrungspräferenzen und Lebensstil kontrolliert werden. Die hochfetthaltige westliche Nahrung ist einer Hauptfaktor, die die Entwicklung von Fettleibigkeit in der menschlichen Bevölkerung fördert. Trotzdem werden nicht alle Konsumenten der Hochfettnahrung fettleibig.

In dieser Studie wurden zwei unterschiedliche Mausinzuchtlinien – AKR/J und SWR/J – entweder mit einer hoch fetthaltigen Nahrung oder der Standardnahrung gefüttert. Der AKR/J Stamm repräsentiert ein Mausmodel für diät-induzierte Fettleibigkeit (*diet-induced obesity* = DIO). Mäuse dieses Stammes wurden fett wenn sie mit der hochfetthaltigen Diät gefüttert wurden, wohingegen sie schlank bei Fütterung mit der Standard-Diät blieben. Im Gegensatz dazu waren die Mäuse des SWR/J Stamm resistent gegenüber der DIO, d.h. es war im Vergleich kein wahrnehmbar Anstieg des Körpergewichts oder von Fettleibigkeit in Mäusen, die mit fetthaltiger Nahrung oder Standard-Diät gefüttert wurden. Genexpressions-Arrays wurden benutzt um differentiell exprimierte Gene im Hypothalamus von AKR/J und SWR/J Mäusen bei fetthaltiger Fütterung zu identifizieren. Um die Kandidatengene, ausgesucht aus der Array Datenanalyse to validieren, wurde Northern Blot Analyse, *in situ* Hybridisierung und real-time RT-PCR durchgeführt.

Hämoglobin alpha, adult chain 1 (Hba-α1) ist auf dem Chromosom 11 der Maus (Chromosom 16p13.3 des Menschen) lokalisiert. Die funktionelle Bedeutung der Expression von Hba-α1 ist unbekannt. Eventuell erleichtert es den Sauerstofftransport im Gehirn in einer ähnlichen Weise wie das Myoglobin im Skelettmuskel. In dieser Arbeit wurde eine höhere ubiquitäre Expression von Hba-α1 im Hirn der SWR/J Maus im Vergleich zur AKR/J Maus beobachtet. Dieser Unterschied könnte mit der höheren Stoffwechselrate der SWR/J Mäuse zusammenhängen. So weit konnte keine direkte Beziehung zwischen Hba-α1 Expression und Fettleibigkeit hergestellt werden.

Im Gegensatz dazu zeigt die Glyoxalase I (Glo 1) ein spezifisches Expressionsmuster mit stärkster Präsenz im Hippocampus. Im Hypothalamus kann die Glo1 Expression im arquatischen Nukleus (ARC), im ventromedialen hypothalamischen Nukleus (VMH) und im paraventricularen hypothalamischen Nukleus (PVN) detektiert werden. Während die

Expression von Glo1 ausserhalb des Hypothalamus ähnlich in beiden Mausstämmen ist, ist die mRNA Expression in der hypothalamischen Region viel stärker in AKR/J im Vergleich zur SWR/J Mäusen. Das Glo1 Gen befindet sich auf Chromosom 17 der Maus (Chr. 6 des Menschen) und an der Entgiftung von Stoffwechselnebenprodukten beteiligt. Außerdem wurde Glo1 auf der Fettleibigkeits-Genkarte vom Menschen verzeichnet und vermutet eine Verbindung zwischen einer abweichenden Expression des Glyoxalase-Systems und Krankheiten wie Krebs und Diabetes.

Tumor Nekrose Faktor alpha-induziertes Protein 1 (endothelial) (tumor necrosis factor alpha induced protein 1 (TNFAIP1) ist auf Maus-Chromosom 11(45,10 cM) und Mensch-Chromosom 17q22-q23 lokalisiert. Das Protein ist beim Kalium-Eisen-Transport durch Proteinbindung und bei der Einstellung der spannungsabhängigen Kaliumkanal Aktivitäten involviert. TNFAIP1 lokalisiert sich im ARC, im VMH und PVN. Es wurde durch Hochfett-Diäten in den AKR/J aber nicht SWR/J Mäusen hochreguliert, was an den Filterarrays und den Northern Blots, aber nicht mit der real-time RT-PCR und *in situ* Hybridisierungen gezeigt werden konnte. Obwohl bei der *in situ* Hybridisierung eine 1,6fache Steigerung der mRNA Expression im ARC und VMH durch die Hochfettdiät beobachtet werden konnte, war diese Steigerung aufgrund individueller Variationen nicht signifikant. Weitere Experimente mit höherer Stichprobenzahl müssten durchgeführt werden um dieses Ergebnis zu bestätigen. Weil es sich um ein neu annotiertes Gen handelt, ist nicht viel über die pathologische Relevanz bekannt. Bisher hat keine Studie eine Verbindung zwischen TNFAIP1 und Fettleibigkeit beschrieben. Es wird angenommen, dass TNFα einen Einfluss auf Körpergewichtsregulation hat und wahrscheinlich durch einen lokalen Prozess im Fettgewebe wirkt. Möglicherweise führt eine erhöhte Sekretion von TNFα aus Adipozyten in fettleibigen Versuchstieren/-personen zu einer Induktion von TNFAIP1 im Hypothalamus. Weitere Studien sollten durchgeführt werden um die Funktion von TNFAIP1 im Gehirn aufzuklären.

1 Summary

Obesity has developed to a worldwide public health problem. It is caused by a complex disorder of appetite regulation and energy metabolism which are controlled by multiple factors such as genetic predisposition, dietary preferences and life style. The high-fat western-type diet is one of the major factors promoting the development of obesity in the human population. However, not all of the high-fat diet consumers become obese.

In this study, two different inbred mouse strains – AKR/J and SWR/J were either fed a high-fat diet or standard chow diet. The AKR/J strain represents a mouse model for diet-induced obesity (DIO). Mice of this strain developed obesity when fed a high fat diet, whereas they remained lean on a standard chow. In contrast, mice of the SWR/J strain are resistant to DIO, i.e., there was no discernable increase in body weight or adiposity in mice fed a high fat diet as compared to standard chow. The gene expression arrays were applied to identify differentially expressed genes in the hypothalamus of AKR/J and SWR/J mice in response to high-fat diet feeding. For the candidate genes selected from array data analysis, validation was carried out by northern blot analysis, in situ hybridization and real-time PCR.

Hemoglobin alpha, adult chain 1 (Hba-α1) is located on mouse chromosome 11 (human chromosome 16p13.3). The functional significance of Hba-α1 expression is unclear. Perhaps it facilitates oxygen transport in the brain in a similar manner as myoglobin in muscle. In this study, overall the expression of Hba-α1 in brain was higher in SWR/J compared to AKR/J mice. This difference between strains may be related to the fact that SWR/J mice have a higher metabolic rate. So far, no direct relationship between Hba-α1 expression and obesity has been suggested.

In contrast, Glyoxalase I (Glo 1) shows a very distinct expression pattern with highest levels found in the hippocampus. In the hypothalamus, Glo1 expression can be found in the arcuate nucleus (ARC), ventromedial hypothalamic nucleus (VMH) and paraventricular hypothalamic nucleus (PVN). Whereas the expression of Glo1 outside the hypothalamus is similar in both strains, Glo1 mRNA expression within the hypothalamic region is much stronger in AKR/J compared to SWR/J mice. Glo 1 is located on mouse chromosome 17 (human chromosome 6) and involved in the detoxification of metabolic by-products. It was assigned to the human

obesity gene map and has been suggested that aberrant expression of the glyoxalase system is related to cancer and diabetes.

Tumor necrosis factor alpha-induced protein 1 (endothelial) (TNFAIP1) is on mouse chromosome 11 (45.10 cM) and human 17q22-q23. The protein functions in potassium ion transport by protein binding and voltage-gated potassium channel activity adjustment. TNFAIP1 localizes in the ARC, the VMH and PVN. It was upregulated by high fat diet in AKR/J mice but not in SWR/J mice, which was shown in filter array and Northern blot but not in real-time RT-PCR and in situ hybridization. In the in situ hybridization, although it showed 1.6 fold upregulation in the ARC and VMH by high fat diet, this difference was not significant because of the individual variation, further experiment with more samples should be carried out to confirm this conclusion. Because it is a newly assigned gene not much information on its pathological relevance is available. So far, there have been no papers linking TNFAIP1 and obesity. However, many publications report on a role of TNFα in obesity. It is believed that TNFα has an effect on body weight regulation and that it acts probably through a local action on adipose tissue. Possibly, elevated secretion of TNFα from adipocytes in obese subjects leads to induction of TNFAIP1 in the hypothalamus. Further research needs to be conducted to elucidate the function of TNFAIP1 in the brain.

2 Introduction

The word obesity is derived from the Latin – *ob*, means "on account of", and *esito*, means "to keep eating". Obesity is defined by the WHO as a body mass index (BMI) > 30 kg/m^2 (1995;Garrow & Webster, 1985), where BMI is calculated by dividing a person's body weight in kilograms by his or her height in meters squared (weight [kg] / height [m^2]).

2.1 Epidemiology of obesity

The prevalence of obesity has increased markedly over the past few decades (1960s). The WHO has described obesity as the major unmet public health problem worldwide (2000). From 1995 to 2000, the number of obese adults has increased from about 200 million to over 300 million in the world (www.who.int). During the past 20 years there has been a dramatic increase in obesity in the United States (Figure 1.1). In 1991, four states reported adult obesity prevalence rates of 15–19 percent and no states reported rates at or above 20 percent. In 2002, 15 states had obesity prevalence rates of 15–19 percent; 31 states had rates of 20–24 percent; and 4 state reported a rate over 25 percent (Behavioral Risk Factor Surveillance System (BRFSS), CDC www.cdc.gov).

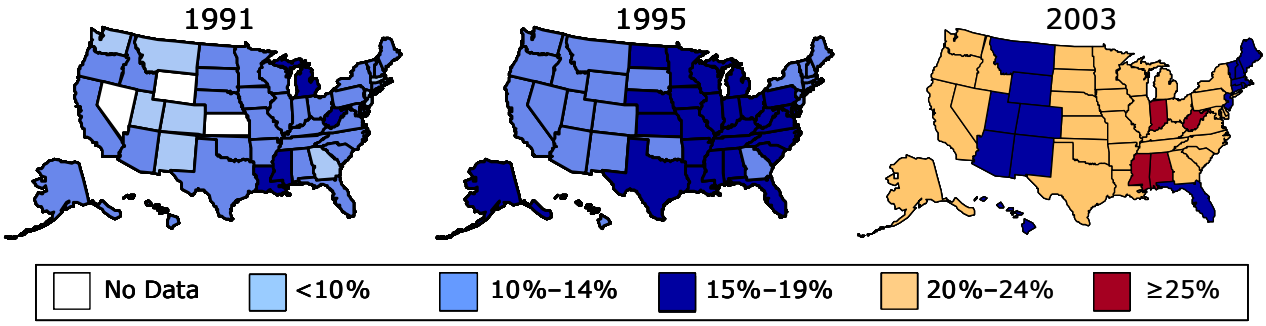

Figure 1.1 Obesity trends (BMI ≥ 30) among U.S. adults in 1991 1995 and 2002.

The data derived from the third National Health and Nutrition Examination Surveys (NHANES III) showed that 56% of adults were overweight (BMI ≥ 25) and nearly a quarter (23%) were obese (Flegal *et al.*, 1998). The data from the 1999-2000 NHANES show almost 65% of the adult population in the United States is overweight and 31% is obese (www.cdc.gov) (Flegal *et al.*, 2002). For the clinically severe obesity (BMI ≥ 45), Sturm reported that from 1986 to 2000

the prevalence of a BMI ≥ 40 in adult Americans quadrupled from 1 in 200 to 1 in 20 and that of a BMI ≥ 50 from 1 in 2000 to 1 in 400 (Sturm, 2003).

In Europe, more than half the adult population between 35 and 65 years of age were either overweight or obese (Kopelman, 2000). The data from International Obesity Task Force (IOTF, http://www.iotf.org) suggest that the range of obesity prevalence in European countries is from 10 to 20% for men, and 10 to 25% for women. In Germany, 50% of the adult population are overweight and 20% are obese (Heseker & Schmid, 2000). Among German school children (7-14 years old), the prevalence of overweight increased between 1975 and 1995 from 10.0 to 16.3% in boys and from 11.7 to 20.7% in girls (Kromeyer-Hauschild *et al.*, 1999). For the pre-school children (5-6 years of age), in 1982, 8.5% of all children were overweight and 1.8% were obese; in contrast in 1997 12.3% were overweight and 2.8% were obese (Kalies *et al.*, 2002).

Although it is widely acknowledged that obesity has emerged as an epidemic in the recent two to three decades in developed countries, it is not just a disease there. Popkin *et al.* collected the data from different countries and reported that adult obesity levels in developing countries are as high as or even higher than those reported for the United States and other developed countries, and are increasing rapidly (Popkin & Doak, 1998). In China, the prevalence of overweight individuals doubled in women (10.4 to 20.8%) and almost tripled in men (5.0 to 14.1%) from 1989 to 1997 (Bell *et al.*, 2001). In developing countries this problem does not emerge only in adults but also in children and adolescents (Popkin *et al.*, 1996;Wang *et al.*, 2002).

2.2 Effects of obesity

Obesity is not just a matter of being obese but it has also dramatic effect on health. Obesity is an important risk factor for a range of chronic disease conditions, for instance, cardiovascular disease (Pi-Sunyer, 1993;Wilson & Kannel, 2002), type II diabetes (non insulin dependent diabetes mellitus, NIDDM) (Chan *et al.*, 1994;Colditz *et al.*, 1995), and hypertension (Cassano *et al.*, 1990;Huang *et al.*, 1998;Stamler *et al.*, 1978). Overweight and obesity were significantly associated with some kinds of cancer, gallbladder disease and musculoskeletal disorders (Pi-Sunyer, 1993), high cholesterol, asthma, arthritis, and poor health status (Mokdad *et al.*, 2003).

About 300,000 U.S. deaths a year are associated with obesity and overweight, compared to more than 400,000 deaths a year associated with smoking (McGinnis & Foege, 1993) (www.surgeongeneral.gov). In the EU, Banegas *et al.* reported that a minimum of 279,000 deaths were attributable to excess weight (Banegas *et al.*, 2003).

The economic effect of obesity in the United States is estimated at approximately 6% of the national health expenditure and costs of care. The number of physician visits related to obesity has increased 88% in a 6-year period (from 1988 to 1994) (Wolf, 1998). In the United States, the total direct and indirect costs attributed to overweight and obesity amounted to $117 billion (€91 billion) in the year 2000 (2001) (www.surgeongeneral.gov). The total costs to European society are between €70 and €135 billion a year (Rayner & Rayner, 2003). In Germany obesity and the obesity-related morbidity and mortality caused costs of nearly 20.7 billion DM (€10.6 billion) in 1995 (Heseker & Schmid, 2000). The direct cost of obesity to the NHS (National Health Service, UK) is £0.5 billion (€0.7 billion), while the indirect cost to the UK economy is at least £2 billion (€2.8 billion) (Vlad, 2003).

2.3 Etiology

Obesity is not a single disorder but a heterogeneous group of conditions with multiple causes. Obesity involves complex etiological interactions between the genetic, metabolic and neural frameworks on one hand and behavior, food habits, physical activity and socio-cultural factors on the other.

2.3.1 External factors

Energy balance and body composition depend upon energy intake and expenditure (Martinez & Fruhbeck, 1996;Friedman, 2000), which appears to be under control on an axis with three components: food intake; fuel utilization and thermogenesis; and adipocyte metabolism.The main reason for the current obesity epidemic is a changing environment that promotes excessive food (calorie) intake and discourages physical activity (Hill & Peters, 1998;Hill *et al.*, 2000;French *et al.*, 2001;Jeffery & Utter, 2003;Stettler, 2002;Jequier, 2002;Poston & Foreyt, 1999). A study based on the area of Washington showed that the main courses of children's

meals in US chain restaurants typically contain 700–900 calories, more than half the total recommended daily amount (Butler, 2004). The U.S. food supply provides 3800 kilocalories per person per day, nearly twice as much as required by many adults (Nestle, 2003). In addition, the physical activity decreased from year to year. The proportion of the U.S. population that reported no leisure-time physical activity was 31% in 1989, 29% in 1992, and 25% in 2002 (U.S. Physical Activity Statistics, www.cdc.gov/). Another survey shows that more than 50% of American adults do not get enough physical activity to provide health benefits; 26% are not active at all in their leisure time (www.cdc.gov).

2.3.2 Internal factors

Environmental factors and lifestyle are important determinants influencing obesity, however, human obesity has also important genetic correlates that interact with relevant environmental factors (Comuzzie *et al.*, 1994;Comuzzie *et al.*, 1996;Comuzzie *et al.*, 2001;Barsh *et al.*, 2000;Clement *et al.*, 2002). Lifestyle factors, especially those related to physical activity levels, may interact with the genetic factors and may mask genotype influences (Bray, 2000;Martinez, 2000). Twin studies, analyses of familial aggregation and adoption studies indicate that obesity is largely the result of genetic factors and that an individual's risk for obesity is increased when he or she has relatives who are obese (Stunkard *et al.*, 1986a;Stunkard *et al.*, 1986b;Stunkard *et al.*, 1990;Sorensen *et al.*, 1992;Vogler *et al.*, 1995). Maes *et al.* concluded in their review article that genetic factors explain 50 to 90% of the variance in BMI from twin studies. Family studies generally report estimates of parent-offspring and sibling correlations in agreement with heritabilities of 20 to 80%. Data from adoption studies are consistent with genetic factors accounting for 20 to 60% (Maes *et al.*, 1997). The importance of genes in the development of obesity can be estimated by calculating the family risk. Data obtained from NHANES III showed the prevalence of obesity is twice as high in families of obese individuals than in the normal population (Lee *et al.*, 1997). Data from Canada Fitness Survey showed that the familial risk of obesity was five times higher for relatives in the upper 1% distribution of BMI than in the general Canadian population (Katzmarzyk *et al.*, 1999).

The discovery of the 'ob' gene, which was mapped to human chromosome 7, has led to a renewed interest in understanding the patho-biological basis of genetic predisposition in obesity. The 'ob' gene encodes a hormone called leptin, a 167 amino acid protein that is produced in white and brown adipose tissue and placenta (Zhang *et al.*, 1994). A case of human obesity caused by mutation of the leptin gene was first found in two severely obese cousin children in an inbred Pakistani kindred (Montague *et al.*, 1997). Subsequently, the success in the treatment of congenital leptin deficiency with recombinant leptin was reported (Farooqi *et al.*, 1999;Farooqi *et al.*, 2002). Other single gene mutations causing human obesity were found in the leptin receptor (LEPR) (Clement *et al.*, 1998), in the melanocortin precursor, pro-opiomelanocortin (POMC) (Krude *et al.*, 1998;Challis *et al.*, 2002), and in the melanocortin-4 receptor (MC4R) (Yeo *et al.*, 1998;Hinney *et al.*, 1999;Dubern *et al.*, 2001;Farooqi *et al.*, 2003). Although obesity has a genetic component, normally, it is not a simple genetic disorder and cases of obesity caused by single gene mutation are extremely rare.

2.4 Hypothalamus

Leptin is secreted by adipocytes and its key role is that of communicating to the brain information on long term energy stores. The primary site for the leptin signal is in the hypothalamus (Figure 1.2), where it influences food intake/appetite and its absence triggers a series of neuroendocrine responses that conserve energy when food availability is limited.

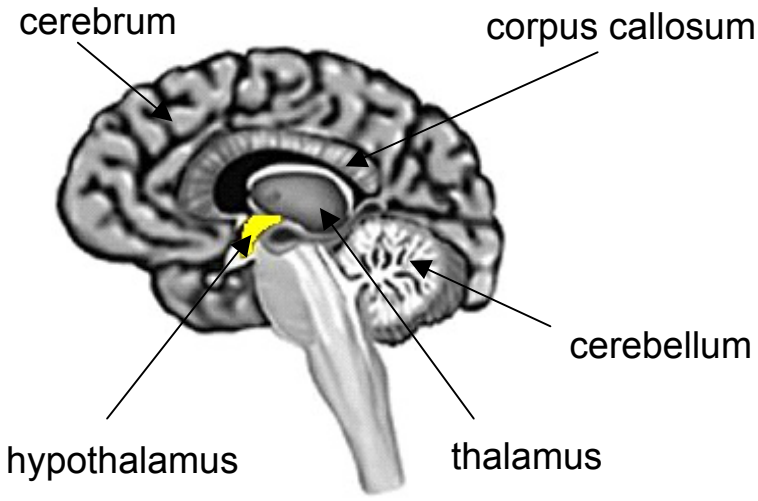

Figure 1.2 Anatomy of human brain showing the hypothalamus and other components.

Energy balance is regulated by an interplay of hormonal and neural mechanisms in response to afferent information from peripheral adiposity signals such as leptin and insulin. It has long been recognized that the hypothalamus plays a key role in the mechanisms regulating food intake and fat accumulation (Anand & Brobeck, 1951a;Anand & Brobeck, 1951b;Kennedy, 1950;Panksepp, 1974). The major hypothalamic regions implicated in adiposity signalling and regulation of food intake are shown in Figure 1.3. For instance, bilateral lesions of the ventromedial (VMH) or paraventricular nucleus (PVN) of the hypothalamus cause hyperphagia, decreased energy expenditure and pronounced weight gain (Leibowitz *et al.*, 1981;Aravich & Sclafani, 1983). Conversely, lesions of the lateral hypothalamic area (LHA) induce hypophagia, increased energy expenditure and weight loss (Bernardis & Bellinger, 1993;Milam *et al.*, 1980;Milam *et al.*, 1982). Electrical stimulation of this area causes hyperphagia and obesity (Bray *et al.*, 1990;Hernandez & Hoebel, 1989;Shiraishi, 1991).

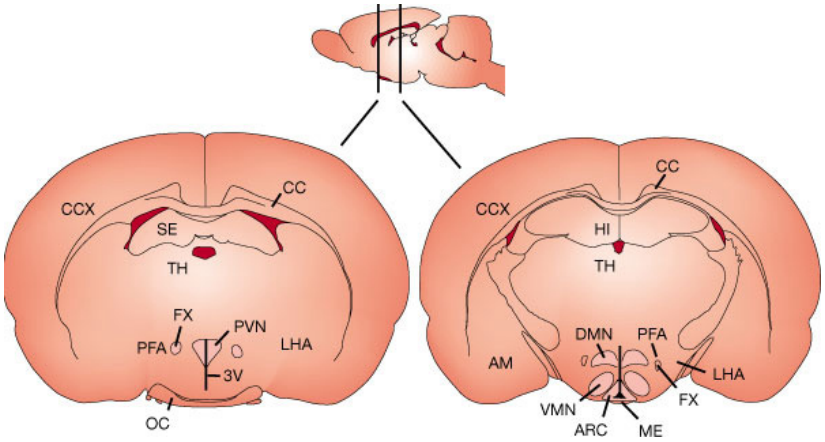

Figure 1.3 Schematic representation of hypothalamic regions implicated in adiposity signalling and regulation of food intake. Abbreviations of brain structures: AM, amygdala; CC, corpus callosum; CCX, cerebral cortex; HI, hippocampus; ME, median eminence; OC, optic chiasm; SE, septum; TH, thalamus; 3V, third ventricle.

Recent studies focused on the role of the hypothalamus reveal that several pathways in the central nervous system (CNS) forming a complex web of neuropeptide interactions are important for body weight regulation. The expression of orexigenic and anorexigenic genes shows contrary direction of regulation in response to fasting. Starvation induces an increase in the gene expression of orexigenic neuropeptides such as neuropeptide Y (NPY) (Davies & Marks, 1994;Schwartz *et al.*, 1992), agouti-related peptide (AgRP) (Hahn *et al.*, 1998),

melanin-concentrating hormone (MCH) (Qu *et al.*, 1996) and orexin (ORX) (Sakurai *et al.*, 1998). The gene expression of anorexigenic neuropeptides such as corticotropin-releasing hormone (CRH) (Brady *et al.*, 1990;Fekete *et al.*, 2000) and POMC (Bergendahl *et al.*, 1992;Brady *et al.*, 1990) are depressed by starvation. These are also supported by other related studies (Adam *et al.*, 2002;Bertile *et al.*, 2003;Savontaus *et al.*, 2002). Cocaine- and amphetamine-regulated transcript (CART) is normally categorized as an anorexigenic gene, which is downregulated by fasting (Robson *et al.*, 2002). However, the effects of CART injection into different region of the hypothalamus are variable: intracerebroventricular (i.c.v.) injection reduced food intake (Asakawa *et al.*, 2001;Volkoff & Peter, 2000) while injection into the area of arcuate nucleus neurons (ARC) increased food intake (Abbott *et al.*, 2001;Kong *et al.*, 2003). Furthermore, injections of NPY, AgRP, MCH, and ORX directly into the brain increased food intake (Qu *et al.*, 1996;Sakurai *et al.*, 1998;Morley *et al.*, 1987;Rossi *et al.*, 1998), whereas CRH, and POMC derivatives such as α-MSH, have the opposite effect (Britton *et al.*, 1982;Tsujii & Bray, 1989). Concerning the localization, NPY and AgRP are co-localized in ARC (Broberger *et al.*, 1998;Hahn *et al.*, 1998;Adam *et al.*, 2002), POMC and CART are co-localized in a distinct, but adjacent, subset of arcuate nucleus neurons (Elias *et al.*, 1998;Adam *et al.*, 2002). The arcuate nucleus transduces the information provided by the leptin signal into a neuronal response. This hypothesis is supported by the anorexic response to local microinjection of leptin into this area (Satoh *et al.*, 1997), and the inability of i.c.v. leptin to reduce food intake after the arcuate nucleus has been destroyed (Tang-Christensen *et al.*, 1999;Dawson *et al.*, 1997). A majority of both NPY/AgRP and POMC/CART neurons have been found to co-express leptin receptors (Baskin *et al.*, 1999;Cheung *et al.*, 1997) and both types of neurons are regulated by leptin, but in an opposing manner. Schwartz *et al.* also reported that leptin can suppress NPY and upregulate POMC (Schwartz *et al.*, 1996;Schwartz *et al.*, 1997).

From ARC, the signals are mainly sent to the PVN (Gale *et al.*, 2004) and other areas such as zona incerta, perifornical area (PF-A) and LHA, all of which are richly supplied by axons from arcuate nucleus NPY/AgRP and POMC/CART neurons (Elmquist *et al.*, 1998;Elmquist *et al.*, 1999). In the PVN, several neuropeptides such as CRH (Bray *et al.*, 1990;Fekete *et al.*, 2000), thyrotropin-releasing hormone (TRH) (Kow & Pfaff, 1991), and oxytocin (McMahon & Wellman, 1997;Blevins *et al.*, 2003) were found to reduce food intake. Whereas in the LHA

and adjacent areas such as PF-A, MCH (Qu *et al.*, 1996;Saito *et al.*, 1999) and orexins A and B were found as orexgenic peptides (Hagan *et al.*, 1999;Sakurai *et al.*, 1998).

2.5 Animal model for research

The first recorded use of mice as research animals occurred in 1664, when the English physicist Robert Hooke studied the reactions of mice in experiments on air. The remarkable genetic similarity of mice to humans, combined with great conveniences of small size and inexpensive maintenance, accounts for mice so often being the experimental model of choice in research. Over the past two decades, the mouse has emerged as the preeminent model organism because of many physiological, anatomical and metabolic parallels with humans (Bradley, 2002). The mouse and human genomes each contains about 30,000 protein-coding genes. The proportion of mouse genes with a single identifiable orthologue in the human genome seems to be approximately 80%, while less than 1% of mouse genes has not any homologue detectable in the human genome (and vice versa) (Mouse Genome Sequencing Consortium, 2002).

Since the obese (ob) mouse and the diabetes (db) mouse were discovered at The Jackson Laboratory in 1950 and 1966 respectively (www.jax.org), obesity research has been developed accelerative. And then, the obesity research was forever changed when leptin was cloned and identified as the responsible mutation for the obese phenotype of the ob/ob mice in 1994 (Zhang *et al.*, 1994). Later on, after the leptin receptor was cloned (Tartaglia *et al.*, 1995), Friedman's group found that the mutation in the leptin receptor gene was responsible for the obese phenotype of the db/db mice (Lee *et al.*, 1996). Inbred strains have long been used for genetic studies because of the isogenicity within a strain and the genetic heterogeneity between inbred strains. Although the knock -out, -in and –down mice are applied to investigate the function of specific genes, the inbred strain mice are still mainly animal models for obesity research because obesity is a polygenic disease. The quantitative trait loci (QTL) studies have identified many loci (QTL) that control measurable polygenic traits related to obesity (www.obesitygene.pbrc.edu).

In humans, not everyone becomes obese, even for the high fat consumers, not all of them tend to obesity (Macdiarmid *et al.*, 1996). Bachmanov *et al*. investigated male mice from 28 inbred strains and found that the strain differences were significant for all of their analyses: body

weight, food and water intake, and spout preference (Bachmanov *et al.*, 2002). In this atudy it was also shown that AKR/J mice were heavier and ate more (diet g/mouse) than SWR/J mice. However, if the food intake was adjusted by body weight, SWR/J mice ate more (diet g/body weight g) (Bachmanov *et al.*, 2002). In other studies with respect to the preference of macronutrient diet selection, the lean strain of SWR/J consumed more calories from carbohydrate diet whereas AKR/J consumed more calories in form of fat (Smith *et al.*, 1997;Smith *et al.*, 1999;Smith *et al.*, 2000;Smith *et al.*, 2001). The sensitivity of dietary obesity was reported by West *et al.*, when exposed to high fat diet, AKR/J mice consumed more energy and had more fat content (West *et al.*, 1992;West *et al.*, 1995). For these two inbred mouse strains – AKR/J (diet-induce obesity model, DIO) and SWR/J (diet-resistant model, DR), although many dietary studies were reported, only Prpic *et al.* investigated strain specific differences in the gene expression of uncoupling protein (UCP) 1 and 2 in adipocytes during diet-induced obesity (Prpic *et al.*, 2002). They reported that HF diet induced a modest increase in brown adipose tissue (BAT) UCP1 mRNA in SWR/J mice, whereas a large decrease in UCP1 expression in AKR/J mice, and that UCP2 was consistently higher in white adipose tissue (WAT) from AKR/J than in SWR/J mice and induced by the HF diet in AKR/J but not SWR/J mice (Prpic *et al.*, 2002).

2.6 Aim of this study

As described above, many genes related to obesity are expressed predominantly in the hypothalamus. Even so, the genetic etiology of obesity is still unclear and the effective pharmaceutical treatment is still in the development stage. In order to investigate the differences of body weight, body fat content and food (energy) intake as a function of different diets and strains, AKR/J and SWR/J mice were to be fed either a high fat diet or a standard control diet. Furthermore, the influence of the different diets and strains on the hypothalamic gene expression was investigated using array technology – RZPD high density cDNA filter and Affymetrix GeneChip, to identify differentially expressed genes involved in the regulation of body weight and “energy turnover”. For the candidate genes selected from array data analysis, validation was to be carried out by northern blot analysis and in situ hybridization.

3 Materials and Methods

3.1 Diet experiment

The two inbred mouse strains – AKR/J and SWR/J were purchased from The Jackson Laboratory (Bar Harbor, ME, USA) and bred in our animal house. The mice were maintained on a 12:12-h light-dark photoperiod with lights on at 6:00 a.m. CET at an ambient temperature of 25°C and fed control diet (Standard 1413, Altromin).

Totally, 20 litters AKR/J mice yielding 104 individuals and 29 litters SWR/J mice yielding 207 individuals were included in the experiment. Offspring were weaned at 21 days and separated into single cage and fed the control diet for 2 weeks. At the age of 35 days, they were assigned to two diet groups matched for body mass – one group of mice remained on control diet, while the other group was switched to a high fat diet (Sonder C1057, Altromin). The compositions of the two different diets used in the diet experiment are shown in Table 3.1. Body mass (± 0.1 g) and food intake (± 0.1 g) of each mouse was determined every 3 days from day 21 to day 35 and then every 2 days until day 45.

Table 3.1 Metabolic characteristics of control and high fat diet as determined by the supplier (Altromin).

Contents	Control diet	High fat diet
Fat (Energy %)	13.4	40.2
Protein (Energy %)	28.9	23.9
Carbohydrate (Energy %)	57.7	35.9
Water content (weight %)	6.5	6.0
Gross energy (KJ/g dry)	18.3	20.7
Assimilated energy (KJ/g dry)	14.2 ± 0.2	18.2 ± 0.1
Assimilation efficiency (%)	77.6	87.9

On day 45 mice were killed in deep CO_2 anesthesia for the dissection of hypothalamus or intact brain and several other selected organs (liver, kidney, inter scapular brown adipose tissue, inguinal and retroperitoneal white adipose tissue, and skeletal muscle). After weighing (± 0.001 g), all tissues were snap frozen and archived at -80°C. In a subset of individuals, only

the hypothalamus was removed and then body composition (fat + lean mass) was measured using Dual-Energy X-ray Absorptiometry (DEXA PIXImus, GE Medical Systems, Wisconsin, USA). In the group of mice used for in situ hybridization, the intact brain was removed from the skull, placed on aluminum foil on dry ice for at least 30 min to allow freezing through and subsequently stored at –80°C.

3.2 RNA manipulations

3.2.1 RNA isolation

Hypothalamic RNA was isolated with TRIZOL® Reagent (Invitrogen), which is a mono-phasic solution of phenol and guanidine isothiocyanate, and an improvement to the single-step RNA isolation method developed by Chomczynski and Sacchi (Chomczynski & Sacchi, 1987).
The hypothalami were transferred from the freezer (-80°C) to the lab bench in liquid nitrogen. Each sample was homogenized in a 4 ml tube containing 1 ml of TRIZOL, using a Ultra-turrax homogenizator (Janke und Kunkel GmbH) for 30 sec. Following a short centrifugation at 1000 rmp for 1-2 min, the homogenized sample was transferred into a 1.5 ml tube and total RNA was isolated according to the manufacturer's protocol.
To purify the isolated RNA, the RNeasy Mini Kit (QIAGEN) was used according to the manufacturer's protocol.

3.2.2 RNA electrophoresis

The hypothalamic RNA was denatured with formamide and separated in denaturing formaldehyde agarose gel. 100 ml of a 1% agarose gel was prepared by dissolving 1 g RNase-free agarose in 85 ml of ddH_2O. 10 ml of 10 x MOPS and 5 ml of formaldehyde (3.5 %, Merck) were added after cooling the melted agarose below 60°C.
Each RNA sample was pretreated by mixing 10 µl of denature buffer and 2 µl of ethidium bromide (0.5 mg/ml), followed by denaturation at 68°C for 15 min and quick cooling on ice for 5 min. Then 6 x color buffer was added to the samples and they were loaded to the wells of the gel. Electrophoresis was conducted at 5-8V/cm in 1 x MOPS for 1-2 h. The ethidium

bromide-stained RNA in the gel was visualized by 302 nm UV light and pictures were taken with Gel Imager (Intas).

Denature buffer (1.25 ml):	6 x color buffer (1ml):
750 µl formamide	300 µl ddH_2O
150 µl 10x MOPS	500 µl glycerol (86%)
250 µl formaldehyde	100 µl 2.5 % bromophenol blue
100 µl ddH_2O	100 µl 2.5 % xylene cyanol
	2 µl EDTA (0.5 M; pH 8.0)

10 x MOPS:
200 mM MOPS
50 mM NaOAc
10 mM EDTA-Na_2

3.2.3 RNA transfer

The RNA in the electrophoresis gel was transferred to a neutral nylon membrane (Hybond N, Amersham) by Northern blotting (Sambrook & Russell, 2001). After 16-20 h of transfer, the membrane was placed on an UV transilluminator (UV-Stratalinker, Stratagene) and briefly irradiated at 254 nm to link the RNA to the membrane.

3.2.4 Northern hybridization

Northern hybridization (DNA-RNA hybridization) was accomplished as described by Sambrook and Russell (Sambrook & Russell, 2001).

The probes were synthesized from cDNA fragments (see chapters 3.3.2 to 3.3.5) digested by restriction nucleases and labeled with α-^{32}P-dCTP (ICN or Amersham) using the Rediprime II Randome Prime Labelling System (Amersham). Subsequently, probes were purified with the beta-Shield Device System (Stratagene). After overnight hybridization at 64°C and stringent wash, membranes were exposed to Kodak X-QMAT film (Scientific Image Film, Kodak) or Phosphor Imager screen (Molecular Dynamics). The screen was scanned with PhosphoImaging

(Storm, Molecular Dynamics) and the signal intensities were densitometrically quantified using the software package ArrayVision (Imaging Research Inc.).

3.3 DNA manipulations

3.3.1 Genomic DNA isolation

Mouse genomic DNA was isolated from tail biopsy. About 0.5 cm of the tail tip was clipped, put into a polypropylene microfuge tube, and then digested overnight in 0.5 ml DNA digestion buffer at 50-55 °C.

DNA digestion buffer:

50 mM Tris-HCl pH 8.0
100 mM EDTA pH 8.0
100 mM NaCl
1% SDS
0.5 mg/ml proteinase K (fresh)

Neutralization was carried out in 0.7 ml of phenol/chloroform/isoamyl alcohol (25:24:1) at RT for 30 min at gentle agitation. Samples were then centrifuged at 15000 rpm for 10 min at RT and the upper phase (0.5 ml) was transferred to a new microfuge tube. DNA was precipitated in 1 ml of 100% ethanol and centrifuged at 15000 rpm for 10 min at 4°C. After brief washing in 1 ml of cold 70% ethanol, DNA was pelleted at 15000 rpm for 5 min at 4°C. The supernatant was discarded and the DNA pellet was air-dried. The DNA was redissolved in 50 µl of TE buffer at 60°C for 15 min and then stored at -20°C.

3.3.2 Plasmid DNA preparation from *E. coli* cells

The cDNA clones in *E. coli* cells were purchased from RZPD German Resource Center for Genome Research, Berlin, Germany. On arriving, the *E. coli* cells were transferred to LB/ampicillin plates and cultured overnight at 37°C followed by overnight culture in LB medium containing ampicillin (50 µg/ml).

LB-medium (1 l):	LB/ampicillin plate (1 l):
10g tryptone	15 g agar in 1 l of LB-medium
5g yeast extract	100 µg/ml Ampicillin
5g NaCl	
pH was adjusted to 7.0 with NaOH	

Plasmid DNA was isolated with QIAprep Spin Miniprep Kit (Qiagen) from the overnight liquid culture according to the manufacturer's protocol.

3.3.3 Precipitation of plasmid DNA

Contamination by small nucleic acid fragments, protein and salt can be reduced to acceptable levels by precipitating the DNA in 2.5 volumes of ethanol and 1/10 volume of 3.0 M NaAc (pH 5.2). The sample was mixed, kept at -20ºC for more than 30 min and centrifuged at 14000 rpm for 10 min at 4ºC. The supernatant was discarded and the pellet was washed in cold 70% ethanol with subsequent centrifugation at 12000 rpm for 10 min. The purified DNA pellet was completely air-dried and then dissolved in TE buffer.

3.3.4 DNA electrophoresis

Agarose gel DNA electrophoresis is a standard method to separate and purify DNA fragments. An agarose gel of 0.8-2.0% (w/v) was prepared by boiling agarose in 1 x TAE buffer and pouring it into a gel casting tray. DNA samples were mixed with 1/6 volume of 6 x DNA loading buffer. The samples and an appropriate DNA marker (NEB) were separated at 10 V/cm for 0.5 - 2 h in 1 x TAE buffer containing ethidium bromide (0.2 µg/l). The ethidium bromide-stained DNA in the gel was visualized by 302 nm UV light and pictures were taken with Gel Imager (Intas).

1 x TAE buffer:	6 x loading buffer (1ml):
40 mM Tris-HCl	300 µl ddH_2O
0.35% glacial acetic acid	500 µl glycerol (86%)
1 mM EDTA (pH 8.0)	100 µl 2.5 % bromophenol blue
(0.2 µg/l ethidium bromide)	100 µl 2.5 % xylene cyanol
	2 µl EDTA (0.5 M; pH 8.0)

3.3.5 Digestion of DNA by restriction endonucleases

Plasmid DNA (200 ng – 5 µg) was digested by restriction endonuclease(s), using the appropriate reaction buffers. The amount of enzyme, DNA, buffer composition and the duration of the reaction varied depending on the specific requirements of the emzyme (in general: 37°C for 1 h to overnight). In case where it was necessary to treat the same DNA sample with different enzymes, the digestion was either carried out in a buffer compatible to different enzymes, or first in the enzyme buffer of lowest salt concentration, and then the salt concentration was increased to proceed with another enzyme.

3.3.6 DNA isolation from agarose gel

The resulting restriction fragments were separated in agarose as described in chapter 3.3.4. Under UV light, the appropriate DNA band was cut out and DNA purification was carried out with QIAquick Gel Extraction Kit (Qiagen) according to the manufacturer's protocol.

3.3.7 PCR

The Polymerase Chain Reaction (PCR) is an in vitro technique used to amplify a specific region of DNA, which lies between two oligonucleotide sequences (primers). PCRs were accomplished with Taq polymerase (Invitrogen) according to the modified manufacturer's protocol. All primers used in this study (Table 3.2) were synthesized by MWG Biotech. The PCR reactions took place in a Personal Cycler (Biometra). RT-PCR was carried out using SUPERSCRIPT^{TM} II RNase H – Reverse Transcriptase (Invitrogen) according to the manufacturer's protocol.

PCR protocol:

Component	Volume	Final concentration
10x PCR buffer	5 µl	20 mM Tris-HCl (pH8.4)
		50 mM KCl
$MgCl_2$ (50 mM)	1.5 µl	1.5 mM
dNTP mixture (2.5 mM)	4 µl	0.2 mM
0.1 % gelatine	0.6 µl	1.2‰
100 % DMSO	2.6 µl	5.2 %
ddH_2O	32.3 µl	
Forward primer (10 pmol/µl)	1 µl	0.2 pmol/µl
Reverse primer (10 pmol/µl)	1 µl	0.2 pmol/µl
cDNA	1 µl	
Taq Polymerase (1U/µl)	1 µl	20 U/ml
Final volume	50 µl	

A typical PCR program consisted as follows:

Step	Temperature	Duration
(1) Initial denaturation:	94°C	2 min
(2) 25-30 cycles:		
Denaturation:	94°C	1 min
Annealing:	50-60°C	1 min
Extension:	72°C	2 min
(3) Final extension:	72°C	10 min

Table 3.2 Primer sequences for the amplification of candidate genes identified from data analysis II (chapter 4.4.2.1)

Name	**Sequence**
Glo1 primer forward	ACCCCAGCACCAAGGATTTTCTAC
Glo1 primer reverse	ATTTTCCCGTCATCAGGCTTCTTC
J0157-Lisch primer forward	CCTCGGGCCCGCTCTGTGGAT
J0157-Lisch primer reverse	AAGGCGGAGGTGCTGGGGGATAGT
L2249-Ppp3 primer forward	TTGGTAAAAGAAGGGCGGGTGGAT

L2249-Ppp3 primer reverse	GCAAGGGGCAAGCTGTCAAAAG
2-A2416-primer forward	ATTCCGCCAAGCCCGTTCC
2-A2416-primer reverse	GCGCCTAGCAGCCGACTTA
J2454-atp1a1 primer forward	GCCCAGAAACCCCAAAACGGACAA
J2454-atp1a1 primer reverse	TAGGGGAAGGCACAGAACCACCAT
B0812-(rik) primer forward	GTATGCGCCACCGGAAAGGAC
B0812-(rik) primer reverse	AGCGGCCGCCATGAACTGTAA
L2441-T7-Skp1a primer forward	AAGATGACCCTCCTCCTCCTG
L2441-T7-Skp1a primer reverse	GTACCTGGGCCTCTTCCTCTT
O0316-T7-Ubqln2 primer forward	CCGGCGGCGACGACATCAT
O0316-T7-Ubqln2 primer reverse	GCGGCATTCAGCATAGGTTCTTG

3.3.8 PCR purification

The QIAquick PCR purification kit (Qiagen) was used to purify PCR products from the reaction mixture, which contained primers, nucleotides, polymerase and salts. PCR product purification was performed according to the manufacturer's protocol.

3.3.9 DNA ligation

DNA ligation was carried out using the pGEM-T Easy Vector System (Promega) according to the manufacturer's protocol. The A-tailing procedure of each purified PCR fragment was done according to the "Standard Tailing Procedure" in the manufacturer's protocol.

3.3.10 Transformation of *E. coli*

2 µl of ligation reaction and 50 µl of Chemically Competent *E. coli* (Subcloning Efficiency DH5α, Invitrogen) were mixed and incubated on ice for 30 min. Uptake of DNA was induced by heat shock (45 s at 42°C), then the cells were diluted in 950 µl of SOC medium and incubated for 1 h at 37°C by rotating at 250 rpm. 100 µl of the cell suspension were plated on LB plates containing ampicillin and IPTG/X-Gal (MBI Fermentas), and cultured overnight at

37°C. On the following day, the white colonies were selected for LB medium overnight culture and further experimental processing.

SOC medium (100 ml):
2 g tryptone
0.5 g yeast extract
0.5 g NaCl
0.25 ml 1M KCl
1 ml 2 M Mg^{2+}
1 ml 2 M glucose

3.3.11 DNA sequencing

DNA sequencing was done by commercial sequencing (MWG Biotech).

3.4 RZPD filter hybridization

The high density cDNA Filters (Mouse Unigene Set - RZPD 1, RZPD German Resource Center for Genome Research, Berlin, Germany) were applied to investigate gene expression. A filter is a nylon membrane of 22 cm x 22 cm size with 24,532 individual clones printed on in duplicate (49,064 clone spots). There are 48 * 48 blocks per filter and 5 * 5 dots per block. In each block, one Kanamycin guide dot spotted in the center, one pair of Arabidopsis control gene clones spotted in fixed positions and 11 different duplicate clones spotted in the other 22 positions comprise a special pattern which ensures that the duplicate genes do not have the same neighbors.

3.4.1 Quality control of filter

The vectors into which the inserts were cloned contain the sequence of M13 primer. To check the quality of the filters, a quality control hybridization was done with radiolabeled ^{33}P-M13. This ensures that the clones are spotted appropriately. First, the filter was stripped in the stripping solution (5 mM sodium phosphate buffer pH 7.2. 0.1% SDS) at 100°C: it was soaked from one edge and shaken gently till it had re-cooled to room temperature (approx. 30-45 min).

Then the filter was rinsed with TE (100 mM Tris-Cl. 10 mM EDTA. pH 8.0) and left in TE until the M13 hybridization was performed.

The M13 oligonucleotide (MWG Biotech) was labelled with γ-^{33}P ATP (ICN) using T4 polynucleotide kinase (Roche).

M13 labelling:	
M13 vector oligonucleotides (100 ng/µl)	100 ng
10x T4 polynucleotide kinase buffer	2 µl
T4 polynucleotide kinase (10.000 U/ml)	1 µl
γ-^{33}P ATP	3 µl
ddH_2O	13 µl
Final volume	20 µl

The 20 µl of mixture was incubated for 30 min at 37°C.

M13 hybridization:

The labeled M13 sequence was hybridized in 25 ml of Amasino per filter over night at 25°C.

Amasino:	
20% SDS	350 ml
1M sodium phosphate buffer pH 7.2	130 ml
5 M NaCl	50 ml
ddH_2O	470 ml
Final volume	1000 ml

On the next day, the filter was washed with wash buffer (1% SDS. 40mM sodium-phosphate) 2 x 30 min at 25°C and wrapped in Saran film. The filter was then exposed to a Phosphor Imager screen for 18 to 24 h. After scanning by PhosphoImaging (Storm, Molecular Dynamics), the filter was stripped twice and then wrapped in Saran film and kept at –20°C for 4-6 weeks to let the radioactivity fully decay.

3.4.2 Complex hybridization

Prior to the complex hybridization, the filters tested (in section 3.4.1) were exposed to Phosphor Imager screen and checked again to assure that no radioactivity was left.

Four RNA pools were gathered from total RNA isolated from the hypothalami of male mice of the AKR/J Control, AKR/J HF, SWR/J Control and SWR/J HF group. From the 4 different RNA pools radiolabeled ^{33}P-cDNA was synthesized and hybridized with the high density cDNA Filters.

3.4.2.1 Preparation of complex cDNA samples

The complex cDNA samples – 1st strand cDNA were synthesized from total RNA using Superscript II RT (Superscript II Reverse Transcriptase Kit, Life Technologies).

First, 10 µg of total RNA in ddH_2O (for two filters) and 1 µg of dTV primer (anchored dT18; 2 µl of 500 ng/µl) were mixed at RT and the final volume was adjusted to 10.5 µl with ddH_2O. The mixture was heated for 10 min at 70°C and then immediately cooled on ice. Then the following reagents were added on ice in the order indicated:

cDNA labeling:	
RNasin	0.5 µl
5x first strand buffer	5.0 µl
0.1 M DTT	2.5 µl
20 mM dGTP, dATP, dTTP	0.5 µl
[alpha-^{33}P] dCTP (10 µCi/ul)	5.0 µl

The reaction was prewarmed for 1 min at 37°C followed by the addition of 1 µl Superscript II RT (final reaction volume was 25 µl), and vortexed. The reaction was then incubated at 37°C for 1 to 2 h.

The hydrolysis of RNA to generate single strand samples was carried out by adding 1 µl of 0.5 M EDTA pH 8.0, 1 µl of 10% SDS and 3 µl of 3 N NaOH at RT and mixing after addition of each reagent. After incubation for 30 min at 68°C the mix was cooled to RT and then 1 µl of 1 M Tris-HCl pH 8.0 and 3 µl of 2 N HCl were added. The final volume was 50 µl after 16 µl of ddH_2O was added. 1 µl of the sample was transferred to 2 ml scintillation fluid and total activity was measured by a β-counter (Beckmann LS 3801, Beckman Instruments, Inc).

In the last step the labeled cDNA was purified using an S-300 column (Mo Bi Tec). The resin in the S-300 column was resuspended and then the column was pre-spun for 1 min at 2500 rpm. After the cDNA was loaded onto the column it was centrifuged again at 2500 rpm for 2 min.

The volume of flow through and the activity of 1 µl in 2 ml scintillation fluid were measured. The percentage of labeled dCTP incorporation was calculated from these two activity measurements.
Finally, the denatured sample was heated for 5 min at 100°C and immediately placed on ice.

3.4.2.2 Pre-hybridization

Each filter was wetted in 7.5 ml of ddH_2O and then placed into roller bottle, avoiding formation of air bubbles between filter and glass. Salmon sperm DNA (10 mg/ml) was denatured for 5 min at 100°C immediately placed on ice. For two filters, 30 µl of denatured DNA was added into the pre-warmed (65°C) 15 ml of 2x Denhardt's hybridization mix. Finally, 7.5 ml of 2x Denhardt's hybridization mix was added. Because the roller bottle already contained 7.5 ml ddH_2O the final concentration of Denhardt's hybridization mix was 1 x.
Filters were pre-hybridized at least 2 hours at 65°C.

2x Denhardt's hybridization mix:	
20% SDS	2.5 ml
20 x SSC	60 ml
50 x Denhardt's buffer	20 ml
ddH_2O	17.5ml
Final volume	100 ml

50x Denhardt's buffer:	
Ficoll (Type 400)	5 g
Polyvinylpyrrolidone	5 g
BSA (Fraction V)	5 g

The reagents for 50x Denhardt's buffer were dissolved in 400 ml ddH_2O, stirred for a few hours and then adjusted to 500 ml with ddH_2O. After filtered through a 0.45 µm filter, aliquots of 10 and 50 ml were frozen at –20°C.

3.4.2.3 Complex hybridization

The labeled cDNA samples prepared from each pool of total RNA (section 3.4.2.1) were added into the roller bottle and hybridized with the filters for 20 to 24 hours at 65°C. Each time, in complex hybridization, one pair of labeled cDNA samples was used, for instance, AKR/J control and HF or SWR/J control and HF.

3.4.2.4 Post-hybridization

The first 2 wash steps were done in the hybridization roller bottle (50 ml/bottle) at 65°C: 20 minutes in wash buffer 1 (1x SSC, 0.1% SDS) followed by 10 minutes in wash buffer 2 (0.3 x SSC, 0.1% SDS).

Then the filters were transferred into a large plastic box and washed for 10 minutes in 500 ml wash buffer 2 at 65°C in a water bath. A maximum of 8 filters (added one by one) can be washed in one box. The shaking frequency of the water bath was not over 20 movements per minute to prevent the filters moving up the box walls and drying out.

The last wash step was to rinse the filters 10 minutes in 500 ml wash buffer 3 (0.1x SSC, 0.1% SDS) at 65°C.

Finally, the filters were taken out of the wash buffer, and remaining buffer was briefly allowed to drop off. Each filter was then wrapped in the Saran foil, avoiding air bubbles, crinkles and visible liquid drops.

The wrapped filters were then exposed to a Phosphor Imager screen for 18 to 24 h followed by scanning with phosphoimaging (Storm, Molecular Dynamics) and image analysis using the software package ArrayVision (Imaging Research Inc.).

Filters were stripped as described in section 3.4.1 and kept at –20 °C. After scanning, a filter can be re-used for 5 times.

3.5 Affymetrix GeneChip hybridization

The GeneChip® expression arrays (Murine Genome U74Av2) were purchased from Affymetrix. The Murine Genome U74v2 set, consisting of three GeneChip® probe arrays (A, B and C Chip), contains probe sets interrogating approximately 36,000 full-length mouse genes and EST

clusters from the UniGene database (Build 74). In this experiment only the A Chip was applied, which contains 12,488 genes.

3.5.1 RNA isolation

See section 3.2.1.

3.5.2 cDNA synthesis

3.5.2.1 First-strand cDNA synthesis

The first-strand cDNA synthesis was carried out with Superscript II Reverse Transcriptase Kit (Life Technologies) with modification. The primer hybridization reaction, containing 5-20 µg RNA, T7-oligo (dT) primer 2 µl (50 µM) and DEPC-H_2O to 11 µl, was incubated at 70°C for 10 min and immediately placed on ice. Then 4 µl of 5 x first-strand cDNA buffer, 2 µl of 0.1 M DTT and 1 µl of 10 mM dNTP mix were added and incubated at 42°C for 2 min. Finally, 2 µl of Superscript II RT were added and the reaction was incubation at 42°C for 1 h.

3.5.2.2 Second-strand cDNA synthesis

The following reagents were added into the first-strand synthesis tube (20µl):

Second-strand reaction composition:	
DEPC-H_2O	91 µl
5 x second-strand reaction buffer	30 µl
10 mM dNTP mix	3 µl
10 U/µl *E. coli* DNA Ligase	1 µl
10 U/µl *E. coli* DNA polymerase I	4 µl
2 U/µl *E. coli* RNase H	1 µl
Final volume	150 µl

After brief centrifugation the mix was incubated at 16°C for 2 h, then 2 µl of T4 DNA polymerase were added and incubation was continued for another 5 min at 16°C. DNA was purified by adding 10 µl of 0.5 M EDTA.

3.5.2.3 Cleanup of double-strand cDNA

Cleanup of the double-strand cDNA was carried out with the GeneChip Sample Cleanup Module (Affymetrix). After 600 µl of cDNA binding buffer were added to the 162 µl of final double-stranded cDNA, the sample was applied to the cDNA Cleanup Spin Column to centrifuge for 1 min at ≥ 8000 g (≥ 10000rpm). The spin column was washed with 750 µl of cDNA wash buffer by centrifugation for 1 min at the same speed, followed by additional centrifugation for 5 min at maximum speed (≤ 25000 g). The cDNA was eluted from the column by loading 14 µl of elution buffer onto the column, 1 min incubation at RT and 1 min centrifugation at maximum speed.

3.5.3 cRNA synthesis

The Enzo®BioArray™High Yield™ RNA Transcript Labeling Kit (Affymetrix) was used for generating labeled cRNA target.

IVT cRNA labeling:	
Template cDNA	10 µl
ddH_2O	12 µl
10 x HY reaction buffer	4 µl
10 x biotin-labeled ribonucleotides	4 µl
10 x DTT	4 µl
10 x RNase inhibitor mix	4 µl
20 x T7 RNA polymerase	2 µl
Total volume	40 µl

After brief centrifugation the reaction was incubated at 37°C for 4-5 h.

3.5.4 Cleanup and quantification of biotin-labeled cRNA

The cRNA sample mixed with 60 µl of ddH_2O, 350 µl of IVT cRNA binding buffer and 250 µl of ethanol (100%) was loaded to an IVT cRNA cleanup spin column (Affymetrix) and centrifuged for 15 sec at ≥ 800 g (10000 rpm). Then the column was washed with 500 µl of

IVT cRNA wash buffer and 500 µl of 80% ethanol by centrifugation twice for 15 sec at ≥ 800 g (10000 rpm). After an additional centrifugation for 5 min at maximum speed (≤ 25000 g), the cRNA was eluted twice with RNase-free water – first with 11 µl, then with 10 µl, by centrifugation twice for 1 min at maximum speed (≤ 25000 g).
The purified cRNA was quantified with Ultrospec 2100 pro spectrophotometer (Amersham Pharmacia Biotech). The cRNA must be at a minimum concentration of 0.6 µg/µl.

3.5.5 Fragmenting the cRNA for target preparation

Fragmentation of cRNA target before hybridization onto GeneChip arrays has been shown to be critical in obtaining optimal assay sensitivity. 2 µl of 5 x fragmentation buffer was added for 8 µl of cRNA, then the mix was incubated at 95°C for 35 min and immediately placed on ice. The fragmented cRNA was checked on RNA 6000 Nano Labchips (Agilent Technologies).

3.5.6 GeneChip hybridization

The hybridization cocktail was prepared as follows and then incubated at 99°C for 5 min followed by incubation at 45°C for 5 min. Finally, it was centrifuged at maximum speed for 5 min.

Hybridization cocktail:	
Fragmented cRNA	15 µg
Control oligonucleotide B2 (3 nM)	5 µl
20 x eukaryotic hybridization controls	15 µl
Herring sperm DNA (10 mg/ml)	3 µl
Acetylated BSA (50 mg/ml)	3 µl
2 x hybridization buffer	150 µl
H_2O	124 µl
Total volume	300 µl

The GeneChip was equilibrated to RT and filled through one of the septa with 1 x hybridization buffer, followed by incubation at 45°C for 10 min with rotation. After removal of hybridization

buffer and refilling with hybridization cocktail, the chip was put into the hybridization oven for 16 h at 45°C.

12 x MES stock (1 l):	
MES-free acid monohydrate	70.4 g
MES sodium salt	193.3 g
Molecular Biology Grade water	800 ml
After mix the final volume was adjusted to 1 l and then filtered through a 0.2 µm filter.	

2 x hybridization buffer (50 ml):	
12 x MES	8.3 ml
5 M NaCl	17.7 ml
0.5 M EDTA	4.0 ml
10% Tween 20	0.1 ml
ddH_2O	19.9 ml

3.5.7 Post-hybridization

After 16 h of hybridization, the hybridization cocktail was removed and wash buffer (wash A) was filled into the GeneChip. The wash and stain steps (Table 3.3) were carried out in the fluidics station with the program edited in the connected computer.

Table 3.3 Post-hybridization: procedure and buffer

Post Hyb Wash 1	10 cycles of 2 mixes with wash A at 25°C	Wash A: 6 x SSPE, 0.01% Tween 20
Post Hyb Wash 2	4 cycles of 15 mixes with wash B at 50°C	Wash B: 100 mM MES, 0.1 M NaCl, 0.01% Tween 20
Stain	10 min in SAPE solution at 25°C	SAPE: 1 X MES, 2 mg/ml acetylated BSA, 10 µg/ml SAPE
Post stain wash	10 cycles of 4 mixes with wash A at 25°C	
2nd stain	10 min in antibody solution at 25°C	Antibody solution: 1 x MES, 2 mg/ml acetylated BSA, 0.1 mg/ml normal goat IgG, 3 µg/ml biotinylated antibody
3rd stain	10 min in SAPE solution at 25°C	
Final wash	15 cycles of 4 mixes with wash A at 30°C The holding temperature is at 25°C.	

After complete wash and staining the GeneChip was scanned with the GeneChip scanner 2500 (Affymetrix) and the image was analyzed using the R software package (Bioconductor).

3.6 In Situ hybridization

The principle behind in situ hybridization (ISH) is the specific annealing of a labelled nucleic acid probe to complementary sequences in fixed tissue, followed by visualization of the location of the probe. This technique was used here to locate and confirm the differentially expressed genes identified by the complex hybridization.

3.6.1 Brain sectioning

Coronal brain sections (16 µm) spanning the hypothalamic area were prepared from the intact brains with a cryosectioning system (Leica CM 3050). The object temperature was adjusted at –13°C to –14°C after the brain was fixed on it at –50°C. The chamber temperature was 1-2°C lower than object temperature to avoid that the sections melted on the cryostat knife. The first 6 sections were mounted on 6 slides (A1 to F1 in order), and then the second 6 sections were added in the same order, i.e., the distance between sections represented on one slide was 96 µm. When the first 6 slides were completed, another series of 6 slides (A2 to F2) was used for mounting new sections.

3.6.2 Glass slide preparation – silanization

For an initial wash, the glass slides (Menzel) were put into a box containing hot tap water and detergent for 1 h. They were rinsed 3 times in hot tap water for 15 min. Subsequently, they were washed once with deionized H_2O and ddH_2O for 15 min each. Finally, after being washed in 70% ethanol and shaken for 45 min they were dried overnight at 60°C. On the following day, they were washed once for 30 s with 2% TESAP in acetone and twice in 100% acetone. After a brief rinse with deionised H_2O and ddH_2O they were dried overnight at 42°C and stored at RT.

3.6.3 Preparation of the probe

3.6.3.1 Linearization of DNA template from section 3.3.3.

The plasmid DNA was linearized by the digestion of the restriction enzyme close to the end of the insert to avoid transcription from the whole plasmid DNA by RNA polymerase. It is very important that there should be no more cutting between the restriction site (e.g., Spe I) and the

corresponding primer binding site (e.g., T7) (Figure 3.1). The plasmid DNA samples (5 µg – 10 µg) were digested in two reaction tubes by one restriction endonuclease (either Spe I or Apa I) in each reaction using corresponding reaction buffer. The amount of enzyme, DNA, buffer composition and the duration of reaction varied depending on the specific requirements of the enzyme (in general: 37°C for 2 h to overnight).

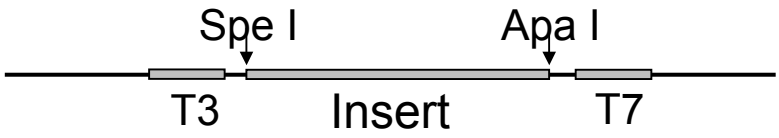

Figure 3.1 linearization of DNA template. The dark line shows part of the vector sequence. The gray box in the middle shows the insert and the other two beside it show the T3/T7 primer binding sites. At both ends of the insert there are restriction sites by Spe I or Apa I.

3.6.3.2 *In Vitro* transcription (IVT)

From this step to hybridization, all solutions and devices used must be RNase free, i.e. DEPC treated solutions, and baked racks and stainless steel tanks, are necessary.

For *In Vitro* transcription the following reagents were added in order indicated:

10 - X µl DEPC H_2O
5 µl 5x transcription buffer
X µl = approx. 1 µg DNA template
1 µl 10 mM rCTP
1 µl 10 mM rGTP
1 µl 10 mM rATP
1 µl 0.75 M DTT
1 µl = 1 U RNase-Block I
4 µl S35-UTP (50 µCi)
1 µl T3 or T7 polymerase (all 20000 U/ml)

The final volume was 25 µl.

This reaction was first incubated at 37°C for 1-1.5 h and then for 0.5-1 h after the addition of 2 U DNase I. During this incubation a ChromaSpin 30 column (BD Biosciences) was prepared by resuspending the loading gel in the column and spinning at 1700 rpm for 5 min at 24°C. After incubation 25 µl DEPC H_2O were added to the reaction and the final volume of 50 µl was pipetted onto the ChromaSpin column, and then centrifuged at 1700 rpm for 5 min. The probe can be stored at -20°C or -70°C for one week if required. 0.5 µl of the purified probe was taken out, diluted to 50 µl and then activity of 5 µl was measured by Beckmann LS 3801.

3.6.4 Pre-hybridization

The slides were brought to RT in a rack and fixed in 4% paraformaldehyde (PFA) in PBS for 20 min on ice followed by 2 x 5 min washes in 0.1 M PBS (0.2 M diluted with DEPC H_2O). Then the slides were immersed in 250 ml of 0.1 M TEA for 2 min; meanwhile, 625 µl of acetic anhydride (AA) (Sigma) was added to another dry tank. Subsequently, the 0.1 M TEA was poured from first tank into acetic anhydride tank, stirred quickly with a sterile tip or Pasteur and then the slides were immersed in this TEA/AA mix for 10 min. After two washes in 0.1 M PBS each lasting 2 min, the slides were dehydrated through gradient increasing concentration of alcohol – 50, 70, 95 and 100% ethanol/DEPC H_2O for 3 min each step. Finally, they were air dried for 1-2 h.

3.6.5 Hybridization

The hybridization buffer and probe mixture were prepared by adding the following reagents and mixing well:

Hybridization buffer (1.5 ml):	Probe mixture (400µl):
300 µl 5 M NaCl	50 µl radioactive probe
100 µl 50 x Denhardts	256 µl tRNA (3.9 mg/ml stock)
50 µl 1 M Tris (pH 8)	20 µl 1 M DTT
10 µl 0.5 M EDTA (pH 8)	74 µl DEPC H_2O
40 µl DEPC H_2O	
1 ml 50% Dextran sulphate	

50% dextran sulphate was prepared by dissolving 1 g of dextran sulphate in 1.5 ml DEPC H_2O in a sterile 4 ml tube at 55-60°C for 2-3 h. After vortexing the solution can be immediately used or stored at 4°C.

The final hybridization cocktail was prepared by mixing 400 µl of probe mixture and 1600 µl of hybridization buffer. The mixture can be stored at -20°C (for 1 week) if necessary.

The radioactivity of the 2000 µl probe was determined. The optimal range of radioactivity is 80000 – 150000 cpm in 10 µl.

50-60 µl of the final hybridization cocktail was loaded to each slide. The slides were covered by cover slips and incubated for 16-22 h at 60°C in the hybridization oven.

3.6.6 Post-hybridization

The slides were taken out of the oven and cooled to RT. Subsequently, they were soaked in 4 x SSC for 30 min to loosen cover slips. The cover slides were removed by joggling and each slide was transferred to another rack in a tank containing 4 x SSC. When all slides were in the rack, they were washed four times in 4 x SSC, 5 min each. After incubation in RNase solution at 37°C for 30 min, the slides were washed in a series of gradient decreasing concentration of SSC dilutions and dehydrated in a series of gradient increasing concentration of ethanol solutions.

RNase solution:

25 ml 5 M NaCl
2.5 ml 1 M Tris (pH 8)
0.5 ml 0.5 M EDTA
0.5 ml RNase (10 mg/ml)
222ml dd H_2O

Slide wash:

4 x SSC	RT	4 x 5 min
2 x SSC	RT	2 x 5 min
1 x SSC	RT	1 x 10 min
0.5 x SSC	RT	1 x 10 min
0.1 x SSC	60°C	1 x 30 min

Slide dehydration:

50% ethanol	RT	1 x 3 min
70% ethanol	RT	1 x 3 min
95% ethanol	RT	1 x 3 min
100% ethanol	RT	1 x 1 min

3.6.7 Signal detection

The well-dried slides were fixed in an X-ray cassette and exposed to BioMax MR Film (Kodak) for 3-7 days.

3.7 Quantitative real-time RT-PCR

Quantitative real-time reverse transcription polymerase chain reaction (real-time RT-PCR) is based on the detection of fluorescence produced by a reporter molecule – e.g., SYBR® Green I, which binds to double-stranded DNA (dsDNA) but not to single-stranded DNA. In real-time RT-PCR, as PCR product – dsDNA accumulates, the fluorescent dye generates a signal that is proportional to DNA concentration and that can be measured using instruments.

3.7.1 First-strand cDNA synthesis

Hypothalamic RNA isolation is described in section 3.2.1. SuperScript™ III Platinum® Two-Step qRT-PCR kit (Invitrogen) was used to generate first-strand cDNA for real-time RT-PCR. 1 µg RNA was added into a tube containing 10 µl of 2 x RT Reaction Mix and 2 µl of RT Enzyme Mix. DEPC-treated water was filled up to the final volume of 20 µl. After gentle mixing, the reaction was incubated at 25°C for 10 min and at 42°C for 50 min. Subsequently, the reaction was terminated at 85°C for 5 min and chilled on ice. Finally, 1 µl (2U) of E. coli RNase H was added followed by incubation at 37°C for 20 min. The first-strand cDNA was diluted with DEPC-treated water to 100 µl.

3.7.2 Primer design

Primers (Table 3.4) were designed at www.invitrogen.com using the primer design software – OligoPerfect™ Designer and synthesized by MWG Biotech. The amplicon length defined by the primer was approximately 80–250 bp to optimize the efficiency of real-time RT-PCR.

Table 3.4 Primer sequences for real-time RT-PCR.

Name	Sequence
Glo1 primer forward	ATGCCTCATGGTACCTCCTG
Glo1 primer reverse	TCCCCTAGAGCAGCCTTGTA
Hba-α1 primer forward	GACGTTGGTTAGCCACCAC
Hba-α1 primer reverse	CTGCAGAAGGGAGCTTATCG
Ppp3cb primer forward	GAGGAGAGCAGTGAGCAAGG
Ppp3cb primer reverse	GGGGGAGTTCCACGTTATCT
TNFAIP1 primer forward	CCTGGGCTCAATCTCCAGTA
TNFAIP1 primer reverse	GGTCCTGGCACTCTGCTTAG

3.7.3 Real-time RT-PCR protocol and program

Fluorescein (Bio-Rad) was added to the Platinum® SYBR® Green qPCR SuperMix UDG (Invitrogen) as internal reference to a final concentration of 20 nM. Each real-time qRT-PCR reaction contained 25 µl of Platinum® SYBR® Green qPCR SuperMix UDG with fluorescein, 1 µl of forward and reverse primer (10 µM) respectively and 1 µl of first-strand cDNA (see 3.7.1) and DEPC water to a final volume of 50 µl. Beta actin was used as standard gene for control because it is expressed identically in all cells.

A typical real-time RT-PCR cycling program using the iCycler™ (Bio-Rad) is shown below:

Cycle 1: (1X)
- Step 1: 50.0ºC for 2 min
- Step 2: 95.0ºC for 2 min

Cycle 2: (45X)
- Step 1: 95.0ºC for 15 sec
- Step 2: 55.0ºC for 30 sec
- Step 3: 72.0ºC for 30 sec
- Data collection enabled.

Cycle 3: (100X)
- Step 1: 70.0ºC for 7 sec
- Increase setpoint temperature after cycle 2 by 0.2ºC
- Melt curve data collection and analysis enabled.

Cycle 4: (1X)
- Step 1: 4.0ºC for 5 min

The fluorescence in each well of the 96-well plate was measured after each extension step (Cycle 2, Step 3) during the PCR reaction. As DNA is synthesized, more SYBR Green will bind and the fluorescence will increase.

3.8 Data analysis

Totally 3 sets of data analysis were done. The first set (Data analysis I) was from 8 filters hybridized with the probes synthesized from the first set of 4 RNA pools – 2 RNA samples for each group. The second set of RNA pools was gathered from the selected RNA after transthyretin screening in Northern blot – 11 from SWR/J control groups as well as HF, and 5 from AKR/J control groups as well as HF. Data analysis II was done using the second set of data coming out of second 8 filter hybridizations and 8 GeneChip hybridizations with the same second set of RNA pools. Data analysis III was focus on the data from second filter hybridization.

3.8.1 Data analysis I

The signal intensity of each spot on the filters was determined using ArrayVision procedure AR VOL that means artifact-removed density value multiplied by its area. To reduce biasdue to technical varision between filters quantile normalization was done for filters using AR VOL data corrected with local background. The local background was median intensity of one Kanamycin and one pair of Arabidopsis spots in each 5*5 block. For each spot, the intensity after background correction was transformed to $\log_2$. Next, for each filter the average intensity of the duplicate genes was calculated, and then the average intensity of this gene on two repeated filters was calculated. An MA plot was made for each comparison, where M means the difference of $\log_2$-intensity of one gene at two conditions and A means the mean of $\log_2$-intensity of one gene at two conditions, in other words, M shows $\log_2$-ratio (fold change = 2^M) and A shows mean intensity. The candidate genes were selected according to the MA plot using a threshold of > 2 fold change in the following 4 comparisons: AKR/J Control vs. AKR/J HF, SWR/J Control vs. SWR/J HF, AKR/J Control vs. SWR/J Control and AKR/J HF vs.

SWR/J HF. Low quality spots were detected and eliminated by checking the differences between the duplicates on filter in relation to the M values.

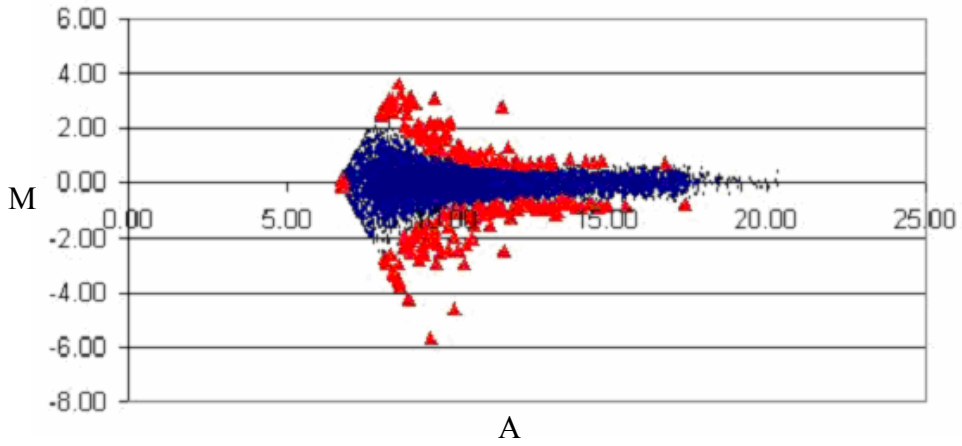

Figure 3.2 MA blot of AKR/J control vs. AKR/J HF. M shows difference of $\log_2$-intensity of one gene at two conditions while A is the mean of $\log_2$-intensity of one gene at two conditions. The selected candidate genes were marked as "▲".

3.8.2 Data analysis II

The second set of data from 8 RZPD cDNA Filter hybridizations and 8 Affymetrix GeneChip hybridizations was analyzed with different strategy.

Table 3.5 Array hybridization with the same original RNA pools.

RNA pools	**RZPD cDNA Filter**	**Affymetrix GeneChip**
AKR/J Control	2 x	2 x
AKR/J HF	2 x	2 x
SWR/J Control	2 x	2 x
SWR/J HF	2 x	2 x

The data (AR VOL) from filter hybridization were first corrected with the local background – medium intensity of one Kanamycin and two Arabidopsis spots within each 5 x 5 block. And then, all filters were complemented in a quantile normalization, followed by the 4 different

comparisons: AKR/J Control vs. AKR/J HF, SWR/J Control vs. SWR/J HF, AKR/J Control vs. SWR/J Control and AKR/J HF vs. SWR/J HF. MA plot and M – z-scores plot were made for each comparison, where z-scores tells how many standard deviations away from the mean of M value at this intensity a score resides. The list of candidates was sorted out through several criteria: intensity (A), z-scores, fold-change (M), and differences of one gene between two replicate filters and between the duplicates within one filter. The threshold of >2 fold change was defined for filter data analysis while >1.7 fold change for chip.

The data from GeneChip hybridizations were treated with the similar analysis method as described above.

In filter data, the genes were listed with RZPD clone ID (e.g., IMAGp952F2058) and GenBank accession number (e.g., ai226516, ai266816). However, in chip data the genes were list with Affy ID (e.g., 103361_at). By Internet database searching (DAVID Annotation Tool, http://apps1.niaid.nih.gov/david/), the list of Affy ID was converted to UniGene cluster. The GenBank accession number was converted to UniGene cluster as well. And then the selected candidate lists from filter and chip analyses were compared and the overlapped genes in each of the 4 comparisons were listed out as the analysis result.

The candidates were rechecked and the low quality candidates were eliminated through another approach – direct going over in the original image of filter.

3.8.3 Data analysis III

Only the filter data from the second complex hybridization were used in analysis III. The data were dealt with as described in 3.8.2 followed by only two comparisons – AKR/J Control vs. AKR/J HF and SWR/J Control vs. SWR/J HF.

3.9 Post analysis

After each analysis, the clones of some candidates were obtained from RZPD, followed by over night culture, sequencing, cloning, probe labeling and then Northern blot analysis, In Situ hybridization and real-time RT-PCR.

3.10 Single nucleotide polymorphism (SNP) analysis

Single nucleotide polymorphism (SNP) analysis of mouse gene Glo1 was carried out by Kathrin Reichwald in the Department of Genome Analysis, Institute of Molecular Biotechnology (IMB), Jena, Germany.

4 Results

4.1 Diet induced obesity in mice

4.1.1 Body mass

In weanlings of either strain, body mass increased rapidly from day 24 to 35 by about 8-14 g, corresponding to the maximal growth spurt in mice. After 2 days on the high fat diet, the body mass in the AKR/J high fat diet groups was already 1.5 to 2.0 g higher than in the controls (Table 4.1 and Figure 4.1). After 10 days on the diet experiment, both female and male AKR/J mice fed the high fat diet were significantly heavier than mice in the control groups. In contrast, body mass of both male and female SWR/J mice showed no difference between the high fat diet and control groups. In corresponding feeding groups, AKR/J mice were heavier than SWR/J mice.

Table 4.1 Effect of different diets on body mass.

Strain	**Diet group[a] and number of mice**	**Body mass (mean ± SD) (g)**		
		Day 21	**Day 35**	**Day 45**
AKR/J (37 mice in 8 litters)	Female C: n = 10	8.95 ± 2.39	19.88 ± 2.16	21.51 ± 1.98
	Female HF: n = 8	8.85 ± 2.14	19.70 ± 1.88	23.61 ± 2.76
	Male C: n = 10	10.27 ± 2.31	23.69 ± 2.65	26.07 ± 2.51
	Male HF: n = 9	10.52 ± 2.22	23.77 ± 2.57	29.01 ± 3.30
SWR/J (104 mice in 14 litters)	Female C: n = 30	8.17 ± 0.71	16.28 ± 0.99	17.08 ± 0.96
	Female HF: n = 25	8.35 ± 0.67	16.24 ± 0.85	17.56 ± 0.93
	Male C: n = 27	8.65 ± 1.29	20.96 ± 1.79	21.77 ± 1.48
	Male HF: n = 22	8.54 ± 0.97	20.76 ± 1.19	21.84 ± 1.18

[a] C: control diet; HF: high fat diet.

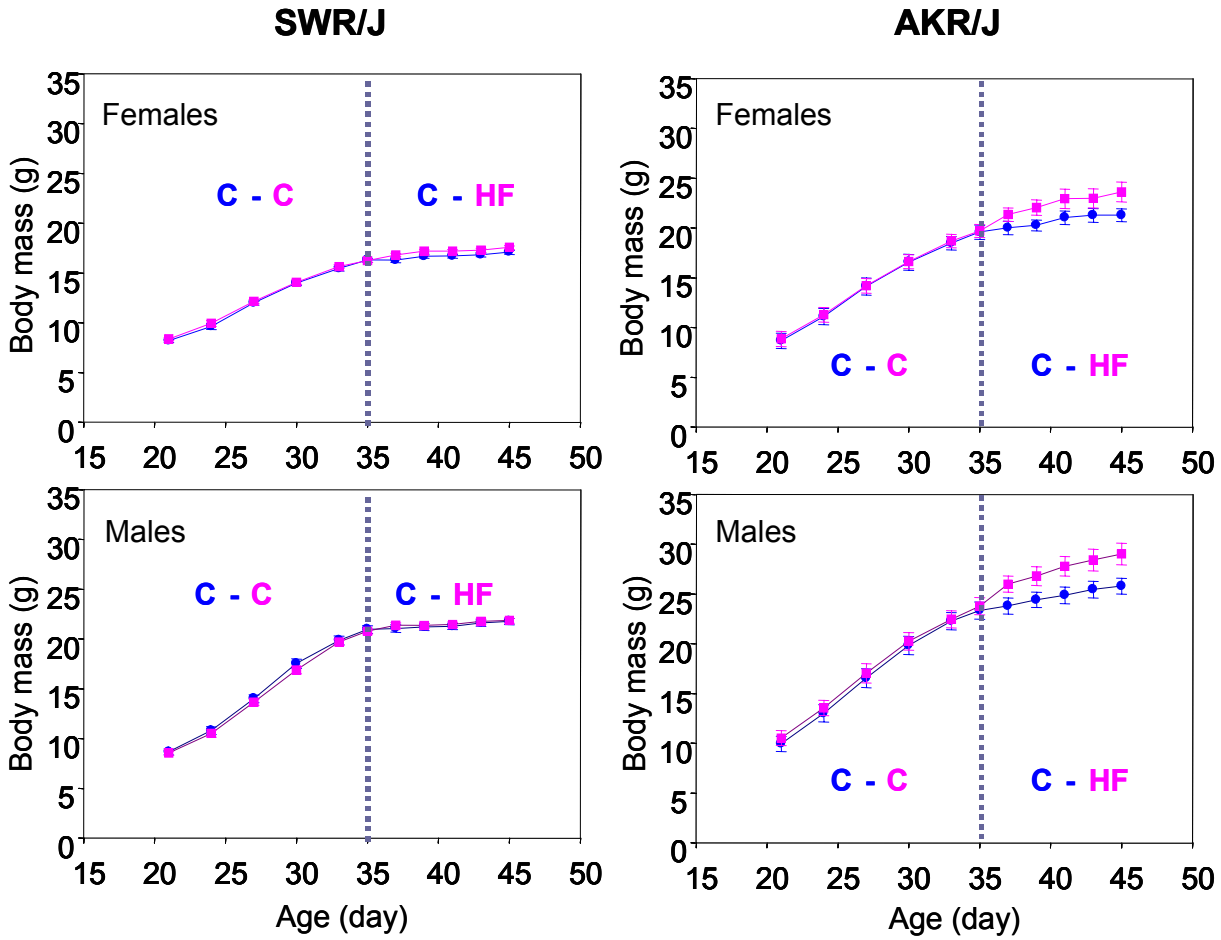

Figure 4.1 Effect of diet on body mass in two inbred mouse strains fed either control (C –●–) or high fat (HF –■–) diet. n = 8-30 individuals per group (Table 4.1). Data indicate means ± SD. The dotted lines match the day of diet change for the HF groups.

4.1.2 Energy intake

After weaning, during the first two weeks at the control diet, all mice consumed comparable amounts of energy per day, regardless of strain. Energy intake (food intake (g) * energy content of diet (KJ/g)) was slightly higher in males than in females, corresponding to sexual dimorphism (Figure 4.2). During the subsequent 10-day experimental period, energy intake was slightly increased in the control groups reflecting the age-related increase in body mass. In contrast, in the high fat diet groups, energy intake was significantly higher in the 10 days after the diet change compared to pre-diet change levels and also to the control groups.

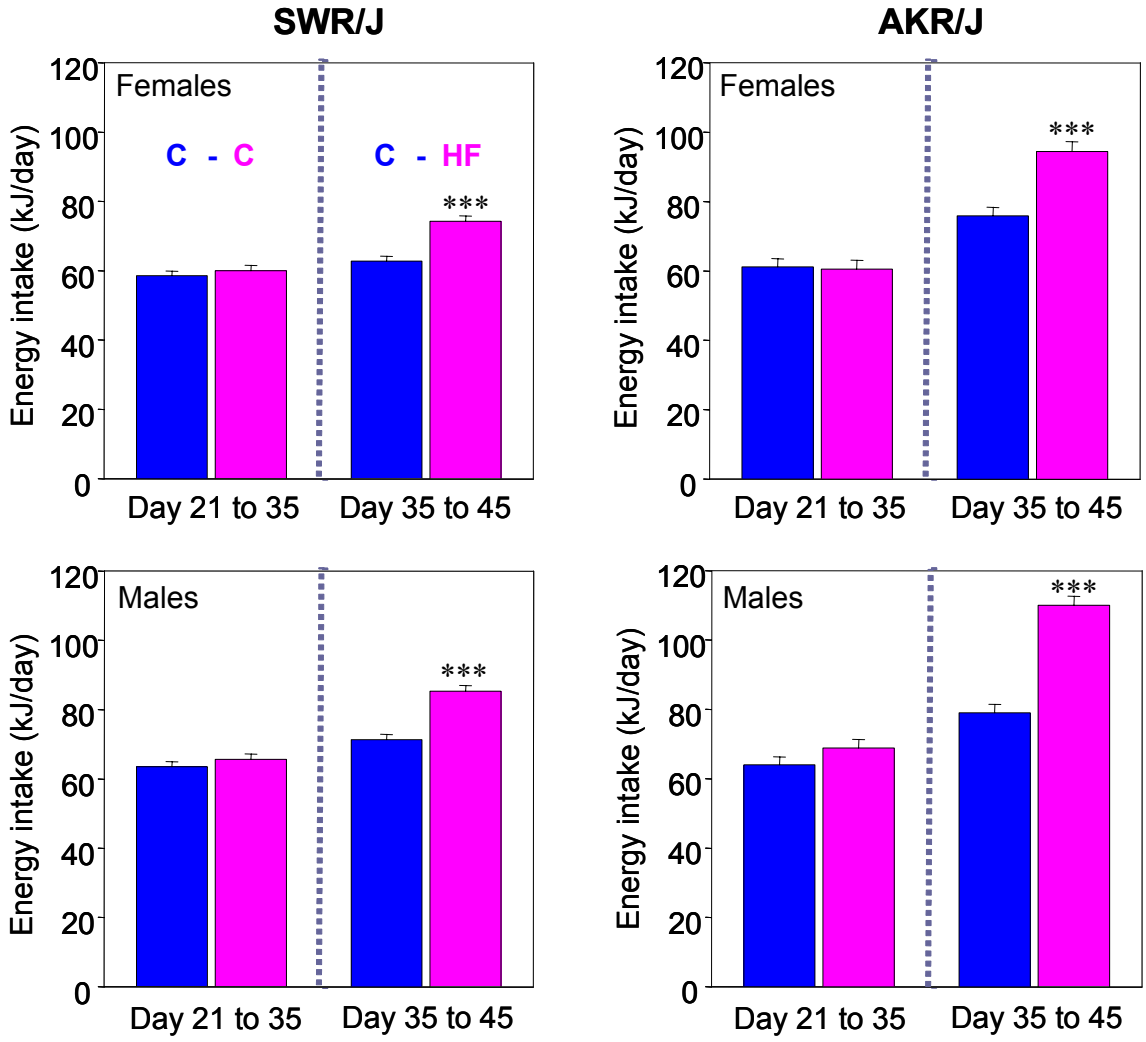

Figure 4.2 Daily energy intake. Bars indicate mean energy intake per day as assessed from the 2 weeks period on the control diet and the 10-day experimental period on the control (C) vs. high fat diet (HF). n = 8-30 (Table 4.1). *** $P < 0.001$ for HF vs. C.

4.1.3 Body fat

The mean total body fat and its proportion to body mass are plotted in Figure 4.3. Both fat mass and the proportion of fat in the AKR/J high fat diet groups were significantly higher than in the control groups. In contrast, total fat mass and the percentage of body fat in the SWR/J high fat diet groups were only slightly elevated compared to the control groups, and this difference was not statistically significant.

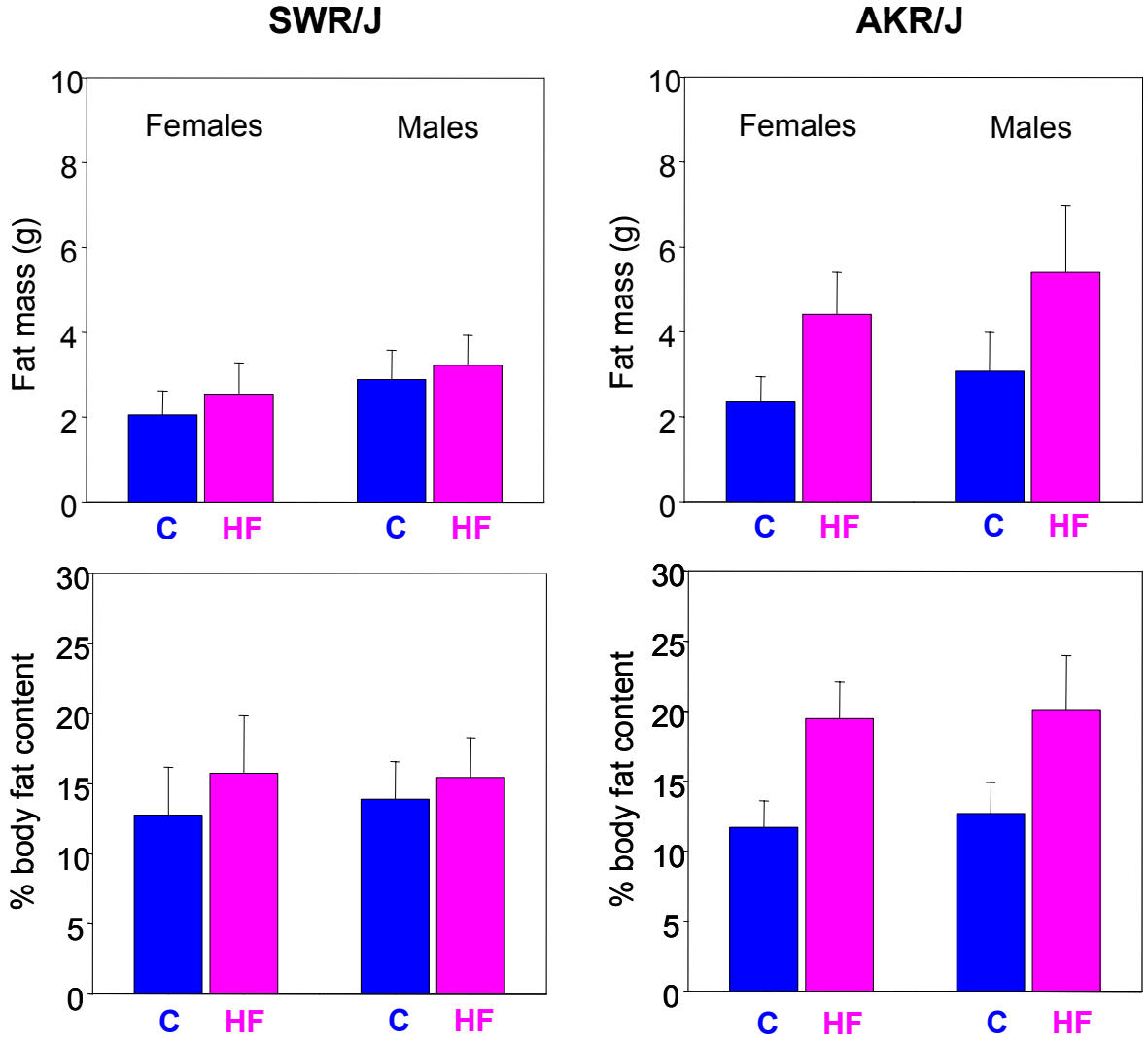

Figure 4.3 Mean body fat (mass (g) or content (%)) on day 45 of control (C) and high fat diet (HF) in two inbred mouse strains. n = 11-12 for SWR/J and 5-6 for AKR/J. * $P < 0.05$, ** $P < 0.01$, *** $P < 0.001$ for HF vs. C.

Individual body fat and lean mass content in relation to body mass are shown in Figure 4.3. In SWR/J HF and control mice, lean mass and fat mass respectively fall within the same line of regression. In AKR/J mice, the high fat diet group did not only have a heavier body mass and a lower lean mass than the control group, but also contained more fat and less lean mass at the same body mass, i.e., body fat content is disproportionally enlarged with body mass in AKR/J mice fed a high fat diet.

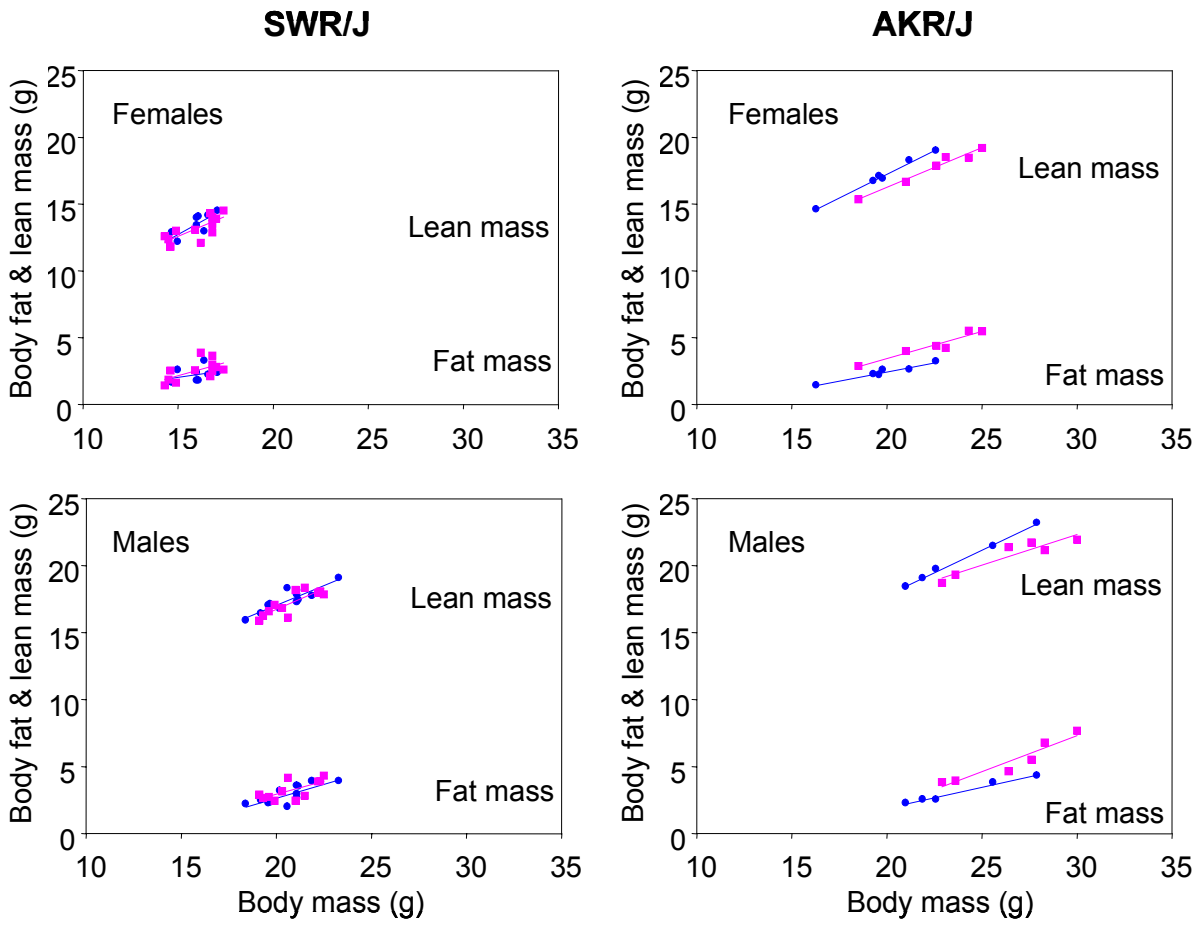

Figure 4.4 Individual body fat/lean mass on day 45 in two inbred mouse strains fed either control (C –●–) or high fat (HF –■–) diet. n = 11-12 for SWR/J and 5-6 for AKR/J. Lines indicate least square regression estimates for the linear relationship between body mass and fat or lean mass in each group.

4.1.4 Tissue mass

For inguinal and retroperitoneal white adipose tissue pads, inter scapular brown adipose tissue pad, femoral skeletal muscle, liver and spleen, whole tissue/organ masses and their proportion to whole body mass are listed in Tables 4.2 and 4.3. Both the inguinal and the retroperitoneal white adipose tissue pads were significantly larger in the AKR/J high fat diet group than in the control group. Concerning these comparisons, no difference between control and HF was found in the SWR/J groups. In the interstrain comparison, inguinal fat mass in AKR/J control mice was smaller than in SWR/J mice ($P<0.001$), while in the HF groups there was no difference between AKR/J and SWR/J mice. Moreover, AKR/J mice had larger femoral muscles and smaller spleens than SWR/J mice. Although AKR/J mice had larger livers (mass) than SWR/J mice, this difference was reduced after whole body mass correction.

Table 4.2 Tissue/organ mass on day 45 in control (C) and high fat diet (HF) groups in both SWR/J and AKR/J strains.

Data / Tissue	Tissue/organ mass			
	SWR/J		AKR/J	
	C (n=11)	HF (n=13)	C (n=8)	HF (n=9)
White adipose tissue:				
- iWAT (mg)	329.4±57.0[a]	372.0±110.0	219.1±47.1[b]	345.3±91.0[c]
- rpWAT (mg)	65.8±20.8	78.8±34.6	71.6±23.3[d]	147.7±36.4[e]
Brown adipose tissue:				
- isBAT (mg)	70.6±10.2	73±10.3	86.6±15.4	103.6±17.2
Skeletal muscle:				
- femoral (mg)	111.9±10.8	116.1±10.0	145.3±13.9	155.0±15.4
Liver (g)	1.37±0.17	1.29 ±0.10	1.50 ±0.15	1.57 ±0.17
Spleen (mg)	101.1±11.0	102.7±12.8	55.0 ±8.0	60.4 ±1.7

Data indicate mean ± SD. P^{a-b} and $P^{d-e} < 0.001$, $P^{b-c} < 0.01$.
iWAT: inguinal white adipose tissue
rpWAT: retroperitoneal white adipose tissue
isBAT: inter scapular brown adipose tissue

Table 4.3 Proportion of tissue/organ mass to whole body mass on day 45 in control (C) and high fat diet (HF) groups in both SWR/J and AKR/J strains.

Data / Tissue	Tissue/organ mass (%)			
	SWR/J male		AKR/J male	
	C (n=11)	HF (n=13)	C (n=8)	HF (n=9)
White adipose tissue:				
- iWAT	1.513±0.267[a]	1.690±0.418	0.904±0.148[b]	1.312±0.250[c]
- rpWAT	0.299±0.086	0.355±0.137	0.293±0.080[d]	0.560±0.093[e]
Brown adipose tissue:				
- isBAT	0.326±0.041	0.340±0.005	0.358±0.050	0.396±0.044
Skeletal muscle:				
- femoral	0.516±0.059	0.527±0.049	0.604±0.054	0.596±0.061
Liver	6.131±0.387	5.901±0.189	6.228±0.578	6.045±0.410
Spleen	0.465±0.043	0.467±0.065	0.228±0.017	0.234±0.011

Data indicate mean ± SD. P^{a-b} and $P^{d-e} < 0.001$, $P^{b-c} < 0.01$.
iWAT: inguinal white adipose tissue
rpWAT: retroperitoneal white adipose tissue
isBAT: inter scapular brown adipose tissue

4.1.5 Litter size

In this study, litter size was investigated in both 29 litters of SWR/J and 20 litters of AKR/J mice. Litter size at birth was 7±2 individuals in SWR/J mice whereas 5±2 in AKR/J mice (Figure 4.5). On day 21 offspring from large litters tended to be smaller than individuals from small litters. And the relationship between body mass and litter size is shown in Figure 4.6. The body mass of SWR/J mice at age of 21 days was 8.41±0.92 g, lower than SWR/J mice (9.50±2.34 g). The variation of body mass in small litter size was higher. To exclude this influence, only mice from large litters (>5) were selected for the further experiment.

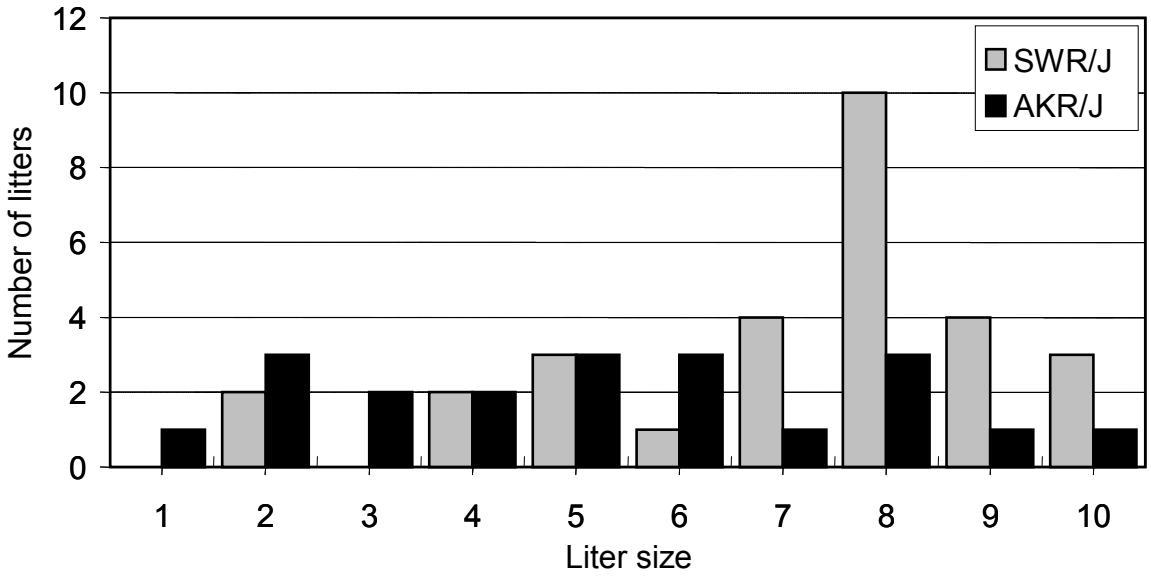

Figure 4.5 frequency distribution of litter size in two inbred mouse stains. Bars indicate the number of litters in corresponding litter sizes in SWR/J and AKR/J mice.

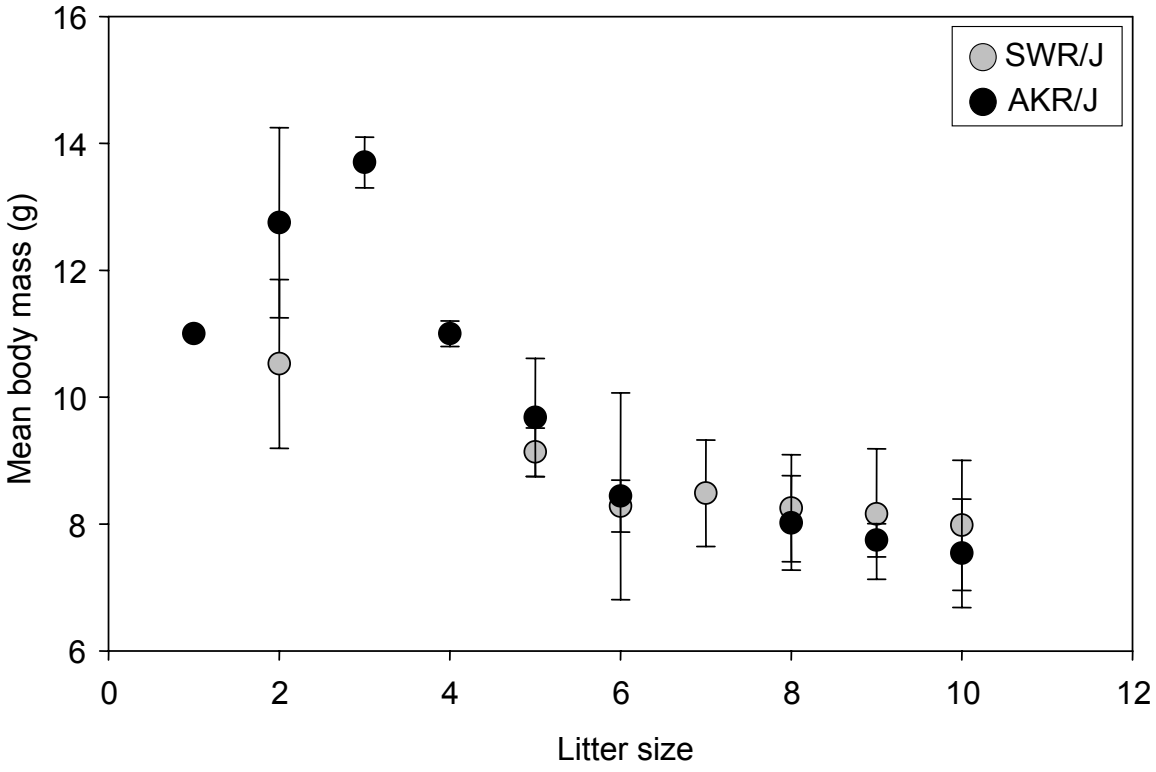

Figure 4.6 The relationship between body mass (day 21) and litter size in two inbred mouse strains. The inverse relation is shown in both strains with r^2=0.86 in SWR/J and 0.75 in AKR/J mice.

4.2 Gene expression study

The in vivo feeding experiments confirmed that in comparison to AKR/J mice, SWR/J mice were resistant to high fat diet feeding in terms of body mass increase and adiposity (body fat content). Using array (filter and chip) technology, it was investigated whether these phenotypic differences between strains were associated with differential gene expression in the hypothalamus.

4.2.1 Data analysis I

4.2.1.1 Array hybridization

The numbers of selected candidate genes from the first set of filter complex hybridizations are listed in Table 4.3. there were more differentially expressed genes found in the inter-strain comparison than in the intra-strain diet comparison, i.e., the impact of genetic background (strain) on differential gene expression appeared to be larger than the diet effect.

Table 4.3 Number of candidate genes in different comparison groups identified from data analysis I.

Comparison group		Number of candidates
AKR/J	Control vs. HF	10
SWR/J	Control vs. HF	13
Control	AKR/J vs. SWR/J	60
HF	AKR/J vs. SWR/J	28

Focused on the diet related genes, the fold changes in SWR/J gene expression were larger than in AKR/J. The candidate genes regulated by different diet within either AKR/J or SWR/J strain are shown in Table 4.4 and 4.5. The candidate genes in the inter strain comparison are shown in Appendix.

Table 4.4 List of candidate genes regulated by diet in AKR/J mice from data analysis I.

AKR/J RZPD clone ID	**GenBank accession number**	**Cluster description by RZPD**	**Fold change[a]**
IMAGp952A0616	aa030182, ai323327, ai894083	SRY-box containing gene 3	2.68
IMAGp952A0534	aa289979, ai661640	ribosomal protein L21	2.55
IMAGp952I2410	ai413755, ai425782, w80260	chaperonin subunit 3 (gamma)	2.26
IMAGp952F0922	aa119175	serine/threonine kinase 19	2.17
IMAGp952D0658	ai226511, ai266811	ornithine transcarbamylase	2.12
IMAGp952O0249	aa673382	mitogen-activated protein kinase kinase kinase kinase 6	2.84
IMAGp952F0432	aa272827	wingless-related MMTV integration site 11	-2.34
IMAGp952P1311	w97066	transgelin	2.32
IMAGp952A1121	aa086944, ai595208	ESTs, Weakly similar to S55051 Bicaudal-C - fruit fly [D.melanogaster]	-2.29
IMAGp952H1522	aa119208	M.musculus mRNA for e1 protein	2.10

[a]: positive means upregulated in HF group while negative means downregulated

Table 4.5 List of candidate genes regulated by diet in SWR/J mice from data analysis I.

RZPD clone ID	GenBank accession number	Cluster description by RZPD	Fold change[a]
IMAGp952C1431	aa048282	ESTs, Highly similar to T17338 hypothetical protein DKFZp434O125.1 - human [H.sapiens]	13.59
IMAGp952F2058	ai226516, ai266816	transthyretin	10.16
IMAGp952F0714	aa011728	ESTs, Weakly similar to KIAA0672 protein [H.sapiens]	10.07
IMAGp952J1319	aa049077	ESTs, Weakly similar to AF161429_1 HSPC311 [H.sapiens]	9.16
IMAGp952N1531	aa060121	Down syndrome critical region homolog 2 (human)	8.76
IMAGp952E149	w71639	ESTs, Weakly similar to matrin cyclophilin [R.norvegicus]	4.02
IMAGp952L0560	ai227481	programmed cell death 4	-3.36
IMAGp952B1828	aa267461	ESTs, Weakly similar to TIG1_human retinoic acid receptor responder protein 1 [H.sapiens]	2.81
IMAGp952L1821	aa117451	ESTs, Weakly similar to y+L amino acid transporter 1 [R.norvegicus]	-2.62
IMAGp952K0127	aa168457	ESTs, Weakly similar to ZIP-kinase [M.musculus]	2.59
IMAGp952L1859	ai117643, ai151964	ESTs, Moderately similar to glucose inhibited division protein A [Pseudomonas putida]	2.51
IMAGp952A245	w41629	ESTs, Highly similar to NADH-ubiquinone oxidoreductase SGDH subunit precursor [Bos taurus]	2.51
IMAGp952A1547	aa547134, ai505917	baculoviral IAP repeat-containing 6	2.50

[a]: positive means upregulated in HF group while negative means downregulated

IMAGp952F2058 (Transthyretin, TTR) was found in the comparisons of SWR/J Control vs. HF and HF SWR/J vs. AKR/J (Appendix 2), and it was shown upregulated >10 fold by high fat diet.

4.2.1.2 Visual inspection of the filter array image

Each filter image was analyzed using ArrayVision software. All of the candidate genes selected in data analysis I (Table 4.4 and 4.5) were checked to find whether the expression image was affected by neighbor spots, dirt or other biasing effects. Each candidate (in duplicate) was circled both in the control and the HF filter, and the result of the filter image inspection (intensity) was consistent with the data analysis result. Examples are given in Figure 4.7.

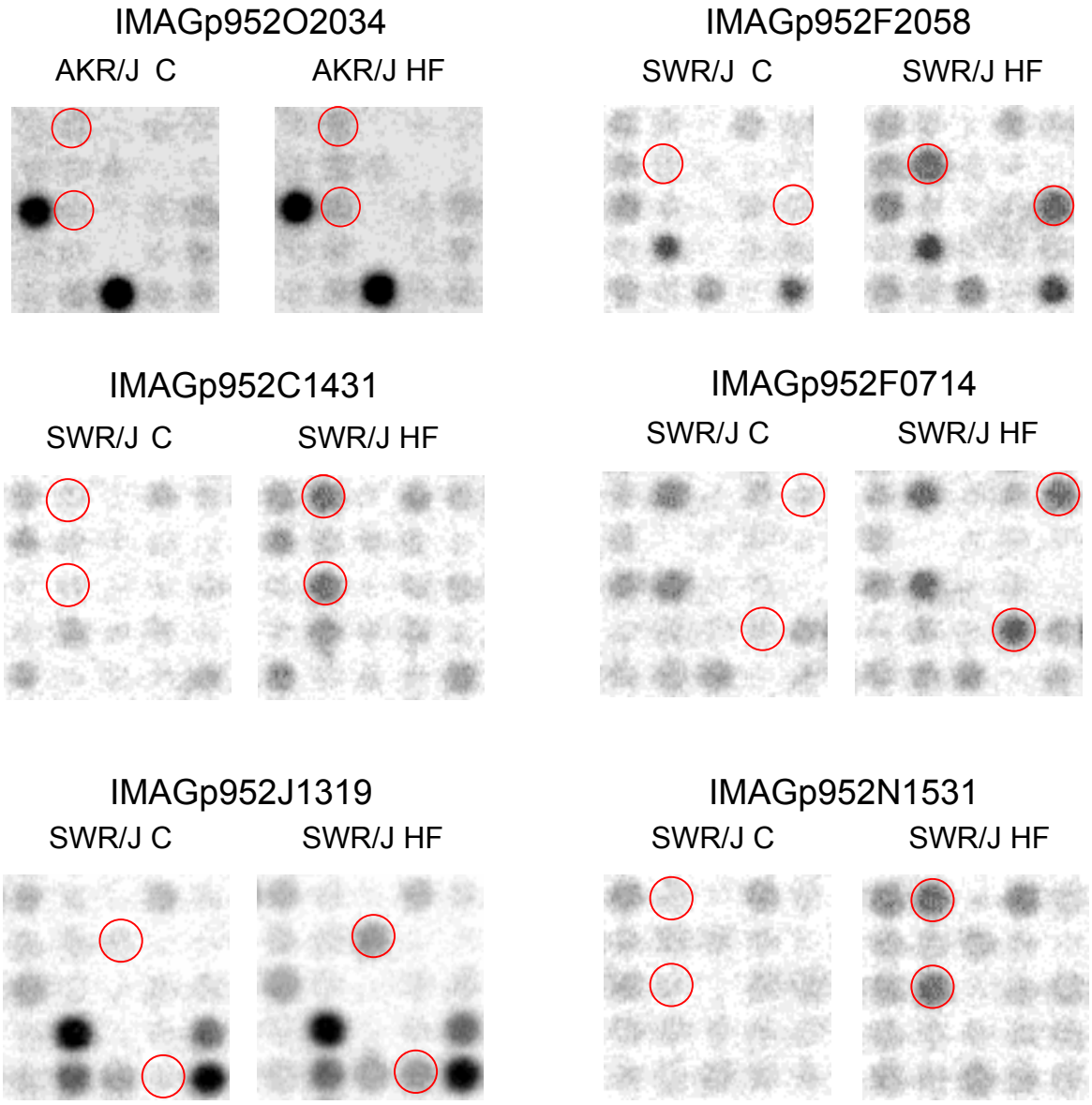

Figure 4.7 Filter image inspections of IMAGp952 O2034, F2058, C1431, F0714, J1319 and N1531. The candidate (in duplicate) was circled both in the control and the HF filter.

4.2.1.3 Northern blot analysis

Two candidates, one from AKR/J Ctrl vs. HF – IMAGp952O2034 (aa289615) and the other one from SWR/J control vs. HF – IMAGp952F2058 (Transthyretin, TTR) were tested on Northern blot analysis loaded with the same RNA as used in the cDNA synthesis for the filter hybridization.

On the filter, IMAGp952O2034 (aa289615) was two fold upregulated in AKR/J HF compared with AKR/J control. However, this result was not confirmed on Northern blot analysis (Figure 4.8). IMAGp952F2058 (Transthyretin, TTR) was > 10 fold upregulated in SWR/J HF compared with SWR/J control but not in AKR/J mice, and this finding was confirmed on Northern blot analysis (Figure 4.9).

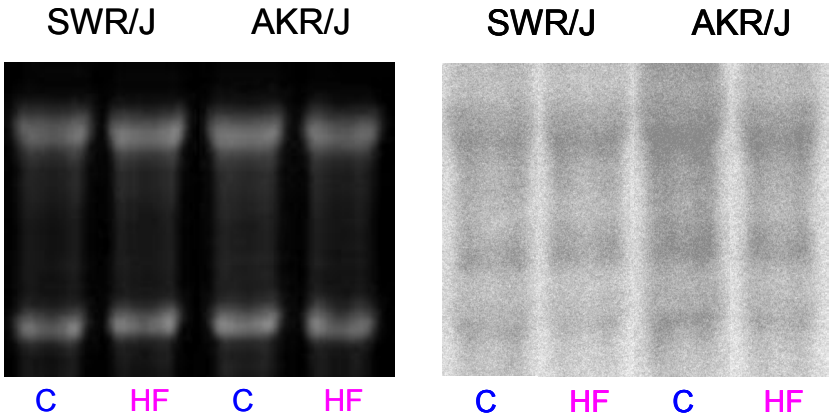

Figure 4.8 IMAGp952O2034 in Northern blot (right) loaded with the same pooled RNA samples as used in the cDNA syntheses for the filter hybridizations. The left is the RNA gel (ethidium bromide staining) used for Northern blotting.

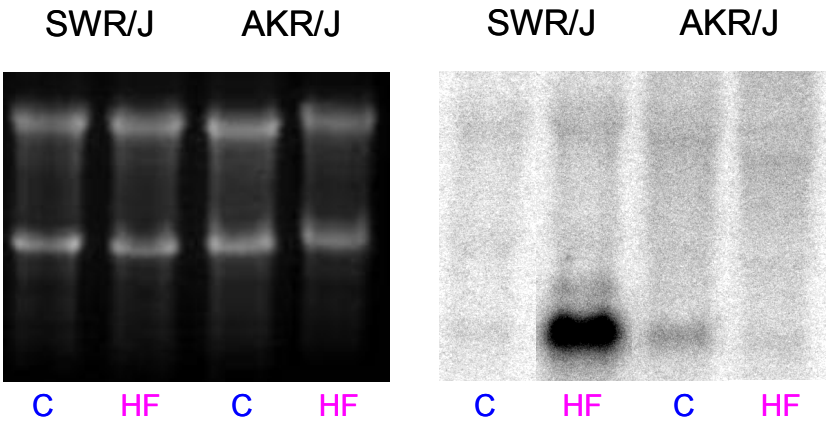

Figure 4.9 IMAGp952F2058 in Northern blot (right) loaded with the same pooled RNA samples as used in the cDNA syntheses for the filter hybridizations. The left is the RNA gel (ethidium bromide staining) used for Northern blotting.

Northern blots loaded with 16 different individual RNA samples were used for further testing of these two candidates. Whereas IMAGp952O2034 (aa289615) (Figure 4.10) was again not confirmed. The expression of IMAGp952F2058 (Transthyretin, TTR) showed a marked variation in different RNA samples (Figure 4.11).

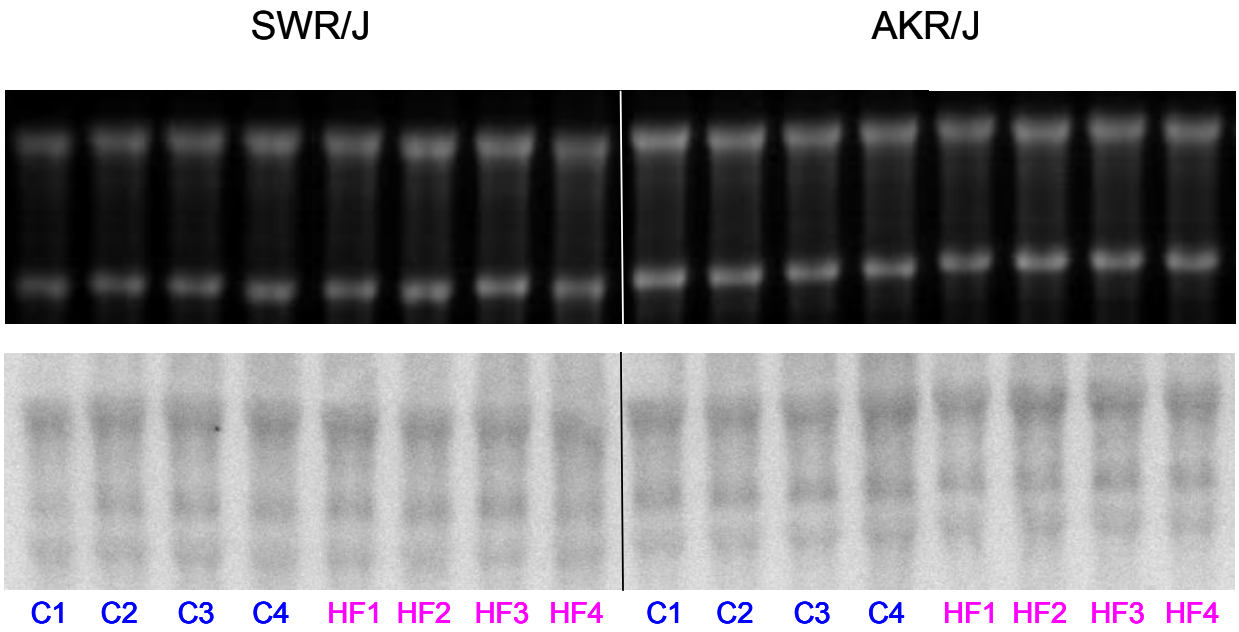

Figure 4.10 Northern blot analysis (with new RNA samples) of IMAGp952O2034. Each lane contains RNA from 4 individual SWR/J or AKR/J mice fed either the control (C1-C4) or the high fat (HF1-HF4) diet. The upper is the RNA gel (ethidium bromide staining) used for Northern blotting.

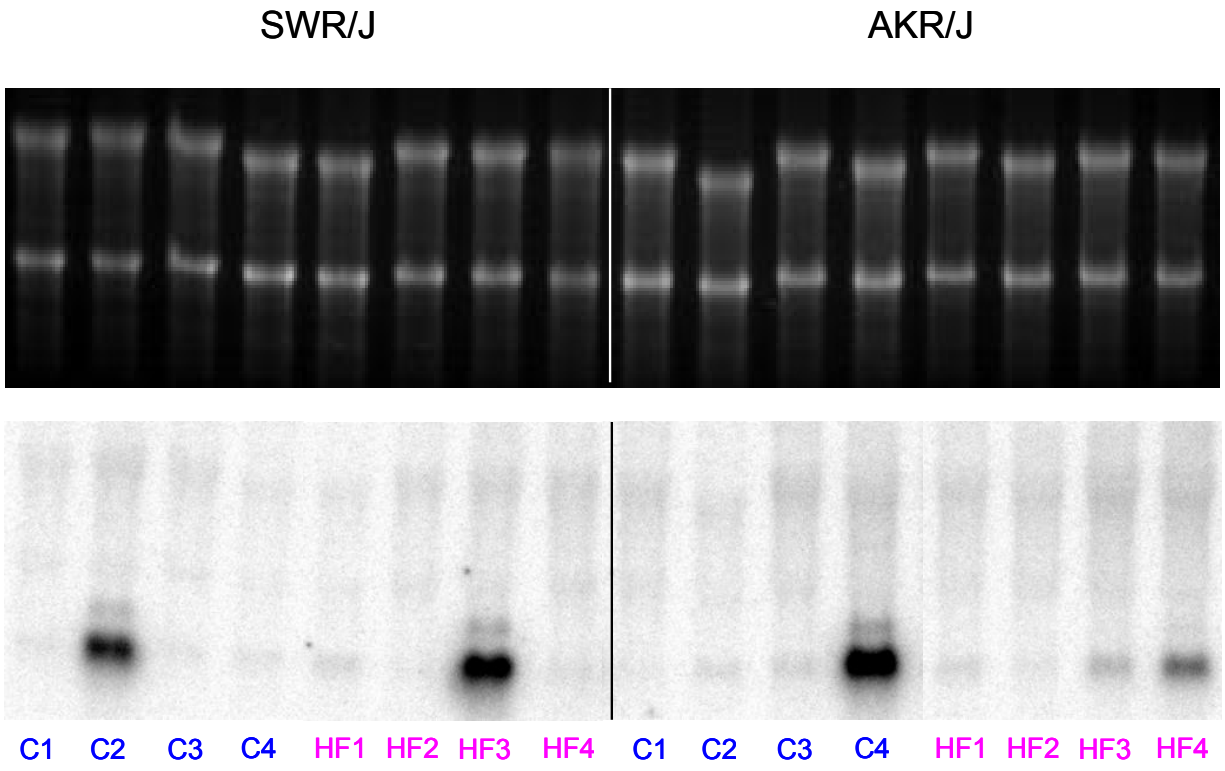

Figure 4.11 Northern blot analysis (with new RNA samples) of IMAGp952F2058. Each lane contains RNA from 4 individual SWR/J or AKR/J mice fed either the control (C1-C4) or the high fat (HF1-HF4) diet. The upper is the RNA gel (ethidium bromide staining) used for Northern blotting.

Another 4 candidates with high fold changes (8 to 13) from SWR/J Ctrl vs. HF were tested by Northern blot analysis (Figure 4.12). The expression patterns were similar to TTR.

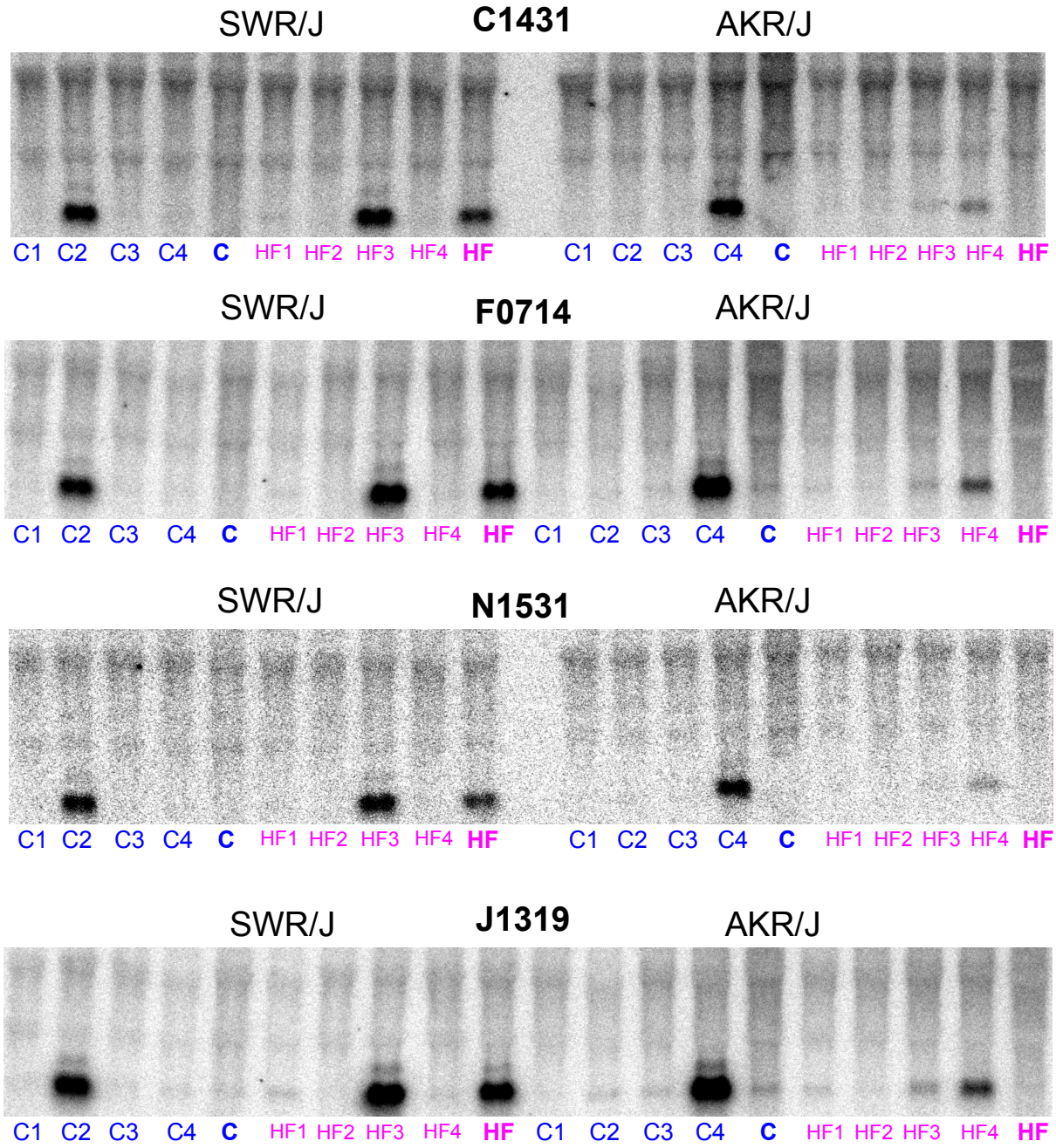

Figure 4.12 Northern blot analyses (with new RNA samples) of 4 different candidates from SWR/J control vs. HF. Each lane contains RNA from 4 individual SWR/J or AKR/J mice fed either the control (C1-C4) or the high fat (HF1-HF4) diet, or the same pooled RNA samples as used in the cDNA syntheses for the filter hybridizations (C or HF).

4.2.1.4 Sequencing

In Table 4.6 the sequencing results of the 6 candidates tested by Northern blot analysis are listed. In RZPD database, these 6 candidates were named differently with different description. However the sequencing results showed that 5 out of the 6 candidates tested are TTR.

Table 4.6 The sequencing results of the 6 candidates tested by Northern blot analysis.

RZPD clone ID	**RZPD description**	**Blast results with commercial sequencing**	**Northern blot analysis**	
			Original RNA Pool	**New RNA from individual mouse**
IMAGp952O2034	aa289615, EST	aa289615, EST	negative	negative
IMAGp952F2058	Transthyretin	Transthyretin	positive	negative
IMAGp952C1431	ESTs, Highly similar to T17338 hypothetical Protein	Transthyretin	positive	negative
IMAGp952F0714	ESTs, Weakly similar to KIAA0672 protein	Transthyretin	positive	negative
IMAGp952J1319	ESTs, Weakly similar to AF161429_1 HSPC311	Transthyretin	positive	negative
IMAGp952N1531	Down syndrome critical region homolog 2	Transthyretin	positive	negative

Negative: the result of Northern blot analysis is not consistent with filter result.

Positive: the result of Northern blot analysis is consistent with filter result.

4.2.1.5 In Situ hybridization

In Situ hybridization (Figure 4.13) showed that Transthyretin (TTR) is localized out side of the hypothalamus – dosal 3rd ventricle and the lateral ventricle, both in AKR/J and SWR/J mice.

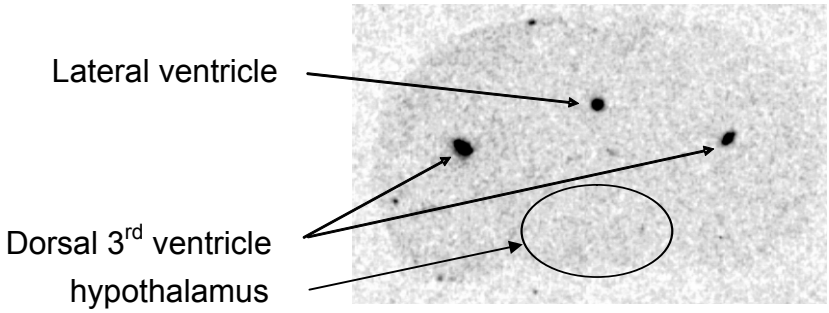

Figure 4.13 Representative in situ hybridization image demonstrating the expression of TTR (trsnsthyretin) in the mouse brain. A section from an AKR/J / SWR/J muse is shown. The hypothalamus is circled.

4.2.2 Data analysis II

4.2.2.1 Array hybridization

The 17 selected candidates are listed in Table 4.7 and 4.8. The majority of candidates (13 out of 17) emerged from the interstrain comparison.

Table 4.7 Number of candidates in different comparison groups from data analysis II

Comparison group		**Number of candidates**
AKR/J	Control vs. HF	2
SWR/J	Control vs. HF	2
Control	AKR/J vs. SWR/J	10
HF	AKR/J vs. SWR/J	3

Table 4.8 List of candidates from data analysis II (Part I-IV)

Part I – AKR/J control vs. HF:

GenBank accession number	**RZPD Clone ID**	**Affy ID**	**Blast result**	**Filter fold change[a]**	**Chip fold change[a]**
ai119403, ai131627	IMAGp952 J2454	93797_g_at	Atp1a1 ATPase, Na+/K+ transporting, alpha 1 polypeptide	-1.80	1.25
w91276	IMAGp952 B0812	160289_s_at	Mm.29482, 1110019C08Rik	-2.04	-1.14

[a]: positive means upregulated in the HF group while negative means downregulated

Part II – SWR/J control vs. HF:

GenBank accession number	**RZPD Clone ID**	**Affy ID**	**Blast result**	**Filter fold change[a]**	**Chip fold change[a]**
ai196320	IMAGp952 J0157	162274_f_at	Lisch7-pending liver-specific bHLH-Zip transcription factor	-2.10	-1.27
aa607542	IMAGp952 L2249	97989_at	similar to gb:M29551 protein phosphatase 2b, catalytic subunit 2 (human); mRNA sequence	2.15	1.16

[a]: positive means upregulated in the HF group while negative means downregulated

Part III – AKR/J control vs. SWR/J control:

GenBank accession number	RZPD Clone ID	Affy ID	Blast result	Filter fold change[a]	Chip fold change[a]
aa413119	IMAGp952A1740	93721_at	Cap1 adenylyl cyclase-associated CAP protein homolog 1 (S. cerevisiae, S. pombe)	2.03	1.32
aa036456, ai323372, ai325380	IMAGp952H2117	93630_at	CUGBP1 CUG triplet repeat, RNA binding protein 1	-2.07	-1.20
aa009082	IMAGp952C2231	94522_at	Dctn3 dynactin 3	-2.02	-1.36
w75791	IMAGp952L059	98525_f_at	similar to edr erythroid differentiation regulator	2.39	4.29
aa475583	IMAGp952K0643	100494_at	Fgf1 fibroblast growth factor 1	-2.44	-1.20
ai097693, ai118254	IMAGp952J2356	93269_at	Glo1 glyoxalase 1	-2.44	-1.88
ai119514, ai158857	IMAGp952K1155	93269_at		-2.11	-1.88
ai196289, ai196587	IMAGp952P0557	93269_at		-2.58	-1.88
ai413558, "w34034"	IMAGp952B243	162457_f_at	Hba- α1 hemoglobin alpha, adult chain 1	2.01	1.64
aa052364	IMAGp952H105	96667_at	Mm.7418, Ppp2cb protein phosphatase 2a, catalytic subunit, beta isoform	2.23	1.32
aa473963	IMAGp952A2437	95508_at	Nckap1 NCK-associated protein 1	-2.02	-1.65
aa509365	IMAGp952L2441	101024_i_at	Skp1a S-phase kinase-associated protein 1A	-2.65	-1.32

[a]: positive means upregulated in the SWR/J group while negative means downregulated

Part IV – AKR/J HF vs. SWR/J HF:

GenBank accession number	**RZPD Clone ID**	**Affy ID**	**Blast result**	**Filter fold change[a]**	**Chip fold change[a]**
w97978	IMAGp952 L0912	101102_at	Igbp1 immunoglobulin binding protein 1	3.76	1.22
aa146387, ai326750, ai528541	IMAGp952 P2126	162137_f_at	Txk TXK tyrosine kinase	-2.48	-1.16
aa030192, ai430809, ai509123	IMAGp952 O0316	102002_at	Ubqln2 ubiquilin 2	2.23	1.24

[a]: positive means upregulated in the SWR/J group while negative means downregulated

From this list, Hba-α1 and Glo1 were selected according to the fold change in filter and chip for further experiments. Although the fold change of candidate edr (w75791) is high in both arrays the blast result is not satisfactory so that it was not selected.

4.2.2.2 Visual inspection of the filter array image

The expression patterns of Hba-α1 (hemoglobin alpha, adult; IMAGp952B243) and Glo1 (glyoxalase 1; IMAGp952J2356, K1155 and P0557) were confirmed by filter image inspections (Figure 4.14).

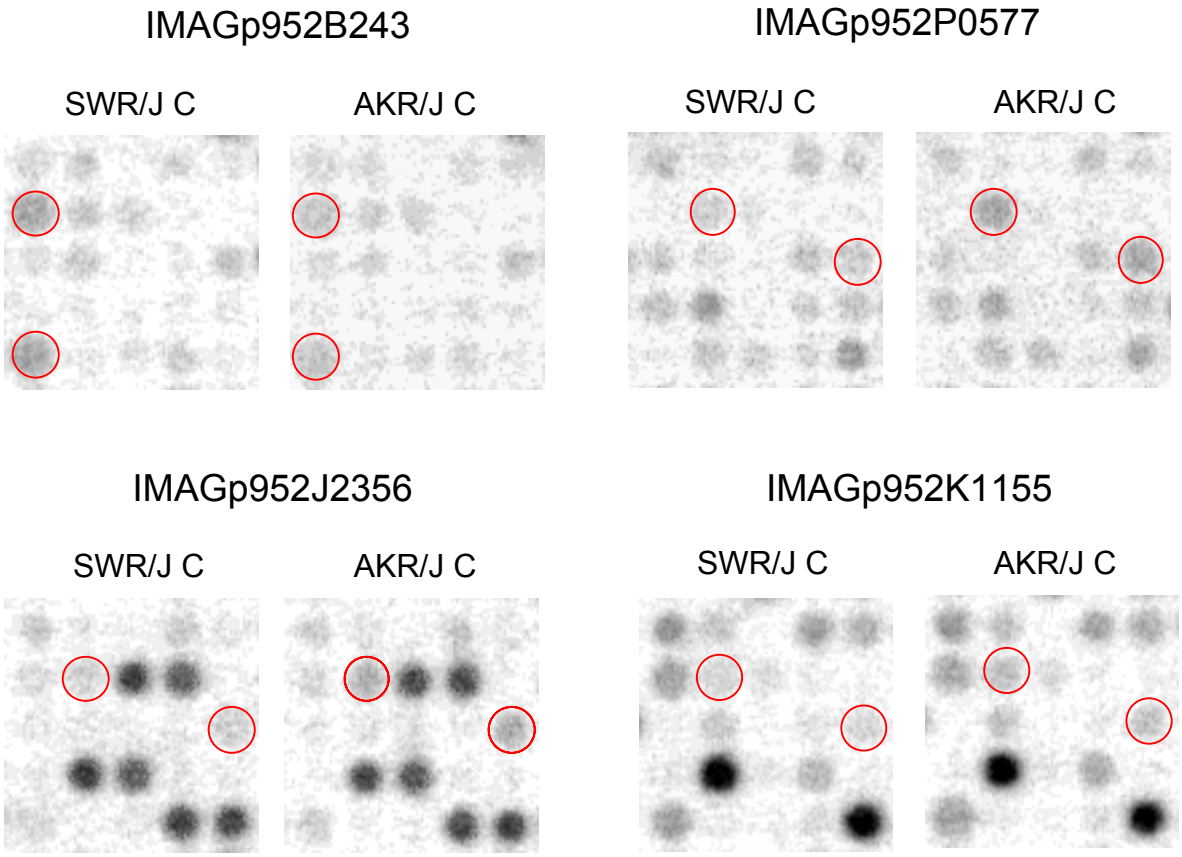

Figure 4.14 Filter image inspections of IMAGp952B243, P0577, J2356 and K1155. The candidate (in duplicate) was circled both in SWR/J and AKR/J control filter.

4.2.2.3 Northern blot analysis of Glo1

The higher array Glo1 RNA expression level in AKR/J mice was confirmed by Northern blot analysis (Figure 4.15). Within strains, there was no difference in Glo1 expression, i.e., Glo1 was not affected by diet. Because of sample limitation, only Glo1 was tested on Northern blot analysis.

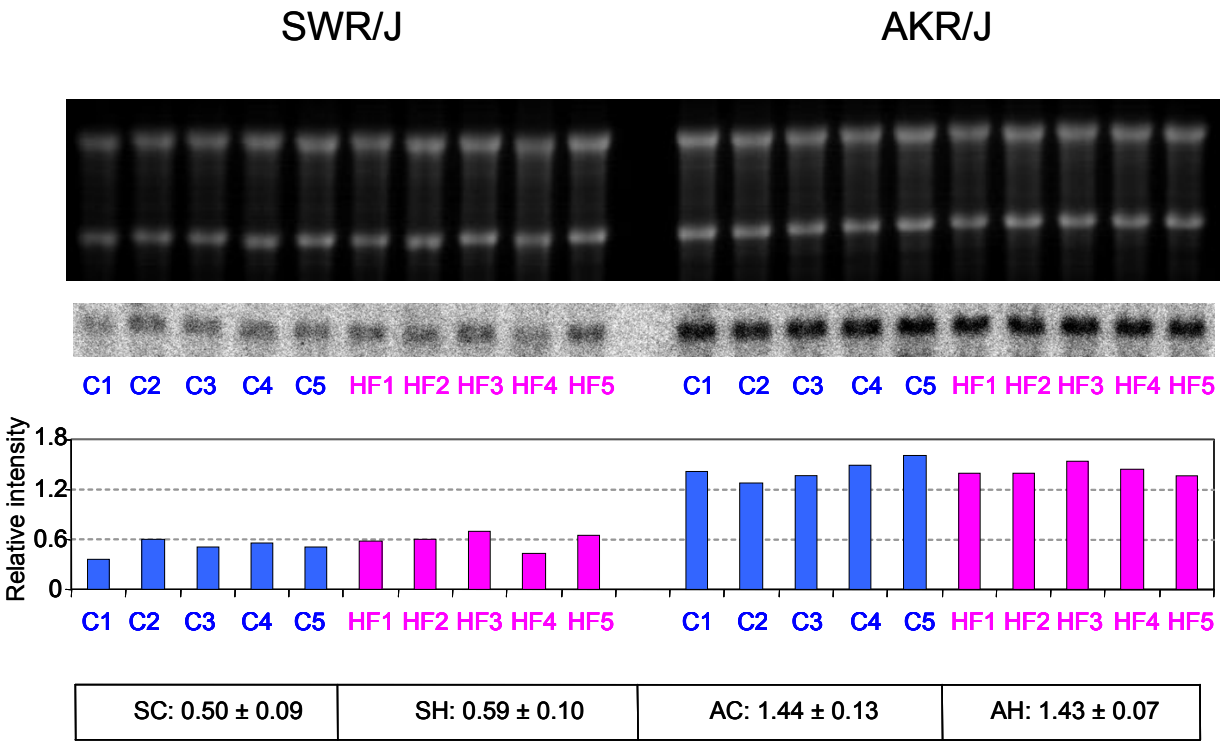

Figure 4.15 Hypothalamic Glo1 mRNA expression in individual SWR/J and AKR/J mice fed either control or HF diet (n = 5 per group). Bars indicate the expression of relative signal intensity of each band. Data indicate signal intensity mean ± SD for each group. The difference in Glo1 expression between strains is significant ($P < 0.001$), but not within strains.

4.2.2.4 PCR

PCR was performed with gene-specific primers designed for 8 selected candidates. Only one was consistent with the array result (Ppp2cb) but the difference was not significant and the fold change (1.16 in PCR) was lower than in array (2.15 in filter and 1.16 in chip). Two candidate genes showed regulation in the opposite direction and five showed high individual variation but no systematic effect of strain or diet. Glo1 was not confirmed in this normal RT-PCR, however, it was confirmed in real time RT-PCR.

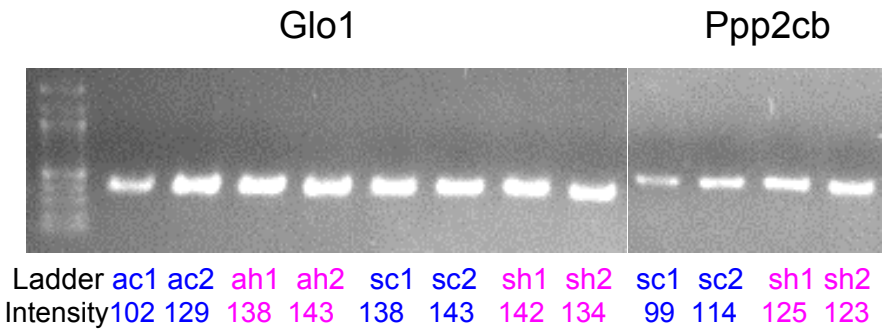

Figure 4.16 RT-PCR analysis of candidates selected from array data analysis II. Band intensity was analyzed by Image station (Kodak). Glo1 showed slightly downregulated in ac compared with sc. Ppp2cb was consistent with the array result, but the fold change is lower in PCR (1.16) and the difference was not significant. ac: AKR/J control, sc: SWR/J control, ah: AKR/J high fat, sh: SWR/J high fat.

4.2.2.5 In Situ hybridization

In Situ hybridization of Hba-α1 (Figure 4.17) showed that the expression of Hba-α1 is not restricted to the hypothalamus but the signals are almost randomly distributed all over the brain. A hotspot of Hba-α1 expression appears to be in the region of dorsal 3rd ventrile and supraoptic nucleus. In general SWR/J mice have a higher Hba-α1 expression than AKR/J both inside and outside the hypothalamus. In contrast, Glo1 shows a very district pattern of expression preferably in the hippocampus (Figure 4.18). In the hypothalamus, Glo1 expression indicates in the arcuate nucleus (ARC), ventromedial hypothalamic nucleus (VMH) and paraventricular hypothalamic nucleus (PVN). Whereas the expression of Glo1 outside the hypothalamus is similar in both strains, Glo1 mRNA expression in the hypothalamus is much stronger in AKR/J compared to SWR/J mice. In situ hybridization therefore qualitatively confirms the results by array experiments with respect to Glo1 and Hba-α1.

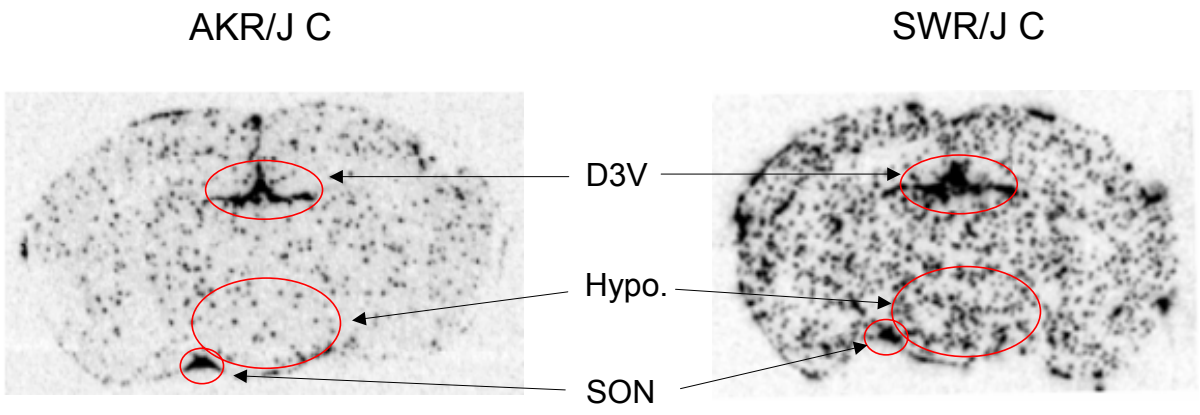

Figure 4.17 Representative image of Hba-α1 mRNA expression in the mouse brain by in situ hybridization. Hba-α1 is distributed all over the brain and its overall expression is higher in SWR/J than in AKR/J mice. D3V: dosal 3rd ventricle, Hypo.: hypothalamus, SON: supraoptic nucleus.

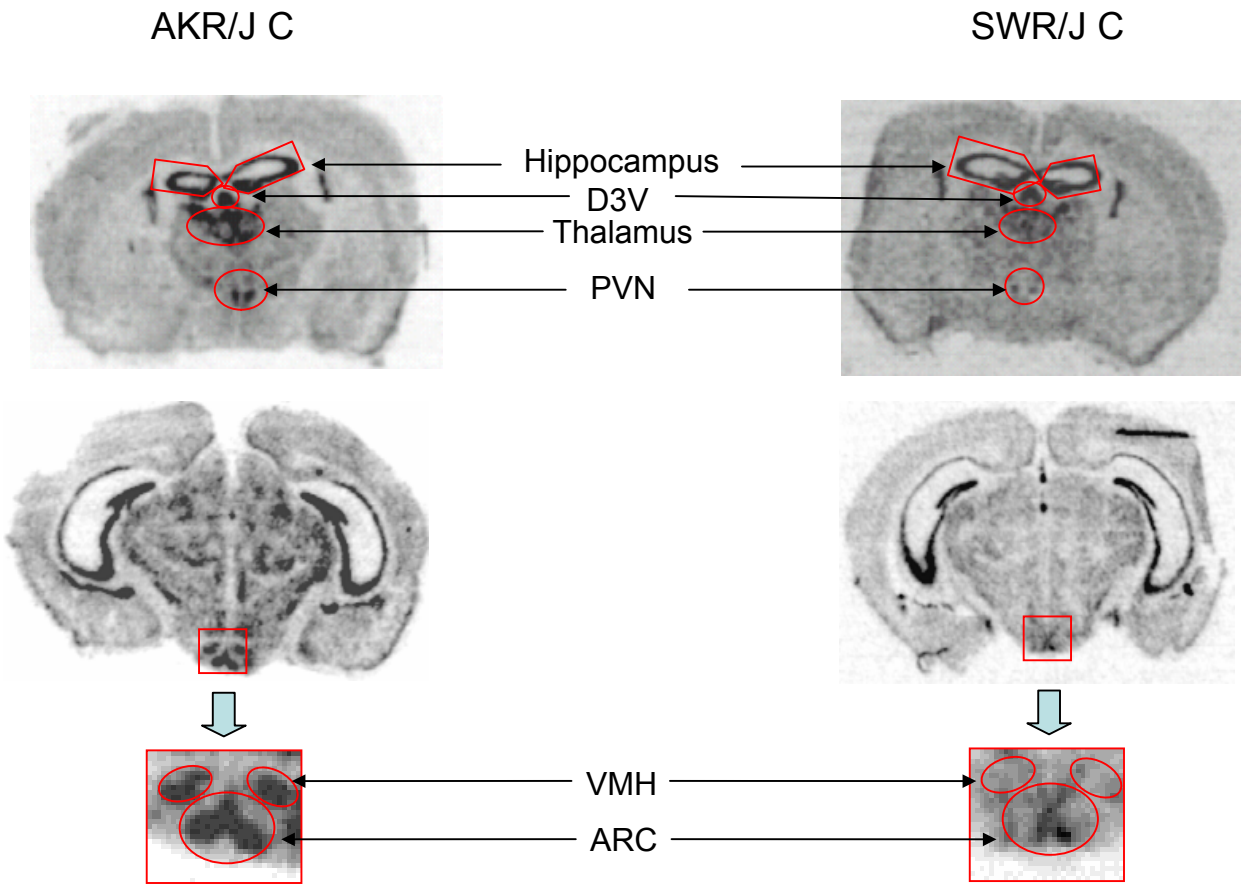

Figure 4.18 Representative image of Glo1 mRNA expression in the mouse brain by in situ hybridization. In the hypothalamus, Glo1 is expressed in the ARC, VMH and PVN, and its hypothalamic expression is higher in AKR/J compared to SWR/J mice.

4.2.2.6 Alignment of hemoglobin and neuroglobin gene sequences

Hemoglobin in the erythrocyte is produced from bone marrow. It is surprising to find hemoglobin expressed in the brain. There are several members in the globin family – hemoglobin, myoglobin and neuroglobin. To check the similarity of sequences between neuroglobin (which localizes in the brain) and hemoglobin probe which was used for in situ hybridization, alignment analysis was carried out and it showed only 42% similarity (Figure 4.19).

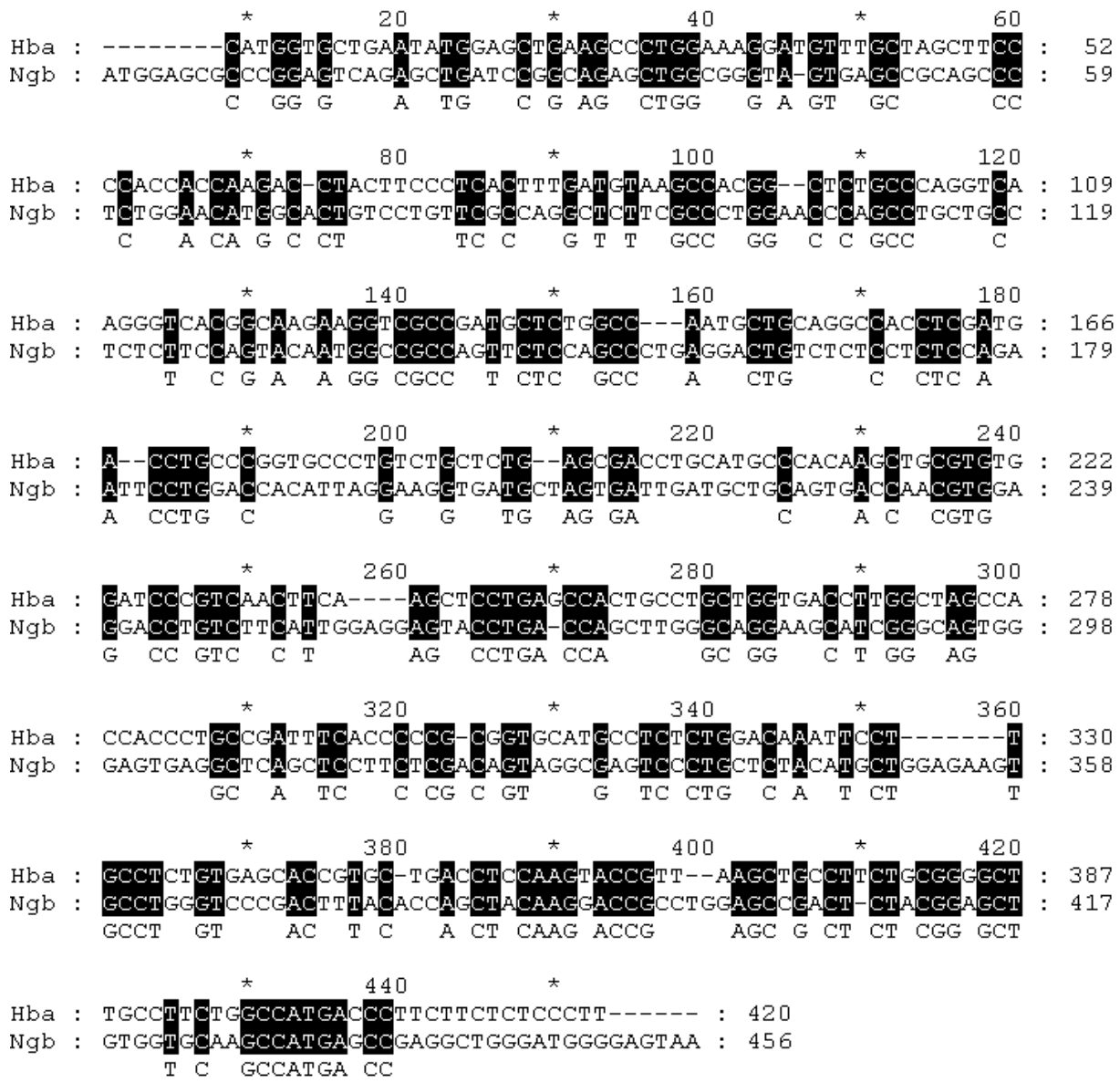

Figure 4.19 Sequence alignment of neuroglobin and hemoglobin probe which was used for in situ hybridization. Positions with identical nucleotides are drawn against a black background. Dashes represent deletions in the sequence of haemoglobin relative to neuroglobin.

4.2.3 Data analysis III

Focused on diet induced genes, new candidates were selected only from filter data and then 11 clones were ordered from RZPD. 5 of them were verified in Northern blot analysis but only one was confirmed (Table 4.9), which was also confirmed in the filter image inspection (Figure 4.20). Only the positive Northern blot is shown in Figure 4.21, other blots not shown.

Table 4.9 list of data analysis III

GenBank accession number	RZPD Clone ID	Comparison group[a]	Blast result	Fold change[b]	Northern blot analysis[c]
aa451138, ai481012	IMAGp952A0241	ACH	high mobility group AT-hook 2, pseudogene 1	-2.16	
aa051449	IMAGp952J2019	ACH	intestinal cell kinase	-1.99	N
aa451434	IMAGp952G1341	ACH	map2k7 mitogen activated protein kinase kinase 7	-1.52	
aa869362	IMAGp952A1851	ACH	tumor necrosis factor, alpha-induced protein 1 (endothelial)	1.97	P
w41719	IMAGp952B225	SCH	asparaginyl-tRNA synthetase	-2.28	
aa511409	IMAGp952D2441	SCH	glutaminase	-2.73	O
ai385680, ai893963, w79980	IMAGp952M2410	SCH	GPC4 glypican 4	-3.80	N
aa537148	IMAGp952A1947	SCH	laminin, alpha 5	-2.61	O
aa269563	IMAGp952C0733	SCH	RIKEN hypothetical protein	-3.75	
aa546545	IMAGp952C2147	SCH	Thrap6-thyroid hormone receptor associated protein 6 or hypothetical protein	-2.09	
aa451295	IMAGp952A1941	SCH	ubiquitin-like 3	-2.71	

[a]: ACH means AKR/J control vs. HF; SCH means SWR/J control vs. HF

[b]: negative means downregulated in HF

[c]: N means no difference between two groups; P means positive; O means not detectable.

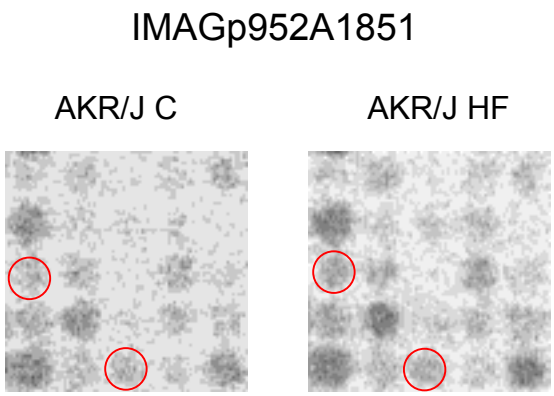

Figure 4.20 Filter image inspection of TNFAIP1. The candidate (in duplicate) was circled both in control and HF filter.

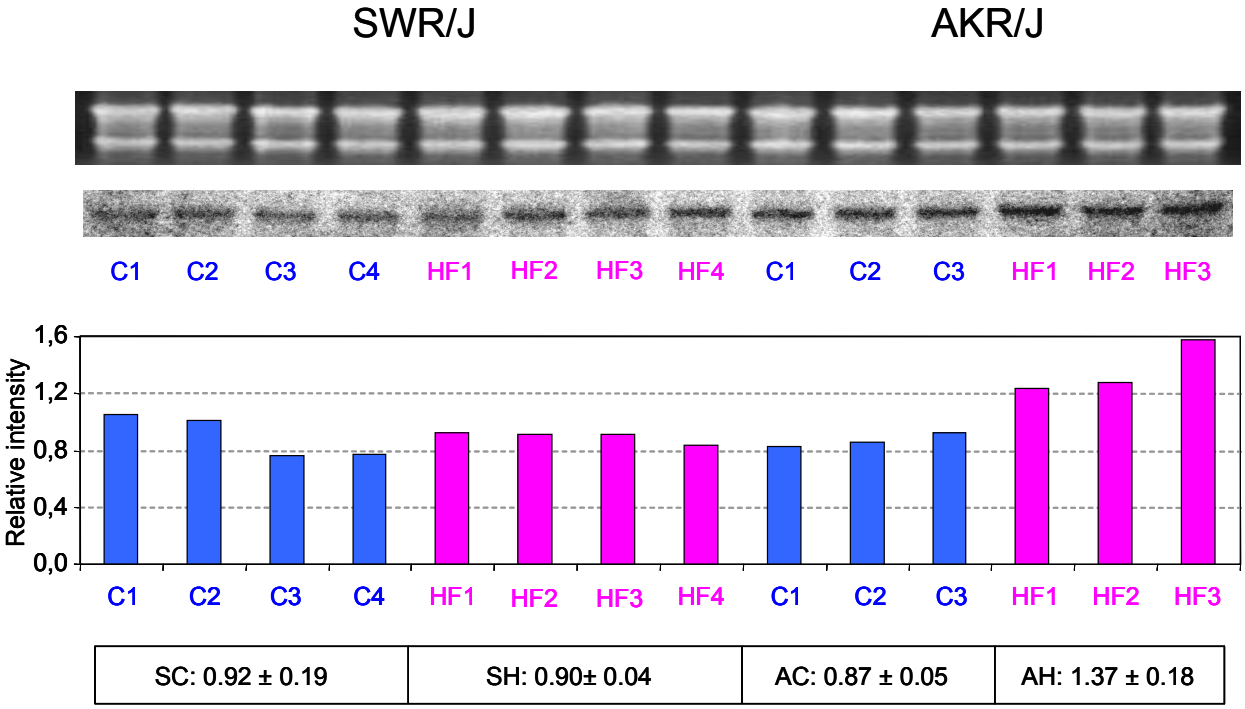

Figure 4.21 TNFAIP1 mRNA expression in individual SWR/J and AKR/J mice fed either control or HF diet (n = 3-4 per group). Bars indicate the relative signal intensity of each band and the data indicate signal intensity mean ± SD for each group. There is a significant difference in TNFAIP1 expression between HF and control mice in AKR/J, but not in SWR/J.

In Situ hybridization shows that TNFAIP1 localizes in the arcuate nucleus, the ventromedial hypothalamic nucleus and the paraventricular hypothalamic nucleus (Figure 4.22). Quantification of TNFAIP1 expression in the hypothalamic region was performed using

Image-Pro Plus (Media Cybernetics). Although it showed 1.6 fold upregulation in the ARC by high fat diet, this difference was not significant because of the individual variation (Figure 4.22), further experiment with more samples should be carried out to confirm this conclusion.

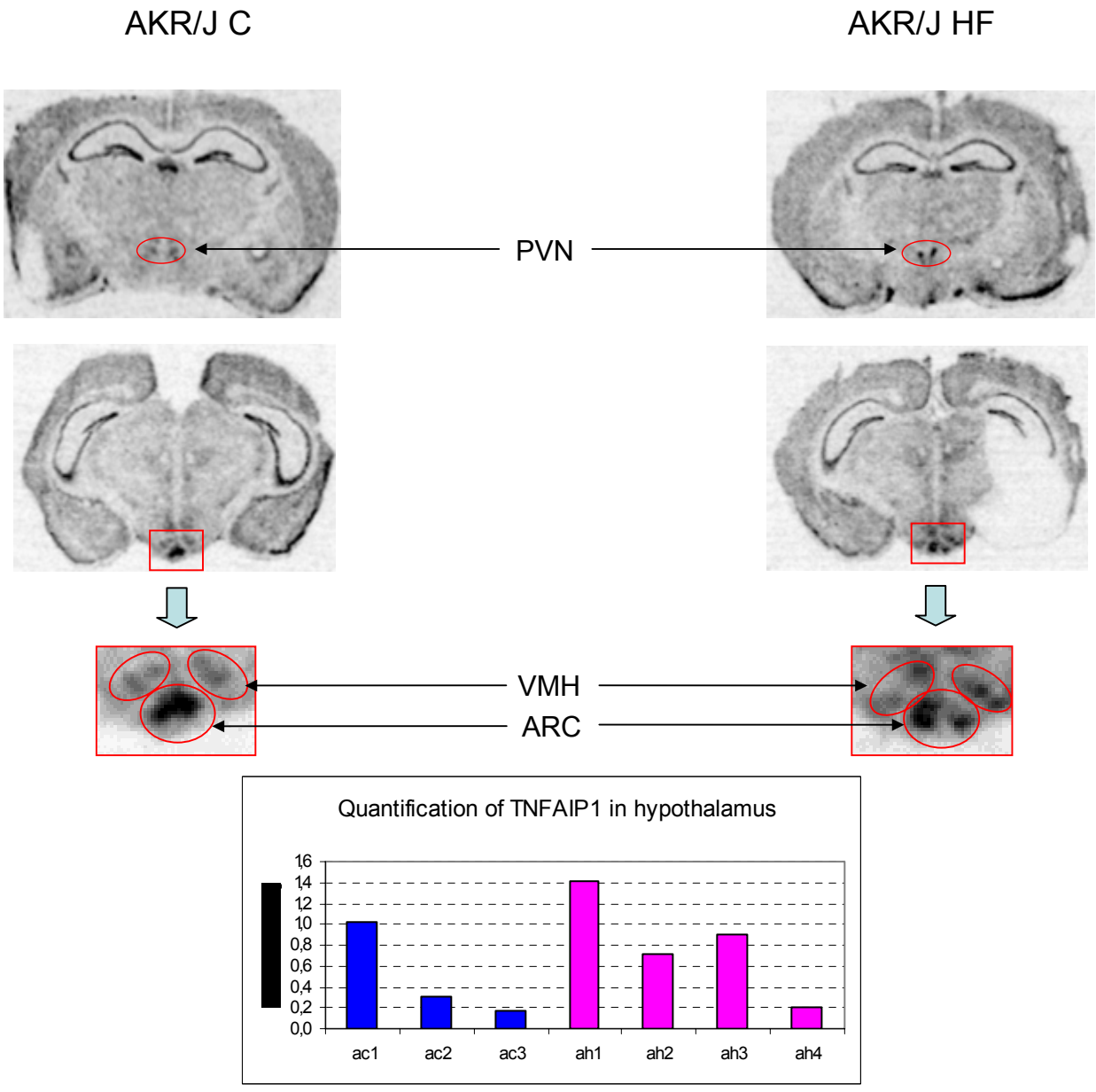

Figure 4.22 representative image of TNFAIP1 mRNA expression in the mouse brain by in situ hybridization and its quantification analysis. In the hypothalamus, TNFAIP1 is expressed the ARC, VMH and PVN. Bars indicate relative signal intensity of TNFAIP1 expression in each hypothalamus. ac: AKR/J control, ah: AKR/J high fat.

4.2.4 Real-time RT-PCR

A real-time RT-PCR trace for 32 wells on a 96-well plate is shown in Figure 4.23. The threshold was defined by the software in the region associated with an exponential growth of PCR product. The point at which the fluorescence crosses the threshold is called the Ct value which is inversely proportional to the logarithm value of starting amount of target DNA.

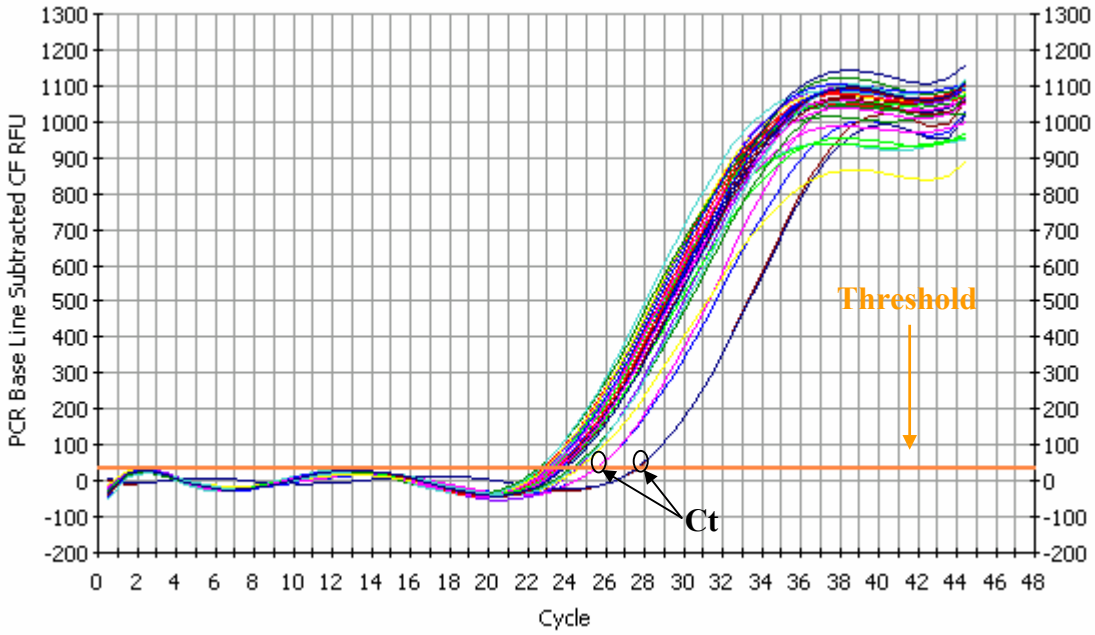

Figure 4.23 A real-time RT-PCR trace for 32 wells on a 96-well plate. Cycles are shown along the X-axis, and background corrected arbitrary fluorescence units are shown on the Y-axis. The real-time RT-PCR traces are indicated with different colors. The orange horizontal line indicates the threshold. CF RFU: curve fit relative fluorescence units; Ct: threshold cycle.

The real-time RT-PCR standard curve is shown in Figure 4.24. The standard curve is generated from a dilution series (1, 1:4, 1:16, 1:64) of cDNA. From the standard curve, PCR efficiency was calculated and relative values for the respective target gene in each experimental and control sample were extrapolated.

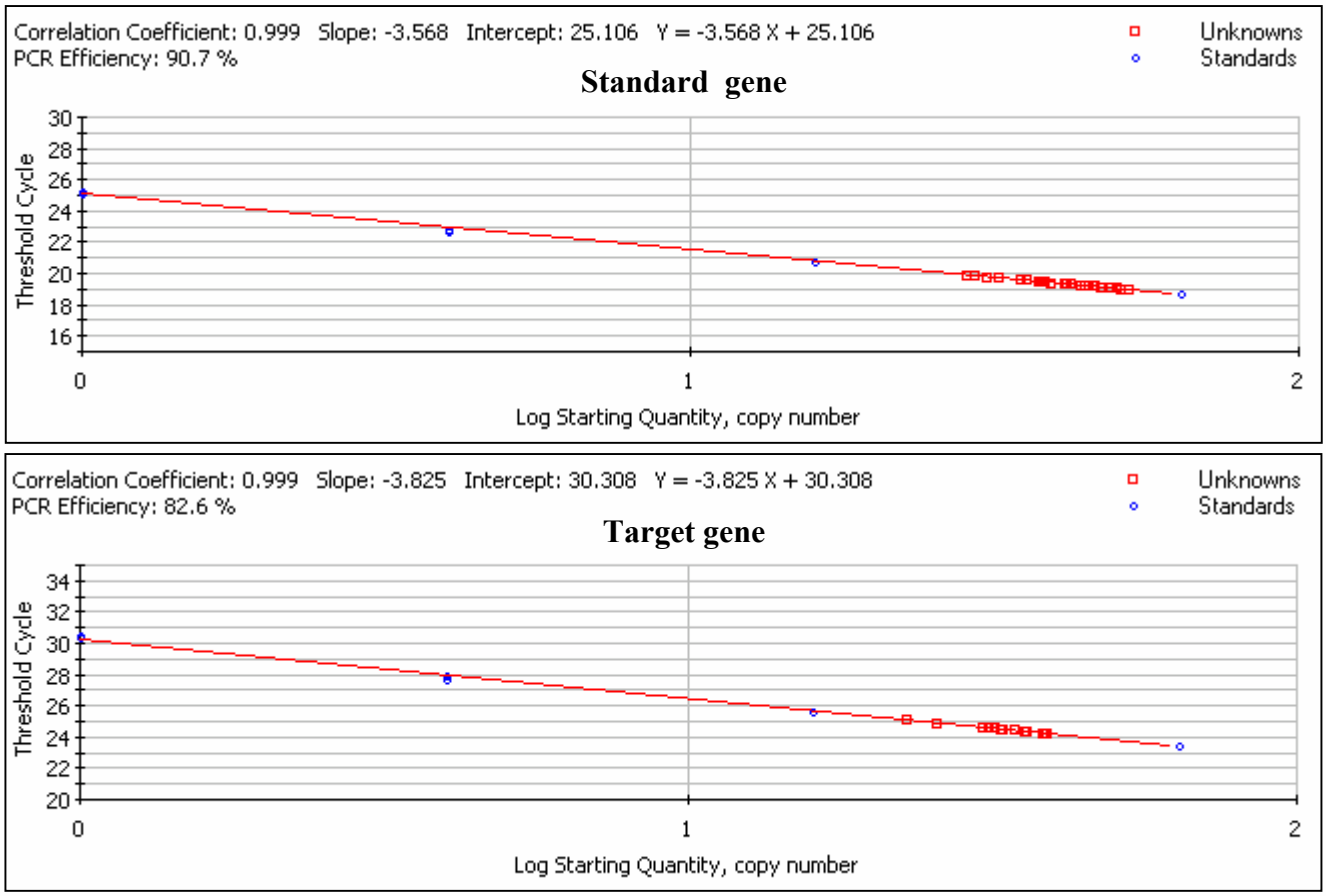

Figure 4.24 Real-time RT-PCR standard curve. Cycles (○) indicate the duplicates of 4 dilutions (1, 1:4, 1:16, 1:64) and squares (□) indicate the duplicates of unknown samples.

Four candidate genes were tested in real-time RT-PCR. The relative value was the normalized data which was derived from the mean of target gene starting quantity (SQ) divided by the mean of corresponding beta actin SQ. However, only strain specific genes – Glo1 and Hba-α1 were found significantly differentially expressed between strains. No significant difference was found for diet-induced genes – Ppp2cb and TNFAIP1 between the control and high fat diet groups within strains (Figure 4.25).

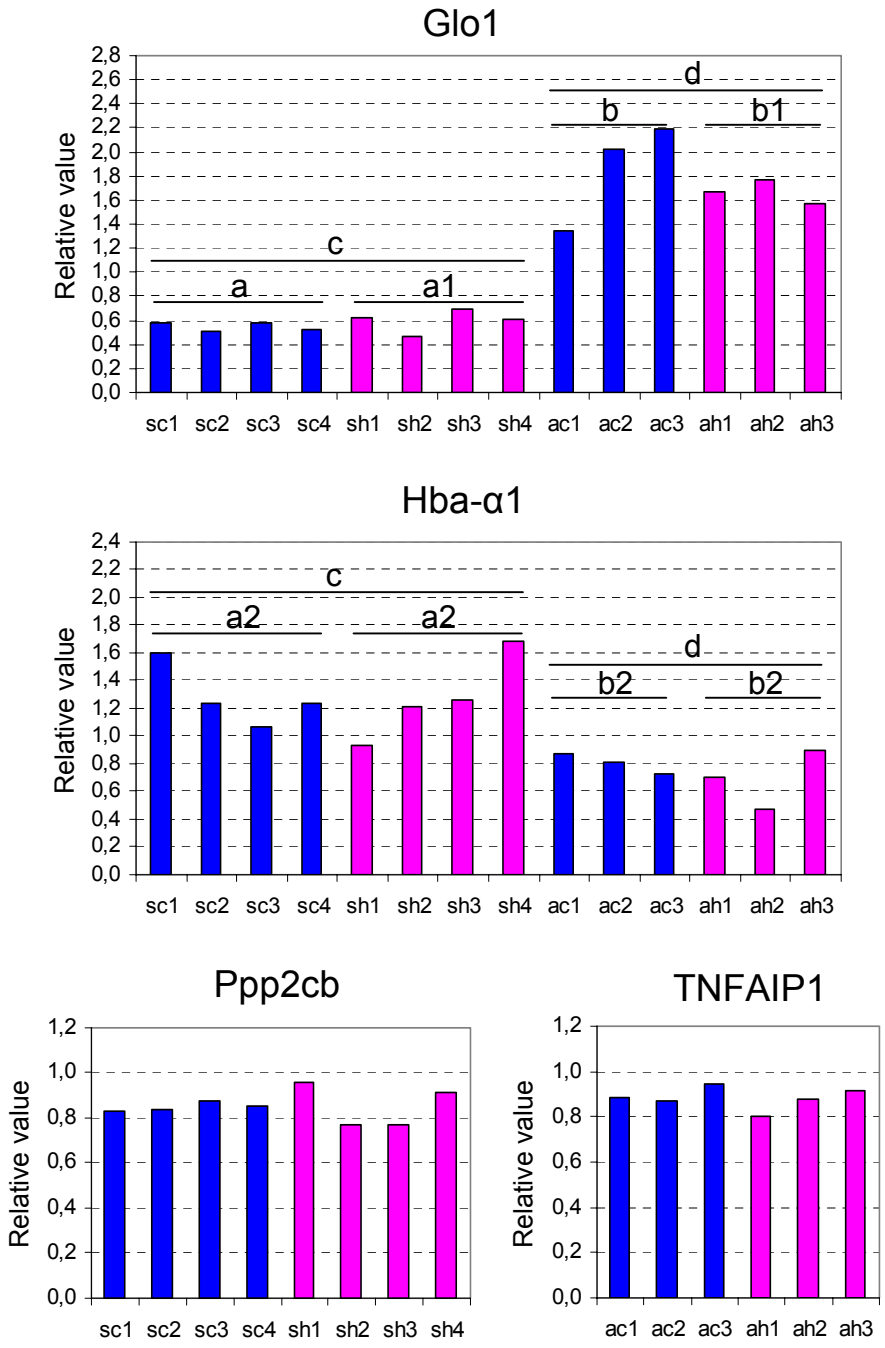

Figure 4.25 Real-time RT-PCR analyses of 4 candidate genes. Bars indicate relative value of candidate gene in individual animal sample. Strain specific genes – Glo1 and Hba-α1 were found significantly differentially expressed between strains, whereas diet-induced genes – Ppp2cb and TNFAIP1 were found no difference within strains. $P^{a2-b2} < 0.05$, $P^{a-b} < 0.01$, P^{a1-b1} and $P^{c-d} < 0.001$. sc: SWR/J control, sh: SWR/J high fat, ac: AKR/J control, ah: AKR/J high fat.

4.3 SNP analysis of gene Glo1

Kathrin Reichwald (IMB, Jena) resequenced the Glo1 gene and revealed several sequence variations in non-coding and coding regions by SNP analysis (Table 4.10). The reference DNA sequence (rc.mm.Glo1.genomic.040120, 24665 bp) used in SNP analysis consists of 19665 bp of Glo1 gene and twice 2500 bp of upstream and down stream sequences. Furthermore, the online program – Match™ at www.gene-regulation.com was used to search different potential binding sites for transcription factors due to the single nucleotide polymorphism between AKR/J and SWR/J strains. Some transcription factor binding sites are changed by the nucleotide exchange, which is shown different between these strains.

Table 4.10 SNP analysis of Glo1 gene in AKR/J and SWR/J

	5' upstream region						**Exon 1**	**Intron 1**	**Exon3**		**Intron 5**	
Position in the genomic DNA	858	925	1057	1374	1601	2158	2485	2732	14878	14882	18737	20730
Sequence in reference DNA	C	A	M	G	A	C	G	A	T	G	G	G
Sequence in AKR/J	M	M	M	AA	AA	C/T	GG	AA	CC	GG	GG	TT
Position in AKR/J sequence	857	923	1055	1372	1599	2156	2483	2730	14876	14880	18735	20728
Sequence in SWR/J	M	M	CC	GG	M	CC	CC	TT	CC	AA	AA	TT
Position in SWR/J sequence	857	923	1056	1373	1599	2156	2483	2730	14876	14880	18735	20728
Transcription factor bound	ND	ND	ND	ND	ND	B1	ND	B2	ND	B3	B4	ND

M: insertion or deletion; AA: homozygote; CT: heterozygote; ND: no difference; B1: T bind s c-Ets-1(p54) and FOXD3; B2: A binds CHOP-C/EBPalpha; B3: G binds GATA-1, -2 and -X; B4: G binds HNF-4 and Oct-1, A binds HNF-1 and Pax-4.

5 Discussion

5.1 Diet experiment

In this study, two different diets – a standard control diet and a high fat diet, and two different inbred mouse strains –AKR/J and SWR/J – were applied to investigate the effect of diet-induced obesity on hypothalamus gene expression. The energy from the high fat diet is mainly derived from fat, whereas > 50% of the energy in the control diet comes from carbohydrates. AKR/J and SWR/J mice represent a useful model for diet research because of their differential response to HF feeding. AKR/J mice prefer HF and are prone to obesity, and on the contrary, SWR/J mice prefer carbohydrates and are obesity resistant. (Bachmanov *et al.*, 2002;Prpic *et al.*, 2002;Smith *et al.*, 1997;Smith *et al.*, 1999;Smith *et al.*, 2000;Smith *et al.*, 2001).

5.1.1 Body mass and body fat

On given the high fat diet, AKR/J mice increased their body mass rapidly within the first 1-2 days, after which, body mass increased at a stable level, similar to control mice. After 10 days on the diet experiment, both female and male AKR/J mice fed the high fat diet were significantly heavier than the control groups. In contrast, SWR/J mice showed no difference in body mass between the high fat diet and the control groups (Figure 4.1).

Not only body mass but also body fat (body fat mass and body fat percentage) in the AKR/J high fat groups was higher than in the control groups (Figure 4.3). Compared with the control group, the AKR/J high fat diet group had lighter body lean mass (Figure 4.4). This suggests that the increase of body mass in AKR/J high fat diet feeding group was primarily due to an increase in body fat content, This was reflected in the white adipose tissue depots (inguinal and retroperitoneal), which were larger in the AKR/J high fat groups compared with the control groups. Similar results were obtained by Prpic *et al.* in a 4-week high fat diet experiment (Prpic *et al.*, 2002) and also by West *et al*. in a 7-week high fat diet experiment (West *et al.*, 1992). Moreover, fat distribution also showed difference between strains. Originally, AKR/J mice had smaller inguinal fat pad and similar retroperitoneal fat pad compared with SWR/J mice. After 10 days on high fat diet, because both were significantly increased only in AKR/J mice, inguinal fat pad became similar in two strains and retroperitoneal fat pad was larger in AKR/J

than in SWR/J mice. The difference of regional fat distribution may also a phenotype in DIO model.

5.1.2 Energy intake

In the present 10-day diet experiment, energy intake in both strains was significantly higher in the high fat diet groups than in the control groups (Figure 4.2), which is consistent with the report of Smith *et al.* (Smith *et al.*, 1999), but is different from the results shown in other studies where only AKR/J mice exposed to high fat diet took more energy but not SWR/J mice (Prpic *et al.*, 2002;West *et al.*, 1992).

The reason for this difference could be the different exposure time to high fat diet feeding. Ziotopoulou *et al.* reported that significant difference of energy intake between high fat and low fat feeding groups appeared on day 2 but disappeared on day 7, and then again appeared on day 14 (Ziotopoulou *et al.*, 2000). This was also supported by West *et al.*, who reported that some high fat diet groups consumed significantly more energy than the controls only in the first week but not in the following 7 weeks (West *et al.*, 1992). It is also possible that the behavior of the same mouse strain in different laboratories is different even if the equipment, test protocols and many environmental variables are rigorously standardized (Crabbe *et al.*, 1999).

5.1.3 Energy expenditure

Different genetic background results in the different phenotype between these two strains. The observation that the high fat groups in both SWR/J and AKR/J strains consumed more energy but only AKR/J mice became obese suggests that SWR/J mice may be able to increase their energy expenditure and thereby counterbalance obesity when confronted with HF feeding supplies. In agreement, Wahlsten *et al.* reported that SWR/J mice were particularly difficult to handle and much wilder than AKR/J mice (Wahlsten *et al.*, 2003). Moreover, this hypothesis is also supported by West *et al.* who measured energy expenditure by doubly labeled water and found that energy expenditure per mouse was higher in SWR/J than in AKRJ mice (West *et al.*, 1994). In another study, AKR/J mice ate more than SWR/J mice when using the unadjusted daily food intake (g/mouse), on the contrary, when the adjusted daily food intake related to

body mass (g/30g body mass) was calculated, SWR/J mice consumed more (Bachmanov *et al.*, 2002), because AKR/J mice are heavier. Konarzewski and Diamond measured basal metabolic rate (BMR) in AKR/J and SWR/J mice and showed no difference (Konarzewski & Diamond, 1995), however, because AKR/J mice are heavier, SWR/J consumed more oxygen.

5.1.4 Litter size

In this study, SWR/J mice had a higher breeding performance than AKR/J mice (www.jax.org; (Osman *et al.*, 1997) and litter size in SWR/J (7.7 ± 1.8) was larger than in AKR/J mice (5.7 ± 2.4). The smaller litter size caused heavier body masses on day 21 in AKR/J (9.50 ± 2.34 g) than in SWR/J mice (8.41 ± 0.92 g) (Figure 4.5). In agreement, Epstein reported the inverse relation between litter size and body mass (Epstein, 1978). This may be a point to help us to understand why AKR/J is prone to obese. It was reported that animals (mice, rats and rabbits) in small litters were heavier and gained more rapidly than animals in large litters (Roberts *et al.*, 1988;Cryer & Jones, 1980;Rommers *et al.*, 2001).

5.2 Gene expression profiling

5.2.1 Normalization

The RZPD filter hybridization was made twice with the same sample from each group to check reproducibility of the results. Because of the difference in radioactive labelling efficiency, cDNA filter quality, and exposure time, raw data can not be compared and therefore a normalization procedure is required. Different normalization methods have been developed and discussed since array technology is used more and more widely. For instance, the MAS 5.0 Statistical algorithm from Affymetrix (www.affymetrix.com, 2001), intensity-dependent normalization (Yang *et al.*, 2002), non-linear normalization (Workman *et al.*, 2002), and so on. The advantage and disadvantage of different methods have been still in discussion. After comparison, the latest published quantile normalization (Bolstad *et al.*, 2003) was performed for the whole set of filter data to reduce technical bias between filters (Figure 5.1). For chip data, the same normalization procedure was applied. After normalization it is possible to make the following quantitative comparisons of signal intensities between filters and chips

respectively: SWR/J control vs. HF, AKR/J control vs. HF, SWR/J control vs. AKR/J control, and SWR/J HF vs. AKR/J HF.

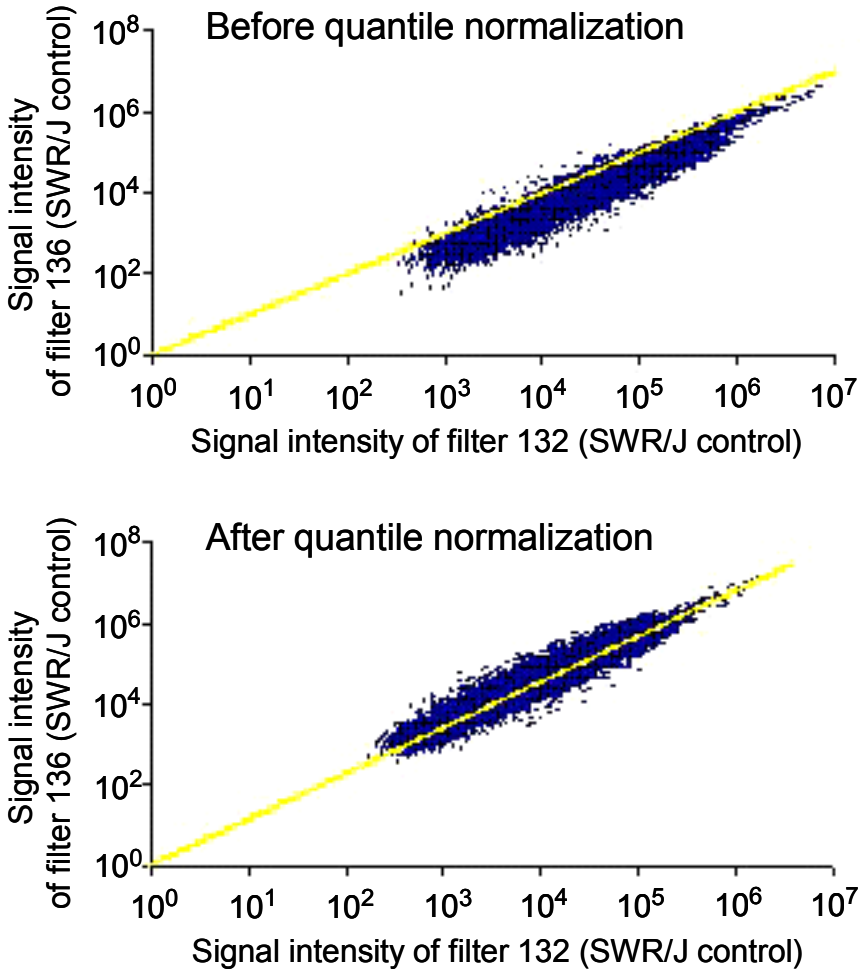

Figure 5.1 Quantile normalization. The x- and y-axes indicate the intensity of individual spots from filters 132 and 136 respectively, which in this example were both hybridized with the same probe from SWR/J control mice. The solid straight line in each plot represents the line of equality of signal intensity.

5.2.2 Candidate selection criteria

Although the fold change is the most important factor for the differentially expressed gene, the candidate selection must go through several criteria including it because all of others can affect

it. The candidate selection procedure was based on the following criteria: M value (indicates fold change of signal intensity between comparison groups), A value (indicates intensity), standard deviation of duplicates within array and of the same candidate gene between arrays, and z-scores of signal intensity between comparison groups. The MA plot is first described by Dudoit *et al.* (Dudoit *et al.*, 2002) and widely applied in array data analysis. The M value is a quantitative measure for the between-group difference in signal intensity of a specific gene spot. However, M values are not independent of absolute signal intensity: for low intensities, M values are not reliable because technical variance such as background or neighbouring spots can produce large effects, which have no biological significance. Therefore, genes with low M values, or even high M values but with low A values were removed from the candidate lists. By checking z-scores, most of the genes with relative high M value but in the range of low intensity were also eliminated. In addition, differences in spot intensity of each duplicate gene within arrays and between arrays was calculated, and only the genes which exhibited low differences were short-listed for further analysis.

5.2.3 RZPD high density cDNA Filters and Affymetrix GeneChips

A filter is an array of clones printed on nylon membrane while a chip is an array of oligonucleotides (25-mers) that are synthesized in a photolithographic process directly onto chip's surface (glass) at very high density. Filters are hybridized to radioactive labelled cDNA synthesized from RNA, while chips are hybridized to biotin-labelled cRNA generated via cDNA from RNA. Compared with chips, filters are cheaper and can be reused up to 10 times. The disadvantage is that there are 20-30% false spots (telephone communication with RZPD) on the filters of the first generation (used in this study), i.e., 20 –30% of clones spotted on a filter do not match the gene description supplied by the RZPD. Therefore, the original spotted clones of the candidates selected must be sequenced for confirmation. This shortage is now overcome in the product of the second generation: all clones are sequenced before they are spotted onto the filters. In this gene expression study, it shows that filters are more sensitive than chips, because the fold change of the same gene in the filter is higher than in the chip, but the variation in filter is also higher than in chip. The optimal method would be to combine these

two technologies. In summary, filters appear to be more sensitive at the detection of small effects than filters.

5.2.4 Validation of candidate genes from array analysis

There are a variety of methods for the validation of candidate genes selected from array analysis. These include: Northern blot analysis, in situ hybridization, traditional RT-PCR and real-time RT-PCR. However, not all of the candidates from array analysis can be validated in other methods. Using real-time RT-PCR Mutch *et al.* examined 27 candidates selected from microarray data and found a concordance of 77.7% (Mutch *et al.*, 2002). Similar results (71%) were reported by Rajeevan *et al.* in a validation study of array-based gene expression profiles by real-time RT-PCR using the candidates with more than twofold difference (Rajeevan *et al.*, 2001b;Rajeevan *et al.*, 2001a). In this study, 3 of 10 genes from the array analysis were confirmed by Northern blot analysis, 3 of 4 were confirmed by in situ hybridization, and 2 of 4 by real-time RT-PCR. All of these methods worked well, however, there are some difference. Northern blot is the most widely used method in most laboratories, but it requires quite much RNA. Although in situ hybridization is the most complicated method it can be used not only for the investigation of expression but also for the localization. Real-time RT-PCR is relative convenience of use and precise, but expensive.

Traditional RT-PCR uses gel electrophoresis for the detection of PCR amplification at end-point of the PCR reaction. This end-point detection has some problems such as low resolution, poor precision, low sensitivity and the need for post PCR processing. Real-time RT-PCR allows for the detection of PCR product during the early exponential growth phases of the reaction. This ability of measuring the reaction kinetics in the early phases of PCR provides a distinct advantage over traditional PCR detection. Glo1 was not confirmed in the traditional RT-PCR, however, it was validated in the real-time RT-PCR, also in Northern blot analysis and in situ hybridization. It could be concluded that real-time RT-PCR is more sensitive than the traditional RT-PCR.

5.2.4.1 Transthyretin (TTR)

From data analysis I, transthyretin (TTR) was the first candidate to be investigated. The differential effect of HF feeding in the two mouse trains clearly showed in the filter image inspection, and was then confirmed by Northern blot analysis loaded with the same RNA as in the probe synthesis for the filter hybridization. The consistent result of the array and Northern blot analysis supports the view that array technology is a very powerful tool for gene expression profiling.

However, the expression of TTR showed a pronounced individual variation in the Northern blot (Fig. 4.12) loaded with different new RNA samples. To further investigate this finding, in situ hybridization was carried out using radioactive labelled TTR probe and mouse brain sections. The result demonstrates that TTR was not located in the hypothalamus but in the lateral ventricle and dorsal 3rd ventricle. The localization of TTR has been studied by many researchers. Dickson *et al*. isolated TTR RNA from choroid plexus of brain (Dickson *et al.*, 1985), using in situ hybridization Stauder *et al.* reported that TTR mRNA was located in choroid plexus epithelial cells of ventricles (Stauder *et al.*, 1986), Kuchler-Bopp *et al*. showed that only choroidal epithelial cells in the brain synthesized TTR (Kuchler-Bopp *et al.*, 1998), Saraiva reviewed the synthesis of TTR by choroids plexus and liver (Saraiva, 2002).

It is therefore very likely that the apparent difference in TTR expression between strains represents a methodological artifact which results from differential dissection of hypothalami in individual mice. Fresh brains are soft, they need to be dissected rapidly to prevent RNA from degrading, and the hypothalamic boundaries are not easy to define. In this study, hypothalami were dissected according to a fixed protocol, and then adjusted by weighing (20-25 g/hypothalamus), which in the case of TTR was obviously not sufficient to uniformly eliminate adjacent regions which express this extra-hypothalamic transcript from all samples. The localization of hypothalamus, lateral ventricle and dorsal 3rd ventricle is shown in Figure 5.2.

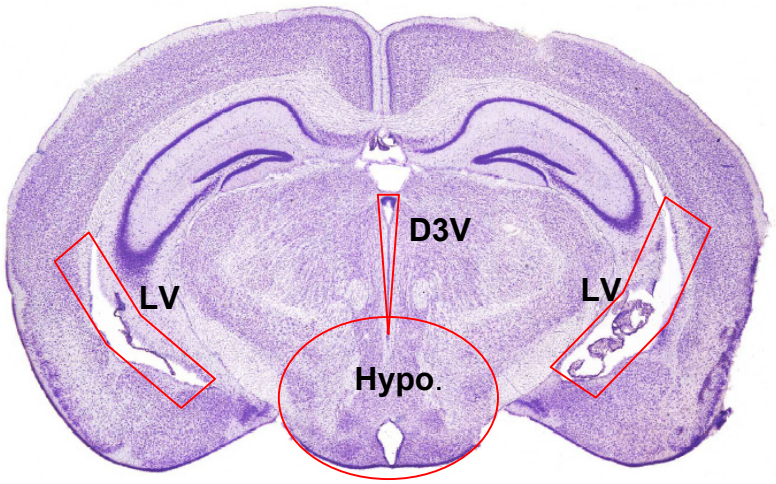

Figure 5.2 Image of brain section showing the localization of hypothalamus (Hypo.), dorsal 3rd ventricle (D3V) and lateral ventricle (LV).

To overcome the "contamination", all of the RNA samples isolated from hypothalami were loaded onto Northern blot and then screened by radioactive labelled TTR to select negatives for the second set of RNA pool for further experiments – filter and chip hybridizations.

5.2.4.2 Hemoglobin alpha, adult chain 1 (Hba-α1)

Hemoglobin alpha, adult chain 1 (Hba-α1) is located on mouse chromosome 11 (human chromosome 16p13.3).

The protein consists of an iron-containing heme moiety, the prosthetic group that mediates reversible binding of oxygen by hemoglobin, and a tetramer of two unlike pairs, α and β, of globin peptide chains surrounding and protecting the heme molecule. The function of hemoglobin is to carry oxygen in arterial erythrocytes from the lung to peripheral tissues. The distribution of Hba-α1 in brain is not only in hypothalamus but also in other areas, even all over the brain (Figure 4.17). Hemoglobin is synthesized in the bone marrow and expressed in the liver and blood (www.jax.org). It is surprising to find hemoglobin expressed in the brain. To check the similarity between hemoglobin and neuroglobin (mainly expressed in the brain) gene sequences, alignment analysis was carried out and it showed no significant similarity. Brain consumes 25% of total oxygen supplied by the body so that it is not surprising that Hba-α1 is

widely expressed in this tissue. In this study, overall the expression of Hba-α1 was higher in SWR/J compared to AKR/J mice. This difference between strains may be related to the fact that SWR/J mice have higher metabolic rate. So far, no direct relationship between Hba-α1 expression and obesity has been suggested.

5.2.4.3 Glyoxalase I

Glyoxalase I (Glo 1) (mouse chromosome 17) was the second candidate to be differentially expressed between the two inbred mouse strains. Although it was not diet induced gene in this study, it was assigned to the human obesity gene map (www.obesitygene.pbrc.edu human chromosome 6 (6p21.2)).

The glyoxalase system, catalysing the conversion of toxic endogenously produced 2-oxoaldehydes, such as methylglyoxal (MG) into D-lactate via the intermediate S-D-lactoyglutathione, is composed of two enzymes: lactoylglutathione lyase (glyoxalase I, Glo 1) and hydroxyacylglutathione hydrolase (glyoxalase II, Glo 2) with glutathione (GSH) as the cofactor.

It has been suggested that the aberrant expression of the glyoxalase system is related to cancer and diabetes. Ranganathan and Tew showed an elevation in glyoxalase I activity in 16 out of 21 colon tumors compared to corresponding normal colon tissues (Ranganathan & Tew, 1993). Another study by Di Ilio *et al.* (Di Ilio *et al.*, 1995) measured glyoxalase I and glyoxalase II activities in urogenital tumor and non-tumor tissues and found decreased glyoxalase I levels in 10 out of 15 kidney tumors compared to corresponding normal kidney tissues. Elevated levels of glyoxalase I were also reported in human prostate cancer (Davidson *et al.*, 1999). This system also appeared to be linked to complications involved in clinical diabetes mellitus as a result of increased levels of MG, and affected patients had higher levels of glyoxalase I and glyoxalase II than normal ones (Ratliff *et al.*, 1996). Concentrations of methylglyoxal, S-D lactoyl glutathione and D-lactate were found to be elevated in the blood samples of both insulin-dependent and -independent diabetic patients, compared to normal healthy controls (Thornalley *et al.*, 1989;McLellan *et al.*, 1993).

In this study, glyoxalase I was found total expressed at higher levels in AKR/J than in SWR/J mice. Higher levels of Glo1 expression in the brain has previously been reported for AKR/J

mice, but also BALB/cByJ, C3H/HeJ and A/J mice (Tafti *et al.*, 2003). All of these strains are widely used in cancer research because of their special genetic background (www.jax.org), for instance, AKR/J mice are prone to leukaemia (Myers *et al.*, 1970;Nemirovsky & Trainin, 1973), C3H/HeJ has poor immune response to endotoxic lipopolysaccharide due to a B-cell deficit (Rosenstreich & Glode, 1975;Coutinho, 1976), A/J is a model for lung tumor research (Festing & Blackmore, 1971;Poirier *et al.*, 1975). Interestingly, not only AKR/J, but also C3H/HeJ and A/J are also models for research on diet induced obesity (DIO). This suggests that Glo1 may be related to obesity.

One possible explanation for the observed strain difference in Glo1 gene expression would be that certain essential transcription factor binding sites (response elements) are mutated in the Glo1 gene of SWR/J mice. Kathrin Reichwald (IMB, Jena) has resequenced the Glo1 gene in order to test this idea, which revealed several sequence variations in non-coding and coding regions (Table 4.10). Our analysis identified several sites in the 5' upstream region, in the intron 1, 5 and exon 3, which may exhibit altered binding properties for transcription factors. The functional significance of these sequence variations for Glo1 gene transcription will be tested in future experiments by reporter gene assays.

5.2.4.4 Tumor necrosis factor alpha-induced protein 1 (endothelial) (TNFAIP1)

TNFAIP1 was upregulated by high fat diet in AKR/J mice but not in SWR/J mice, which was shown in filter array and Northern blot but not in real-time RT-PCR and in situ hybridization. In the in situ hybridization, although it showed 1.6 fold upregulation in the ARC by high fat diet, this difference was not significant because of the individual variation, further experiment with more samples should be carried out to confirm this conclusion. The map location of TNFAIP1 is on mouse chromosome 11 (45.10 cM) and human 17q22-q23. TNFAIP1 was first characterized by Wolf *et al.* as a novel cDNA by differential screening of a tumor necrosis factor-alpha (TNFα) induced human umbilical vein endothelial cell library (Wolf *et al.*, 1992). The intron/exon structure of TNFAIP1 was reported in 1998 by Stift *et al.* (Swift *et al.*, 1998). The protein functions in potassium ion transport by protein binding and voltage-gated potassium channel activity adjustment (www.niaid.nih.gov). Because it is a newly assigned gene not much information on its pathological relevance is available. In 2003, Link *et al.*

reported TNFAIP1 was increased in Alzheimer's disease brains (Link *et al.*, 2003). So far, there have been no papers linking TNFAIP1 and obesity. However, many publications report on a role of TNFα in obesity.

TNFα is located on mouse chromosome 17 (19.06cM) and human chromosome 6p21.3. Adipocytes secrete TNFα – a multifunctional proinflammatory cytokine with effects on lipid metabolism, coagulation, insulin resistance, and endothelial function. It was assigned to the human obesity gene map (www.obesitygene.pbrc.edu). Gene expression studies by Hotamisligil *et al.* showed that TNFα may induce insulin resistance in peripheral tissues both in rodent models of obesity and in people with obesity and diabetes (Hotamisligil *et al.*, 1993;Hotamisligil *et al.*, 1995;Zinman *et al.*, 1999). Using mice lacking TNFα function, Uysal *et al.* reported that TNFα was an important mediator of insulin resistance in obesity through its effects on several important sites of insulin action (Uysal *et al.*, 1997). The role of TNFα in the state of insulin resistance associated with obesity was to interfere with phosphorylation of insulin receptor substrate 1 (IRS-1) (Hotamisligil *et al.*, 1994a;Hotamisligil *et al.*, 1994b;Peraldi *et al.*, 1996) via stimulation of p55 TNF receptor (Peraldi *et al.*, 1996;Uysal *et al.*, 1998). Moreover, TNFα was reported to be involved in the regulation of plasma leptin concentration in obese subjects (Corica *et al.*, 1999). The long term effect of TNFα on adipocytes is inhibition of leptin synthesis and release (Fawcett *et al.*, 2000;Medina *et al.*, 1999), whereas its short term effect is stimulation of leptin release (Finck *et al.*, 1998;Kirchgessner *et al.*, 1997). Herrmann *et al.* in a promoter polymorphism study showed that the carriers of TNFα/-308A allele were more frequently obese than the non-carriers (Herrmann *et al.*, 1998). It is followed by other evidences for the association between the TNFα/-308A polymorphism and obesity, with high rates of glucose oxidation in normal weight subjects and with lipid storage in overweight subjects (Pihlajamaki *et al.*, 2003), with excessive fat accumulation (Hoffstedt *et al.*, 2000), with the development of insulin resistance (Dalziel *et al.*, 2002) and higher BMI (Brand *et al.*, 2001).

It is believed that TNFα has an effect on body weight regulation and that it acts probably through a local action on adipose tissue. Possibly, elevated secretion of TNFα from adipocytes in obese subjects leads to induction of TNFAIP1 in the hypothalamus. Further research needs to be conducted to elucidate the function of TNFAIP1 in the brain.

6 Reference list

(1995). Physical status: the use and interpretation of anthropometry. Report of a WHO Expert Committee. *World Health Organ Tech.Rep.Ser.* **854**, 1-452.

(2000). Obesity: preventing and managing the global epidemic. Report of a WHO consultation. *World Health Organ Tech.Rep.Ser.* **894**, i-253.

The Surgeon General's call to action to prevent and decrease overweight and obesity. [Rockville, MD]. U.S.Department of Health and Human Services, Public Health Service Office of the Surgeon General and [2001]. 2001.
Ref Type: Report

Abbott, C. R., Rossi, M., Wren, A. M., Murphy, K. G., Kennedy, A. R., Stanley, S. A., Zollner, A. N., Morgan, D. G., Morgan, I., Ghatei, M. A., Small, C. J., & Bloom, S. R. (2001). Evidence of an orexigenic role for cocaine- and amphetamine-regulated transcript after administration into discrete hypothalamic nuclei. *Endocrinology* **142**, 3457-3463.

Adam, C. L., Archer, Z. A., Findlay, P. A., Thomas, L., & Marie, M. (2002). Hypothalamic gene expression in sheep for cocaine- and amphetamine-regulated transcript, pro-opiomelanocortin, neuropeptide Y, agouti-related peptide and leptin receptor and responses to negative energy balance. *Neuroendocrinology* **75**, 250-256.

Anand, B. K. & Brobeck, J. R. (1951a). Hypothalamic control of food intake in rats and cats. *Yale J Biol Med.* **24**, 123-140.

Anand, B. K. & Brobeck, J. R. (1951b). Localization of a "feeding center" in the hypothalamus of the rat. *Proc.Soc.Exp.Biol Med.* **77**, 323-324.

Aravich, P. F. & Sclafani, A. (1983). Paraventricular hypothalamic lesions and medial hypothalamic knife cuts produce similar hyperphagia syndromes. *Behav Neurosci.* **97**, 970-983.

Asakawa, A., Inui, A., Yuzuriha, H., Nagata, T., Kaga, T., Ueno, N., Fujino, M. A., & Kasuga, M. (2001). Cocaine-amphetamine-regulated transcript influences energy metabolism, anxiety and gastric emptying in mice. *Horm.Metab Res.* **33**, 554-558.

Bachmanov, A. A., Reed, D. R., Beauchamp, G. K., & Tordoff, M. G. (2002). Food intake, water intake, and drinking spout side preference of 28 mouse strains. *Behav Genet.* **32**, 435-443.

Banegas, J. R., Lopez-Garcia, E., Gutierrez-Fisac, J. L., Guallar-Castillon, P., & Rodriguez-Artalejo, F. (2003). A simple estimate of mortality attributable to excess weight in the European Union. *Eur.J Clin.Nutr.* **57**, 201-208.

Barsh, G. S., Farooqi, I. S., & O'Rahilly, S. (2000). Genetics of body-weight regulation. *Nature* **404**, 644-651.

Baskin, D. G., Breininger, J. F., & Schwartz, M. W. (1999). Leptin receptor mRNA identifies a subpopulation of neuropeptide Y neurons activated by fasting in rat hypothalamus. *Diabetes* **48**, 828-833.

Bell, A. C., Ge, K., & Popkin, B. M. (2001). Weight gain and its predictors in Chinese adults. *Int.J Obes.Relat Metab Disord.* **25**, 1079-1086.

Bergendahl, M., Wiemann, J. N., Clifton, D. K., Huhtaniemi, I., & Steiner, R. A. (1992). Short-term starvation decreases POMC mRNA but does not alter GnRH mRNA in the brain of adult male rats. *Neuroendocrinology* **56**, 913-920.

Bernardis, L. L. & Bellinger, L. L. (1993). The lateral hypothalamic area revisited: neuroanatomy, body weight regulation, neuroendocrinology and metabolism. *Neurosci.Biobehav.Rev.* **17**, 141-193.

Bertile, F., Oudart, H., Criscuolo, F., Maho, Y. L., & Raclot, T. (2003). Hypothalamic gene expression in long-term fasted rats: relationship with body fat. *Biochem.Biophys.Res.Commun.* **303**, 1106-1113.

Blevins, J. E., Eakin, T. J., Murphy, J. A., Schwartz, M. W., & Baskin, D. G. (2003). Oxytocin innervation of caudal brainstem nuclei activated by cholecystokinin. *Brain Res.* **993**, 30-41.

Bolstad, B. M., Irizarry, R. A., Astrand, M., & Speed, T. P. (2003). A comparison of normalization methods for high density oligonucleotide array data based on variance and bias. *Bioinformatics* **19**, 185-193.

Bradley, A. (2002). Mining the mouse genome. *Nature* **420**, 512-514.

Brady, L. S., Smith, M. A., Gold, P. W., & Herkenham, M. (1990). Altered expression of hypothalamic neuropeptide mRNAs in food-restricted and food-deprived rats. *Neuroendocrinology* **52**, 441-447.

Brand, E., Schorr, U., Kunz, I., Kertmen, E., Ringel, J., Distler, A., & Sharma, A. M. (2001). Tumor necrosis factor-alpha--308 G/A polymorphism in obese Caucasians. *Int.J Obes.Relat Metab Disord.* **25**, 581-585.

Bray, G. A., Fisler, J., & York, D. A. (1990). Neuroendocrine control of the development of obesity: understanding gained from studies of experimental animal models. *Frontiers in Neuroendocrinology* **11**, 128-181.

Bray, M. S. (2000). Genomics, genes, and environmental interaction: the role of exercise. *J Appl.Physiol* **88**, 788-792.

Britton, D. R., Koob, G. F., Rivier, J., & Vale, W. (1982). Intraventricular corticotropin-releasing factor enhances behavioral effects of novelty. *Life Sci.* **31**, 363-367.

Broberger, C., Johansen, J., Johansson, C., Schalling, M., & Hokfelt, T. (1998). The neuropeptide Y/agouti gene-related protein (AGRP) brain circuitry in normal, anorectic, and monosodium glutamate-treated mice. *Proc.Natl.Acad.Sci.U.S.A* **95**, 15043-15048.

Butler, D. (2004). Health experts find obesity measures too lightweight. *Nature* **428**, 244.

Cassano, P. A., Segal, M. R., Vokonas, P. S., & Weiss, S. T. (1990). Body fat distribution, blood pressure, and hypertension. A prospective cohort study of men in the normative aging study. *Ann.Epidemiol.* **1**, 33-48.

Challis, B. G., Pritchard, L. E., Creemers, J. W., Delplanque, J., Keogh, J. M., Luan, J., Wareham, N. J., Yeo, G. S., Bhattacharyya, S., Froguel, P., White, A., Farooqi, I. S., & O'Rahilly, S. (2002). A missense mutation disrupting a dibasic prohormone processing site in pro-opiomelanocortin (POMC) increases

susceptibility to early-onset obesity through a novel molecular mechanism. *Hum.Mol.Genet.* **11**, 1997-2004.

Chan, J. M., Rimm, E. B., Colditz, G. A., Stampfer, M. J., & Willett, W. C. (1994). Obesity, fat distribution, and weight gain as risk factors for clinical diabetes in men. *Diabetes Care* **17**, 961-969.

Cheung, C. C., Clifton, D. K., & Steiner, R. A. (1997). Proopiomelanocortin neurons are direct targets for leptin in the hypothalamus. *Endocrinology* **138**, 4489-4492.

Chomczynski, P. & Sacchi, N. (1987). Single-step method of RNA isolation by acid guanidinium thiocyanate-phenol-chloroform extraction. *Anal.Biochem.* **162**, 156-159.

Clement, K., Boutin, P., & Froguel, P. (2002). Genetics of obesity. *Am.J Pharmacogenomics.* **2**, 177-187.

Clement, K., Vaisse, C., Lahlou, N., Cabrol, S., Pelloux, V., Cassuto, D., Gourmelen, M., Dina, C., Chambaz, J., Lacorte, J. M., Basdevant, A., Bougneres, P., Lebouc, Y., Froguel, P., & Guy-Grand, B. (1998). A mutation in the human leptin receptor gene causes obesity and pituitary dysfunction. *Nature* **392**, 398-401.

Colditz, G. A., Willett, W. C., Rotnitzky, A., & Manson, J. E. (1995). Weight gain as a risk factor for clinical diabetes mellitus in women. *Ann.Intern.Med.* **122**, 481-486.

Comuzzie, A. G., Blangero, J., Mahaney, M. C., Haffner, S. M., Mitchell, B. D., Stern, M. P., & MacCluer, J. W. (1996). Genetic and environmental correlations among hormone levels and measures of body fat accumulation and topography. *J Clin.Endocrinol.Metab* **81**, 597-600.

Comuzzie, A. G., Blangero, J., Mahaney, M. C., Mitchell, B. D., Stern, M. P., & MacCluer, J. W. (1994). Genetic and environmental correlations among skinfold measures. *Int.J Obes.Relat Metab Disord.* **18**, 413-418.

Comuzzie, A. G., Williams, J. T., Martin, L. J., & Blangero, J. (2001). Searching for genes underlying normal variation in human adiposity. *J Mol.Med.* **79**, 57-70.

Corica, F., Allegra, A., Corsonello, A., Buemi, M., Calapai, G., Ruello, A., Nicita, M., V, & Ceruso, D. (1999). Relationship between plasma leptin levels and the tumor necrosis factor-alpha system in obese subjects. *Int.J Obes.Relat Metab Disord.* **23**, 355-360.

Coutinho, A. (1976). Genetic control of B-cell responses. II. Identification of the spleen B-cell defect in C3H/HeJ mice. *Scand.J Immunol.* **5**, 129-140.

Crabbe, J. C., Wahlsten, D., & Dudek, B. C. (1999). Genetics of mouse behavior: Interactions with laboratory environment. *Science* **284**, 1670-1672.

Cryer, A. & Jones, H. M. (1980). The development of white adipose tissue. Effect of litter size on the lipoprotein lipase activity of four adipose-tissue depots, serum immunoreactive insulin and tissue cellularity during the first year of life in male and female rats. *Biochem.J* **186**, 805-815.

Dalziel, B., Gosby, A. K., Richman, R. M., Bryson, J. M., & Caterson, I. D. (2002). Association of the TNF-alpha -308 G/A promoter polymorphism with insulin resistance in obesity. *Obes.Res.* **10**, 401-407.

Davidson, S. D., Cherry, J. P., Choudhury, M. S., Tazaki, H., Mallouh, C., & Konno, S. (1999). Glyoxalase I activity in human prostate cancer: a potential marker and importance in chemotherapy. *J Urol.* **161**, 690-691.

Davies, L. & Marks, J. L. (1994). Role of hypothalamic neuropeptide Y gene expression in body weight regulation. *Am.J Physiol* **266**, R1687-R1691.

Dawson, R., Pelleymounter, M. A., Millard, W. J., Liu, S., & Eppler, B. (1997). Attenuation of leptin-mediated effects by monosodium glutamate-induced arcuate nucleus damage. *Am.J Physiol* **273**, E202-E206.

Di Ilio, C., Angelucci, S., Pennelli, A., Zezza, A., Tenaglia, R., & Sacchetta, P. (1995). Glyoxalase activities in tumor and non-tumor human urogenital tissues. *Cancer Lett.* **96**, 189-193.

Dickson, P. W., Howlett, G. J., & Schreiber, G. (1985). Rat transthyretin (prealbumin). Molecular cloning, nucleotide sequence, and gene expression in liver and brain. *J Biol Chem.* **260**, 8214-8219.

Dubern, B., Clement, K., Pelloux, V., Froguel, P., Girardet, J. P., Guy-Grand, B., & Tounian, P. (2001). Mutational analysis of melanocortin-4 receptor, agouti-related protein, and alpha-melanocyte-stimulating hormone genes in severely obese children. *J Pediatr.* **139**, 204-209.

Dudoit, S., Yang, Y. H., Callow, M. J., & Speed, T. P. (2002). Statistical methods for identifying differentially expressed genes in replicated cDNA microarray experiments. *Statistica Sinica* **12**, 111-139.

Elias, C. F., Lee, C., Kelly, J., Aschkenasi, C., Ahima, R. S., Couceyro, P. R., Kuhar, M. J., Saper, C. B., & Elmquist, J. K. (1998). Leptin activates hypothalamic CART neurons projecting to the spinal cord. *Neuron* **21**, 1375-1385.

Elmquist, J. K., Elias, C. F., & Saper, C. B. (1999). From lesions to leptin: hypothalamic control of food intake and body weight. *Neuron* **22**, 221-232.

Elmquist, J. K., Maratos-Flier, E., Saper, C. B., & Flier, J. S. (1998). Unraveling the central nervous system pathways underlying responses to leptin. *Nat.Neurosci.* **1**, 445-450.

Epstein, H. T. (1978). The effect of litter size on weight gain in mice. *J Nutr.* **108**, 120-123.

Farooqi, I. S., Jebb, S. A., Langmack, G., Lawrence, E., Cheetham, C. H., Prentice, A. M., Hughes, I. A., McCamish, M. A., & O'Rahilly, S. (1999). Effects of recombinant leptin therapy in a child with congenital leptin deficiency. *N.Engl.J Med.* **341**, 879-884.

Farooqi, I. S., Keogh, J. M., Yeo, G. S., Lank, E. J., Cheetham, T., & O'Rahilly, S. (2003). Clinical spectrum of obesity and mutations in the melanocortin 4 receptor gene. *N.Engl.J Med.* **348**, 1085-1095.

Farooqi, I. S., Matarese, G., Lord, G. M., Keogh, J. M., Lawrence, E., Agwu, C., Sanna, V., Jebb, S. A., Perna, F., Fontana, S., Lechler, R. I., DePaoli, A. M., & O'Rahilly, S. (2002). Beneficial effects of leptin on obesity, T cell hyporesponsiveness, and neuroendocrine/metabolic dysfunction of human congenital leptin deficiency. *J Clin.Invest* **110**, 1093-1103.

Fawcett, R. L., Waechter, A. S., Williams, L. B., Zhang, P., Louie, R., Jones, R., Inman, M., Huse, J., & Considine, R. V. (2000). Tumor necrosis factor-alpha inhibits leptin production in subcutaneous and omental adipocytes from morbidly obese humans. *J Clin.Endocrinol.Metab* **85**, 530-535.

Fekete, C., Legradi, G., Mihaly, E., Tatro, J. B., Rand, W. M., & Lechan, R. M. (2000). alpha-Melanocyte stimulating hormone prevents fasting-induced suppression of corticotropin-releasing hormone gene expression in the rat hypothalamic paraventricular nucleus. *Neurosci.Lett.* **289**, 152-156.

Festing, M. F. & Blackmore, D. K. (1971). Life span of specified-pathogen-free (MRC category 4) mice and rats. *Lab Anim* **5**, 179-192.

Finck, B. N., Kelley, K. W., Dantzer, R., & Johnson, R. W. (1998). In vivo and in vitro evidence for the involvement of tumor necrosis factor-alpha in the induction of leptin by lipopolysaccharide. *Endocrinology* **139**, 2278-2283.

Flegal, K. M., Carroll, M. D., Kuczmarski, R. J., & Johnson, C. L. (1998). Overweight and obesity in the United States: prevalence and trends, 1960-1994. *Int.J Obes.Relat Metab Disord.* **22**, 39-47.

Flegal, K. M., Carroll, M. D., Ogden, C. L., & Johnson, C. L. (2002). Prevalence and trends in obesity among US adults, 1999-2000. *JAMA* **288**, 1723-1727.

French, S. A., Story, M., & Jeffery, R. W. (2001). Environmental influences on eating and physical activity. *Annu.Rev.Public Health* **22**, 309-335.

Friedman, J. M. (2000). Obesity in the new millennium. *Nature* **404**, 632-634.

Gale, S. M., Castracane, V. D., & Mantzoros, C. S. (2004). Energy homeostasis, obesity and eating disorders: recent advances in endocrinology. *J Nutr.* **134**, 295-298.

Garrow, J. S. & Webster, J. (1985). Quetelet's index (W/H2) as a measure of fatness. *Int.J Obes.* **9**, 147-153.

Hagan, J. J., Leslie, R. A., Patel, S., Evans, M. L., Wattam, T. A., Holmes, S., Benham, C. D., Taylor, S. G., Routledge, C., Hemmati, P., Munton, R. P., Ashmeade, T. E., Shah, A. S., Hatcher, J. P., Hatcher, P. D., Jones, D. N., Smith, M. I., Piper, D. C., Hunter, A. J., Porter, R. A., & Upton, N. (1999). Orexin A activates locus coeruleus cell firing and increases arousal in the rat. *Proc.Natl.Acad.Sci.U.S.A* **96**, 10911-10916.

Hahn, T. M., Breininger, J. F., Baskin, D. G., & Schwartz, M. W. (1998). Coexpression of Agrp and NPY in fasting-activated hypothalamic neurons. *Nat.Neurosci.* **1**, 271-272.

Hernandez, L. & Hoebel, B. G. (1989). Food intake and lateral hypothalamic self-stimulation covary after medial hypothalamic lesions or ventral midbrain 6-hydroxydopamine injections that cause obesity. *Behav Neurosci.* **103**, 412-422.

Herrmann, S. M., Ricard, S., Nicaud, V., Mallet, C., Arveiler, D., Evans, A., Ruidavets, J. B., Luc, G., Bara, L., Parra, H. J., Poirier, O., & Cambien, F. (1998). Polymorphisms of the tumour necrosis factor-alpha gene, coronary heart disease and obesity. *Eur.J Clin.Invest* **28**, 59-66.

Heseker, H. & Schmid, A. (2000). [Epidemiology of obesity]. *Ther.Umsch.* **57**, 478-481.

Hill, J. O., Melanson, E. L., & Wyatt, H. T. (2000). Dietary fat intake and regulation of energy balance: implications for obesity. *J Nutr.* **130**, 284S-288S.

Hill, J. O. & Peters, J. C. (1998). Environmental contributions to the obesity epidemic. *Science.* **280**, 1371-1374.

Hinney, A., Schmidt, A., Nottebom, K., Heibult, O., Becker, I., Ziegler, A., Gerber, G., Sina, M., Gorg, T., Mayer, H., Siegfried, W., Fichter, M., Remschmidt, H., & Hebebrand, J. (1999). Several mutations in the melanocortin-4 receptor gene including a nonsense and a frameshift mutation associated with dominantly inherited obesity in humans. *J Clin.Endocrinol.Metab* **84**, 1483-1486.

Hoffstedt, J., Eriksson, P., Hellstrom, L., Rossner, S., Ryden, M., & Arner, P. (2000). Excessive fat accumulation is associated with the TNF alpha-308 G/A promoter polymorphism in women but not in men. *Diabetologia* **43**, 117-120.

Hotamisligil, G. S., Arner, P., Caro, J. F., Atkinson, R. L., & Spiegelman, B. M. (1995). Increased adipose tissue expression of tumor necrosis factor-alpha in human obesity and insulin resistance. *J Clin.Invest* **95**, 2409-2415.

Hotamisligil, G. S., Budavari, A., Murray, D., & Spiegelman, B. M. (1994a). Reduced tyrosine kinase activity of the insulin receptor in obesity-diabetes. Central role of tumor necrosis factor-alpha. *J Clin.Invest* **94**, 1543-1549.

Hotamisligil, G. S., Murray, D. L., Choy, L. N., & Spiegelman, B. M. (1994b). Tumor necrosis factor alpha inhibits signaling from the insulin receptor. *Proc.Natl.Acad.Sci.U.S.A* **91**, 4854-4858.

Hotamisligil, G. S., Shargill, N. S., & Spiegelman, B. M. (1993). Adipose expression of tumor necrosis factor-alpha: direct role in obesity-linked insulin resistance. *Science* **259**, 87-91.

Huang, Z., Willett, W. C., Manson, J. E., Rosner, B., Stampfer, M. J., Speizer, F. E., & Colditz, G. A. (1998). Body weight, weight change, and risk for hypertension in women. *Ann.Intern.Med.* **128**, 81-88.

Jeffery, R. W. & Utter, J. (2003). The changing environment and population obesity in the United States. *Obes.Res.* **11 Suppl**, 12S-22S.

Jequier, E. (2002). Pathways to obesity. *Int.J Obes.Relat Metab Disord.* **26 Suppl 2**, S12-S17.

Kalies, H., Lenz, J., & von Kries, R. (2002). Prevalence of overweight and obesity and trends in body mass index in German pre-school children, 1982-1997. *Int.J Obes.Relat Metab Disord.* **26**, 1211-1217.

Katzmarzyk, P. T., Perusse, L., Rao, D. C., & Bouchard, C. (1999). Familial risk of obesity and central adipose tissue distribution in the general Canadian population. *Am.J Epidemiol.* **149**, 933-942.

Kennedy, G. C. (1950). The hypothalamic control of food intake in rats. *Proc.R.Soc.Lond B Biol Sci.* **137**, 535-549.

Kirchgessner, T. G., Uysal, K. T., Wiesbrock, S. M., Marino, M. W., & Hotamisligil, G. S. (1997). Tumor necrosis factor-alpha contributes to obesity-related hyperleptinemia by regulating leptin release from adipocytes. *J Clin.Invest* **100**, 2777-2782.

Konarzewski, M. & Diamond, J. (1995). Evolution of basal metabolic rate and organ masses in laboratory mice. *Evolution* **49**, 1239-1248.

Kong, W. M., Stanley, S., Gardiner, J., Abbott, C., Murphy, K., Seth, A., Connoley, I., Ghatei, M., Stephens, D., & Bloom, S. (2003). A role for arcuate cocaine and amphetamine-regulated transcript in hyperphagia, thermogenesis, and cold adaptation. *FASEB J* **17**, 1688-1690.

Kopelman, P. G. (2000). Obesity as a medical problem. *Nature* **404**, 635-643.

Kow, L. M. & Pfaff, D. W. (1991). The effects of the TRH metabolite cyclo(His-Pro) and its analogs on feeding. *Pharmacol.Biochem.Behav* **38**, 359-364.

Kromeyer-Hauschild, K., Zellner, K., Jaeger, U., & Hoyer, H. (1999). Prevalence of overweight and obesity among school children in Jena (Germany). *Int.J Obes.Relat Metab Disord.* **23**, 1143-1150.

Krude, H., Biebermann, H., Luck, W., Horn, R., Brabant, G., & Gruters, A. (1998). Severe early-onset obesity, adrenal insufficiency and red hair pigmentation caused by POMC mutations in humans. *Nat.Genet.* **19**, 155-157.

Kuchler-Bopp, S., Ittel, M. E., Dietrich, J. B., Reeber, A., Zaepfel, M., & Delaunoy, J. P. (1998). The presence of transthyretin in rat ependymal cells is due to endocytosis and not synthesis. *Brain Res.* **793**, 219-230.

Lee, G. H., Proenca, R., Montez, J. M., Carroll, K. M., Darvishzadeh, J. G., Lee, J. I., & Friedman, J. M. (1996). Abnormal splicing of the leptin receptor in diabetic mice. *Nature.* **379**, 632-635.

Lee, J. H., Reed, D. R., & Price, R. A. (1997). Familial risk ratios for extreme obesity: implications for mapping human obesity genes. *Int.J Obes.Relat Metab Disord.* **21**, 935-940.

Leibowitz, S. F., Hammer, N. J., & Chang, K. (1981). Hypothalamic paraventricular nucleus lesions produce overeating and obesity in the rat. *Physiol Behav* **27**, 1031-1040.

Link, C. D., Taft, A., Kapulkin, V., Duke, K., Kim, S., Fei, Q., Wood, D. E., & Sahagan, B. G. (2003). Gene expression analysis in a transgenic Caenorhabditis elegans Alzheimer's disease model. *Neurobiol.Aging* **24**, 397-413.

Macdiarmid, J. I., Cade, J. E., & Blundell, J. E. (1996). High and low fat consumers, their macronutrient intake and body mass index: further analysis of the National Diet and Nutrition Survey of British Adults. *Eur.J Clin.Nutr.* **50**, 505-512.

Maes, H. H., Neale, M. C., & Eaves, L. J. (1997). Genetic and environmental factors in relative body weight and human adiposity. *Behav Genet.* **27**, 325-351.

Martinez, J. A. (2000). Obesity in young Europeans: genetic and environmental influences. *Eur.J Clin.Nutr.* **54 Suppl 1**, S56-S60.

Martinez, J. A. & Fruhbeck, G. (1996). Regulation of energy balance and adiposity: a model with new approaches. *Rev.Esp.Fisiol.* **52**, 255-258.

McGinnis, J. M. & Foege, W. H. (1993). Actual causes of death in the United States. *JAMA* **270**, 2207-2212.

McLellan, A. C., Thornalley, P. J., Benn, J., & Sonksen, P. H. (1993). Modification of the glyoxalase system in clinical diabetes mellitus. *Biochem.Soc.Trans.* **21**, 158S.

McMahon, L. R. & Wellman, P. J. (1997). Assessment of the role of oxytocin receptors in phenylpropanolamine-induced anorexia in rats. *Pharmacol.Biochem.Behav* **57**, 767-770.

Medina, E. A., Stanhope, K. L., Mizuno, T. M., Mobbs, C. V., Gregoire, F., Hubbard, N. E., Erickson, K. L., & Havel, P. J. (1999). Effects of tumor necrosis factor alpha on leptin secretion and gene

expression: relationship to changes of glucose metabolism in isolated rat adipocytes. *Int.J Obes.Relat Metab Disord.* **23**, 896-903.

Milam, K. M., Keesey, R. E., & Stern, J. S. (1982). Body composition and adiposity in LH-lesioned and pair-fed obese Zucker rats. *Am.J Physiol* **242**, E437-E444.

Milam, K. M., Stern, J. S., Storlien, L. H., & Keesey, R. E. (1980). Effect of lateral hypothalamic lesions on regulation of body weight and adiposity in rats. *Am.J Physiol* **239**, R337-R343.

Mokdad, A. H., Ford, E. S., Bowman, B. A., Dietz, W. H., Vinicor, F., Bales, V. S., & Marks, J. S. (2003). Prevalence of obesity, diabetes, and obesity-related health risk factors, 2001. *JAMA* **289**, 76-79.

Montague, C. T., Farooqi, I. S., Whitehead, J. P., Soos, M. A., Rau, H., Wareham, N. J., Sewter, C. P., Digby, J. E., Mohammed, S. N., Hurst, J. A., Cheetham, C. H., Earley, A. R., Barnett, A. H., Prins, J. B., & O'Rahilly, S. (1997). Congenital leptin deficiency is associated with severe early-onset obesity in humans. *Nature* **387**, 903-908.

Morley, J. E., Levine, A. S., Gosnell, B. A., Kneip, J., & Grace, M. (1987). Effect of neuropeptide Y on ingestive behaviors in the rat. *Am.J Physiol* **252**, R599-R609.

Mouse Genome Sequencing Consortium (2002). Initial sequencing and comparative analysis of the mouse genome. *Nature* **420**, 520-562.

Mutch, D. M., Berger, A., Mansourian, R., Rytz, A., & Roberts, M. A. (2002). The limit fold change model: a practical approach for selecting differentially expressed genes from microarray data. *BMC.Bioinformatics.* **3**, 17.

Myers, D. D., Meier, H., & Huebner, R. J. (1970). Prevalence of murine C-type RNA virus group specific antigen in inbred strains of mice. *Life Sci.II* **9**, 1071-1080.

Nemirovsky, T. & Trainin, N. (1973). Leukemia induction in C3H mice following their inoculation with normal AKR lymphoid cells. *Int.J Cancer* **11**, 172-177.

Nestle, M. (2003). The ironic politics of obesity. *Science* **299**, 781.

Osman, G. E., Jacobson, D. P., Li, S. W., Hood, L. E., Liggitt, H. D., & Ladiges, W. C. (1997). SWR: An inbred strain suitable for generating transgenic mice. *Laboratory Animal Science* **47**, 167-171.

Panksepp, J. (1974). Hypothalamic regulation of energy balance and feeding behavior. *Fed.Proc.* **33**, 1150-1165.

Peraldi, P., Hotamisligil, G. S., Buurman, W. A., White, M. F., & Spiegelman, B. M. (1996). Tumor necrosis factor (TNF)-alpha inhibits insulin signaling through stimulation of the p55 TNF receptor and activation of sphingomyelinase. *J Biol Chem.* **271**, 13018-13022.

Pi-Sunyer, F. X. (1993). Medical hazards of obesity. *Ann.Intern.Med.* **119**, 655-660.

Pihlajamaki, J., Ylinen, M., Karhapaa, P., Vauhkonen, I., & Laakso, M. (2003). The effect of the -308A allele of the TNF-alpha gene on insulin action is dependent on obesity. *Obes.Res.* **11**, 912-917.

Poirier, L. A., Stoner, G. D., & Shimkin, M. B. (1975). Bioassay of alkyl halides and nucleotide base analogs by pulmonary tumor response in strain A mice. *Cancer Res.* **35**, 1411-1415.

Popkin, B. M. & Doak, C. M. (1998). The obesity epidemic is a worldwide phenomenon. *Nutr.Rev.* **56**, 106-114.

Popkin, B. M., Richards, M. K., & Montiero, C. A. (1996). Stunting is associated with overweight in children of four nations that are undergoing the nutrition transition. *J Nutr.* **126**, 3009-3016.

Poston, W. S. & Foreyt, J. P. (1999). Obesity is an environmental issue. *Atherosclerosis* **146**, 201-209.

Prpic, V., Watson, P. M., Frampton, I. C., Sabol, M. A., Jezek, G. E., & Gettys, T. W. (2002). Adaptive changes in adipocyte gene expression differ in AKR/J and SWR/J mice during diet-induced obesity. *J Nutr.* **132**, 3325-3332.

Qu, D., Ludwig, D. S., Gammeltoft, S., Piper, M., Pelleymounter, M. A., Cullen, M. J., Mathes, W. F., Przypek, R., Kanarek, R., & Maratos-Flier, E. (1996). A role for melanin-concentrating hormone in the central regulation of feeding behaviour. *Nature* **380**, 243-247.

Rajeevan, M. S., Ranamukhaarachchi, D. G., Vernon, S. D., & Unger, E. R. (2001a). Use of real-time quantitative PCR to validate the results of cDNA array and differential display PCR technologies. *Methods* **25**, 443-451.

Rajeevan, M. S., Vernon, S. D., Taysavang, N., & Unger, E. R. (2001b). Validation of array-based gene expression profiles by real-time (kinetic) RT-PCR. *J Mol.Diagn.* **3**, 26-31.

Ranganathan, S. & Tew, K. D. (1993). Analysis of glyoxalase-I from normal and tumor tissue from human colon. *Biochim.Biophys.Acta* **1182**, 311-316.

Ratliff, D. M., Vander Jagt, D. J., Eaton, R. P., & Vander Jagt, D. L. (1996). Increased levels of methylglyoxal-metabolizing enzymes in mononuclear and polymorphonuclear cells from insulin-dependent diabetic patients with diabetic complications: aldose reductase, glyoxalase I, and glyoxalase II--a clinical research center study. *J Clin.Endocrinol.Metab* **81**, 488-492.

Rayner, G. & Rayner, M. (2003). Fat is an economic issue! Combating chronic diseases in Europe. *EuroHealth* **9**, 17-20.

Roberts, J. L., Whittington, F. M., & Enser, M. (1988). Effects of litter size and subsequent gold-thioglucose-induced obesity on adipose tissue weight, distribution and cellularity in male and female mice: an age study. *Br.J Nutr.* **59**, 519-533.

Robson, A. J., Rousseau, K., Loudon, A. S., & Ebling, F. J. (2002). Cocaine and amphetamine-regulated transcript mRNA regulation in the hypothalamus in lean and obese rodents. *J Neuroendocrinol.* **14**, 697-709.

Rommers, J. M., Kemp, B., Meijerhof, R., & Noordhuizen, J. P. (2001). The effect of litter size before weaning on subsequent body development, feed intake, and reproductive performance of young rabbit does. *J Anim Sci.* **79**, 1973-1982.

Rosenstreich, D. L. & Glode, L. M. (1975). Difference in B cell mitogen responsiveness between closely related strains of mice. *J Immunol.* **115**, 777-780.

Rossi, M., Kim, M. S., Morgan, D. G., Small, C. J., Edwards, C. M., Sunter, D., Abusnana, S., Goldstone, A. P., Russell, S. H., Stanley, S. A., Smith, D. M., Yagaloff, K., Ghatei, M. A., & Bloom, S.

R. (1998). A C-terminal fragment of Agouti-related protein increases feeding and antagonizes the effect of alpha-melanocyte stimulating hormone in vivo. *Endocrinology* **139**, 4428-4431.

Saito, Y., Nothacker, H. P., Wang, Z., Lin, S. H., Leslie, F., & Civelli, O. (1999). Molecular characterization of the melanin-concentrating-hormone receptor. *Nature* **400**, 265-269.

Sakurai, T., Amemiya, A., Ishii, M., Matsuzaki, I., Chemelli, R. M., Tanaka, H., Williams, S. C., Richardson, J. A., Kozlowski, G. P., Wilson, S., Arch, J. R., Buckingham, R. E., Haynes, A. C., Carr, S. A., Annan, R. S., McNulty, D. E., Liu, W. S., Terrett, J. A., Elshourbagy, N. A., Bergsma, D. J., & Yanagisawa, M. (1998). Orexins and orexin receptors: a family of hypothalamic neuropeptides and G protein-coupled receptors that regulate feeding behavior. *Cell* **92**, 573-585.

Sambrook, J. & Russell, D. W. (2001). In *Molecular Cloning: A Laboratory Manual*, eds. Argentine, J., Irwin, N., & Janssen, K. A., pp. 14-20. Cold Spring Harbor Laboratory Press, Cold Spring Harbor.

Saraiva, M. J. (2002). Hereditary transthyretin amyloidosis: molecular basis and therapeutical strategies. *Expert.Rev.Mol.Med.* **2002**, 1-11.

Satoh, N., Ogawa, Y., Katsuura, G., Hayase, M., Tsuji, T., Imagawa, K., Yoshimasa, Y., Nishi, S., Hosoda, K., & Nakao, K. (1997). The arcuate nucleus as a primary site of satiety effect of leptin in rats. *Neurosci.Lett.* **224**, 149-152.

Savontaus, E., Conwell, I. M., & Wardlaw, S. L. (2002). Effects of adrenalectomy on AGRP, POMC, NPY and CART gene expression in the basal hypothalamus of fed and fasted rats. *Brain Res.* **958**, 130-138.

Schwartz, M. W., Seeley, R. J., Campfield, L. A., Burn, P., & Baskin, D. G. (1996). Identification of targets of leptin action in rat hypothalamus. *J Clin.Invest* **98**, 1101-1106.

Schwartz, M. W., Seeley, R. J., Woods, S. C., Weigle, D. S., Campfield, L. A., Burn, P., & Baskin, D. G. (1997). Leptin increases hypothalamic pro-opiomelanocortin mRNA expression in the rostral arcuate nucleus. *Diabetes* **46**, 2119-2123.

Schwartz, M. W., Sipols, A. J., Marks, J. L., Sanacora, G., White, J. D., Scheurink, A., Kahn, S. E., Baskin, D. G., Woods, S. C., Figlewicz, D. P., & . (1992). Inhibition of hypothalamic neuropeptide Y gene expression by insulin. *Endocrinology* **130**, 3608-3616.

Shiraishi, T. (1991). Noradrenergic neurons modulate lateral hypothalamic chemical and electrical stimulation-induced feeding by sated rats. *Brain Res.Bull.* **27**, 347-351.

Smith, B. K., Andrews, P. K., & West, D. B. (2000). Macronutrient diet selection in thirteen mouse strains. *Am.J Physiol Regul.Integr.Comp Physiol* **278**, R797-R805.

Smith, B. K., Andrews, P. K., York, D. A., & West, D. B. (1999). Divergence in proportional fat intake in AKR/J and SWR/J mice endures across diet paradigms. *Am.J.Physiol* **277**, R776-R785.

Smith, B. K., Volaufova, J., & West, D. B. (2001). Increased flavor preference and lick activity for sucrose and corn oil in SWR/J vs. AKR/J mice. *American Journal of Physiology-Regulatory Integrative and Comparative Physiology* **281**, R596-R606.

Smith, B. K., West, D. B., & York, D. A. (1997). Carbohydrate versus fat intake: differing patterns of macronutrient selection in two inbred mouse strains. *Am.J Physiol* **272**, R357-R362.

Sorensen, T. I., Holst, C., Stunkard, A. J., & Skovgaard, L. T. (1992). Correlations of body mass index of adult adoptees and their biological and adoptive relatives. *Int.J Obes.Relat Metab Disord.* **16**, 227-236.

Stamler, R., Stamler, J., Riedlinger, W. F., Algera, G., & Roberts, R. H. (1978). Weight and blood pressure. Findings in hypertension screening of 1 million Americans. *JAMA* **240**, 1607-1610.

Stauder, A. J., Dickson, P. W., Aldred, A. R., Schreiber, G., Mendelsohn, F. A., & Hudson, P. (1986). Synthesis of transthyretin (pre-albumin) mRNA in choroid plexus epithelial cells, localized by in situ hybridization in rat brain. *J Histochem.Cytochem.* **34**, 949-952.

Stettler, N. (2002). Environmental factors in the etiology of obesity in adolescents. *Ethn.Dis.* **12**, S1-S5.

Stunkard, A. J., Foch, T. T., & Hrubec, Z. (1986a). A twin study of human obesity. *JAMA* **256**, 51-54.

Stunkard, A. J., Harris, J. R., Pedersen, N. L., & McClearn, G. E. (1990). The body-mass index of twins who have been reared apart. *N.Engl.J Med.* **322**, 1483-1487.

Stunkard, A. J., Sorensen, T. I., Hanis, C., Teasdale, T. W., Chakraborty, R., Schull, W. J., & Schulsinger, F. (1986b). An adoption study of human obesity. *N.Engl.J Med.* **314**, 193-198.

Sturm, R. (2003). Increases in clinically severe obesity in the United States, 1986-2000. *Arch.Intern.Med.* **163**, 2146-2148.

Swift, S., Blackburn, C., Morahan, G., & Ashworth, A. (1998). Structure and chromosomal mapping of the TNF-alpha inducible endothelial protein 1 (Edp1) gene in the mouse. *Biochim.Biophys.Acta* **1442**, 394-398.

Tafti, M., Petit, B., Chollet, D., Neidhart, E., de Bilbao, F., Kiss, J. Z., Wood, P. A., & Franken, P. (2003). Deficiency in short-chain fatty acid beta-oxidation affects theta oscillations during sleep. *Nat.Genet.* **34**, 320-325.

Tang-Christensen, M., Holst, J. J., Hartmann, B., & Vrang, N. (1999). The arcuate nucleus is pivotal in mediating the anorectic effects of centrally administered leptin. *Neuroreport* **10**, 1183-1187.

Tartaglia, L. A., Dembski, M., Weng, X., Deng, N. H., Culpepper, J., Devos, R., Richards, G. J., Campfield, L. A., Clark, F. T., Deeds, J., Muir, C., Sanker, S., Moriarty, A., Moore, K. J., Smutko, J. S., Mays, G. G., Woolf, E. A., Monroe, C. A., & Tepper, R. I. (1995). Identification and expression cloning of a leptin receptor, OB-R. *Cell* **83**, 1263-1271.

Thornalley, P. J., Hooper, N. I., Jennings, P. E., Florkowski, C. M., Jones, A. F., Lunec, J., & Barnett, A. H. (1989). The human red blood cell glyoxalase system in diabetes mellitus. *Diabetes Res.Clin.Pract.* **7**, 115-120.

Tsujii, S. & Bray, G. A. (1989). Acetylation alters the feeding response to MSH and beta-endorphin. *Brain Res.Bull.* **23**, 165-169.

Uysal, K. T., Wiesbrock, S. M., & Hotamisligil, G. S. (1998). Functional analysis of tumor necrosis factor (TNF) receptors in TNF-alpha-mediated insulin resistance in genetic obesity. *Endocrinology* **139**, 4832-4838.

Uysal, K. T., Wiesbrock, S. M., Marino, M. W., & Hotamisligil, G. S. (1997). Protection from obesity-induced insulin resistance in mice lacking TNF-alpha function. *Nature* **389**, 610-614.

Vlad, I. (2003). Obesity costs UK economy 2bn pounds sterling a year. *BMJ* **327**, 1308.

Vogler, G. P., Sorensen, T. I., Stunkard, A. J., Srinivasan, M. R., & Rao, D. C. (1995). Influences of genes and shared family environment on adult body mass index assessed in an adoption study by a comprehensive path model. *Int.J Obes.Relat Metab Disord.* **19**, 40-45.

Volkoff, H. & Peter, R. E. (2000). Effects of CART peptides on food consumption, feeding and associated behaviors in the goldfish, Carassius auratus: actions on neuropeptide Y- and orexin A-induced feeding. *Brain Res.* **887**, 125-133.

Wahlsten, D., Metten, P., & Crabbe, J. C. (2003). A rating scale for wildness and ease of handling laboratory mice: results of 21 inbred strains tested in two laboratories. *Genes Brain and Behavior* **2**, 71-79.

Wang, Y., Monteiro, C., & Popkin, B. M. (2002). Trends of obesity and underweight in older children and adolescents in the United States, Brazil, China, and Russia. *Am.J Clin.Nutr.* **75**, 971-977.

West, D. B., Boozer, C. N., Moody, D. L., & Atkinson, R. L. (1992). Dietary obesity in nine inbred mouse strains. *Am.J Physiol* **262**, R1025-R1032.

West, D. B., Waguespack, J., & McCollister, S. (1995). Dietary obesity in the mouse: interaction of strain with diet composition. *Am.J Physiol* **268**, R658-R665.

West, D. B., Waguespack, J., York, B., Goudey-Lefevre, J., & Price, R. A. (1994). Genetics of dietary obesity in AKR/J x SWR/J mice: segregation of the trait and identification of a linked locus on chromosome 4. *Mamm.Genome* **5**, 546-552.

Wilson, P. W. & Kannel, W. B. (2002). Obesity, diabetes, and risk of cardiovascular disease in the elderly. *Am.J Geriatr.Cardiol.* **11**, 119-23,125.

Wolf, A. M. (1998). What is the economic case for treating obesity? *Obes.Res.* **6 Suppl 1**, 2S-7S.

Wolf, F. W., Marks, R. M., Sarma, V., Byers, M. G., Katz, R. W., Shows, T. B., & Dixit, V. M. (1992). Characterization of a novel tumor necrosis factor-alpha-induced endothelial primary response gene. *J Biol Chem.* **267**, 1317-1326.

Workman, C., Jensen, L. J., Jarmer, H., Berka, R., Gautier, L., Nielser, H. B., Saxild, H. H., Nielsen, C., Brunak, S., & Knudsen, S. (2002). A new non-linear normalization method for reducing variability in DNA microarray experiments
1. *Genome Biol* **3**, research0048.

Yang, Y. H., Dudoit, S., Luu, P., Lin, D. M., Peng, V., Ngai, J., & Speed, T. P. (2002). Normalization for cDNA microarray data: a robust composite method addressing single and multiple slide systematic variation. *Nucleic Acids Res.* **30**, e15.

Yeo, G. S., Farooqi, I. S., Aminian, S., Halsall, D. J., Stanhope, R. G., & O'Rahilly, S. (1998). A frameshift mutation in MC4R associated with dominantly inherited human obesity. *Nat.Genet.* **20**, 111-112.

Zhang, Y., Proenca, R., Maffei, M., Barone, M., Leopold, L., & Friedman, J. M. (1994). Positional cloning of the mouse obese gene and its human homologue. *Nature* **372**, 425-432.

Zinman, B., Hanley, A. J., Harris, S. B., Kwan, J., & Fantus, I. G. (1999). Circulating tumor necrosis factor-alpha concentrations in a native Canadian population with high rates of type 2 diabetes mellitus. *J Clin.Endocrinol.Metab* **84**, 272-278.

Ziotopoulou, M., Mantzoros, C. S., Hileman, S. M., & Flier, J. S. (2000). Differential expression of hypothalamic neuropeptides in the early phase of diet-induced obesity in mice. *American Journal of Physiology-Endocrinology and Metabolism* **279**, E838-E845.

7 Abbreviations

AA	acetic anhydride
AgRP	agouti-related peptide
ARC	arcuate nucleus
BAT	brown adipose tissue
BMI	body mass index
BSA	bovine serum albumin
CART	cocaine- and amphetamine-regulated transcript
CRH	corticotropin-releasing hormone
DEPC	diethyl pyrocarbonate
DTT	dithiothreitol
EDTA	ethylene diaminetetraacetic acid
EST	expressed sequence tag
Glo1	glyoxalase I
Hba- α1	hemoglobin alpha, adult chain 1
ICV	intracerebroventricular
IPTG	isopropyl-β-D-thiogalactopyranoside
isBAT	inter scapular brown adipose tissue
ISH	in situ hybridization
IVT	*In Vitro* transcription
iWAT	inguinal white adipose tissue
LEPR	leptin receptor
LHA	lateral hypothalamic nucleus
MC4R	melanocortin-4 receptor
MOPS	3-(N-morpholino) propane sulfonic acid
NPY	neuropeptide Y
ORX	orexin
PBS	phosphate buffered saline
PCR	polymerase chain reaction
PFA	paraformaldehyde

PF-A	perifornical area
POMC	proopiomelanocortin
Ppp2cb	protein phosphatase 2a, catalytic subunit, beta isoform
PVN	paraventricular hypothalamic nucleus
rpWAT	retroperitoneal white adipose tissue
SDS	sodium-dodecyl-sulphate
SSC	standard sodium citrate
TAE	Tris-acetate-EDTA
TE	Tris-EDTA
TEA	triethanolamine
TNFAIP1	tumor necrosis factor alpha-induced protein 1 (endothelial)
TRH	thyrotropin-releasing hormone
TTR	transthyretin
VMH	ventromedial hypothalamic nucleus
WAT	white adipose tissue
X-Gal	5’-Bromo-4-chloro-3-indolyl-β-D-galactopyranoside

8 Appendix

8.1 Appendix 1

Appendix 1. List of candidate genes in the inter strain comparison – AKR/J control vs. SWR/J control from data analysis I.

RZPD clone ID	GenBank accession number	Cluster description by RZPD	Fold change[a]
IMAGp952I058	w61435	paternally expressed gene 3	3.44
IMAGp952B1239	aa444730	small inducible cytokine A19	-3.17
IMAGp952O0350	aa672630,ai551192		-3.13
IMAGp952N0950	aa672655	ESTs, Highly similar to hGCN5 [H.sapiens]	3.03
IMAGp952M0615	aa016919		-2.93
IMAGp952C2060	aa981499		-2.84
IMAGp952H1814	aa013674		-2.80
IMAGp952B2215	aa023039		-2.73
IMAGp952P0414	aa013706	ESTs, Moderately similar to dJ622L5.8.1 [H.sapiens]	-2.72
IMAGp952B0414	aa013524	ESTs, Weakly similar to F52C12.2 [C.elegans]	-2.72
IMAGp952B0745	aa538202	ESTs, Weakly similar to putative RNA helicase [M.musculus]	-2.69
IMAGp952E0715	aa034643	ESTs, Weakly similar to HYPOTHETICAL 55.1 KD PROTEIN IN FAB1-PES4 INTERGENIC REGION [Saccharomyces cerevisiae]	-2.64
IMAGp952L0515	aa017937	cleavage and polyadenylation specific factor 4, 30kD subunit	-2.64
IMAGp952H092	w42169	prostaglandin D2 synthase (21 kDa, brain)	2.63
IMAGp952M0260	aa982515	midline 2	-2.60
IMAGp952L1462	aa199543,ai592642, ai666665	ESTs, Moderately similar to ZIC4_MOUSE ZINC FINGER PROTEIN ZIC4 [M.musculus]	-2.59
IMAGp952G1162	aa138161		-2.58
IMAGp952N2214	aa013529	ESTs, Moderately similar to unnamed protein product [H.sapiens]	-2.54
IMAGp952D1420	aa061740,ai327007, ai893662	ESTs, Highly similar to PROTEOLIPID PROTEIN PPA1 [Saccharomyces cerevisiae]	-2.54
IMAGp952B1215	aa023244	M.musculus ASF mRNA	-2.52
IMAGp952L1718	aa049636		-2.48
IMAGp952A1735	aa387581		-2.47

IMAGp952P1054	ai119550,ai119733	hemoglobin alpha, adult chain 1	2.47
IMAGp952A0915	aa015253		-2.46
IMAGp952P1232	aa259445	eukaryotic translation initiation factor 4, gamma 2	2.46
IMAGp952O0249	aa673382	mitogen-activated protein kinase kinase kinase kinase 6	2.45
IMAGp952D054	ai391019,ai415191, w29683	s17 protein	2.42
IMAGp952A1547	aa547134,ai505917	baculoviral IAP repeat-containing 6	-2.39
IMAGp952G1925	aa119613,ai452165		-2.36
IMAGp952B1327	aa168903	m6a methyltransferase	-2.34
IMAGp952P039	w77193		-2.34
IMAGp952O1610	ai413741,ai425768, w76774	transmembrane tryptase	2.34
IMAGp952C1427	aa288756		-2.33
IMAGp952K173	w08585	ESTs, Highly similar to sh3bgr protein [M.musculus]	-2.33
IMAGp952O0232	aa286155	ESTs, Highly similar to SP24_RAT SECRETED PHOSPHOPROTEIN 24 [R.norvegicus]	-2.32
IMAGp952E074	w20733	transmembrane 4 superfamily member 7	2.31
IMAGp952B1363	aa562246		-2.30
IMAGp952L1827	aa172854		2.29
IMAGp952K2216	aa027487	ESTs, Moderately similar to HYPOTHETICAL 63.5 KD PROTEIN ZK353.1 IN CHROMOSOME III [Caenorhabditis elegans]	-2.28
IMAGp952I1416	aa027365,ai324204	connective tissue growth factor	-2.28
IMAGp952L0663	aa572284,ai507498, ai615843		-2.27
IMAGp952O2034	aa289615		2.26
IMAGp952N1054	ai119558	fatty acid Coenzyme A ligase, long chain 2	2.24
IMAGp952I0420	aa060202	Mus musculus clone BAC126c8 Rsp29-like protein (Rsp29) and Als splice variant 2 (Als) genes, partial cds; Als splice variant 1 (Als), TCE2 (Tce2), NDK3-like protein (Ndk3), and TCE4 (Tce4) genes, complete cds; and TCE5 (Tce5) gene, partial cds	2.23
IMAGp952I0764	aa606337		2.23
IMAGp952M2461	aa106149		2.23
IMAGp952I0444	aa516852	ESTs, Highly similar to S-	2.22

		ADENOSYLMETHIONINE SYNTHETASE GAMMA FORM [Rattus norvegicus]	
IMAGp952D2017	aa036096	ESTs, Highly similar to HYPOTHETICAL 25.7 KD PROTEIN IN MSH1-EPT1 INTERGENIC REGION [Saccharomyces cerevisiae]	-2.22
IMAGp952O1022	aa162681	aconitase 2, mitochondrial	2.22
IMAGp952M131	w09175		2.21
IMAGp952M0751	aa673494	Mus musculus cAMP-dependent protein kinase regulatory subunit mRNA, complete cds	3.88
IMAGp952I2410	ai413755,ai425782, w80260	chaperonin subunit 3 (gamma)	3.67
IMAGp952O0238	aa432889		-2.73
IMAGp952L2062	aa184574	ESTs, Weakly similar to PDI_RAT PROTEIN DISULFIDE ISOMERASE PRECURSOR [R.norvegicus]	2.72
IMAGp952L0560	ai227481	programmed cell death 4	2.47
IMAGp952G1034	aa289937,ai661641		2.42
IMAGp952N0262	aa184521		-2.36
IMAGp952N1221	aa117053,ai427057, ai550228		-2.35
IMAGp952P0623	aa396595	granzyme G	-2.28
IMAGp952B052	ai414418,w42098		-2.26

[a]: positive means up regulated in SWR/J group while negative means down regulated

8.2 Appendix 2

Appendix 2. List of candidate genes in the inter strain comparison – AKR/J HF vs. SWR/J HF from data analysis I.

RZPD clone ID	GenBank accession number	Cluster description by RZPD	Fold change[a]
IMAGp952F2058	ai226516,ai266816	transthyretin	12.26
IMAGp952C1431	aa048282	ESTs, Highly similar to T17338 hypothetical protein DKFZp434O125.1 - human [H.sapiens]	10.55
IMAGp952F0714	aa011728	ESTs, Weakly similar to KIAA0672 protein [H.sapiens]	9.07
IMAGp952J1319	aa049077	ESTs, Weakly similar to AF161429_1 HSPC311 [H.sapiens]	8.87
IMAGp952N1531	aa060121	Down syndrome critical region homolog 2 (human)	6.89
IMAGp952E149	w71639	ESTs, Weakly similar to matrin cyclophilin [R.norvegicus]	-5.26
IMAGp952N0950	aa672655	ESTs, Highly similar to hGCN5 [H.sapiens]	3.91
IMAGp952B0663	aa771366	ESTs, Highly similar to I5P1_HUMAN TYPE I INOSITOL-1,4,5-TRISPHOSPHATE 5-PHOSPHATASE [H.sapiens]	3.03
IMAGp952O2334	aa288036,ai644752, ai661644	ESTs, Weakly similar to nuclear receptor RVR [M.musculus],thyroid hormone receptor alpha	-2.86
IMAGp952I0444	aa516852	ESTs, Highly similar to S-ADENOSYLMETHIONINE SYNTHETASE GAMMA FORM [Rattus norvegicus]	2.74
IMAGp952M2461	aa106149		-2.64
IMAGp952O1252	aa688597	ESTs, Highly similar to KERATIN, TYPE II CYTOSKELETAL 4 [Homo sapiens]	-2.52
IMAGp952H1623	aa396515	DNA segment, Chr 11, ERATO Doi 603, expressed	2.50
IMAGp952I058	w61435	paternally expressed gene 3	2.48
IMAGp952O1452	aa681073,aa682096	polynucleotide kinase 3-- phosphatase	2.40
IMAGp952A1710	w98128	low density lipoprotein receptor related protein	2.39
IMAGp952O0565	aa185650	DNA segment, Chr 18, Wayne State University 98, expressed	2.37
IMAGp952A1610	w77706	ESTs, Highly similar to scaffold	-2.32

		attachment factor B [R.norvegicus]	
IMAGp952N2361	aa087689	ESTs, Highly similar to S-ADENOSYLMETHIONINE SYNTHETASE GAMMA FORM [Rattus norvegicus]	-2.32
IMAGp952I244	w29642		-4.06
IMAGp952O224	w29499		3.06
IMAGp952B1828	aa267461	ESTs, Weakly similar to TIG1_HUMAN RETINOIC ACID RECEPTOR RESPONDER PROTEIN 1 [H.sapiens]	-2.96
IMAGp952A1816	aa024120	ESTs, Highly similar to KIAA0121 protein [H.sapiens]	-2.88
IMAGp952M0763	aa212649		-2.64
IMAGp952I2440	aa433525	C-terminal binding protein 2	2.48
IMAGp952J1123	aa108026	protein tyrosine phosphatase, non-receptor type 16	2.41
IMAGp952H2414	aa013792		2.35
IMAGp952A1462	aa139332	ESTs, Moderately similar to T12506 hypothetical protein DKFZp434C212.1 - human [H.sapiens]	-2.33

[a]: positive means up regulated in SWR/J group while negative means down regulated

9 Erklärung

ich versichere, dass ich meine Dissertation

> Hypothalamic gene expression profiling in mouse strains susceptible or resistant to diet-induced obesity

selbstständig, ohne unerlaubte Hilfe angefertigt und mich dabei keiner anderen als der von mir ausdrücklich bezeichneten Quellen und Hilfen bedient habe.

Die Dissertation wurde in der jetzigen oder einer ähnlichen Form noch bei keiner anderen Hochschule eingereicht und hat noch keinen sonstigen Prüfungszwecken gedient.

_____ _____

(Ort/Datum) (Unterschrift mit Vor- und Zuname)

10 Acknowledgements

The success of this work did not come up without kind assistance and cooperation of many persons.

First of all, I would like to thank Prof. Dr. Gerhard Heldmaier for providing me a working place in this excellent research group.

I am particularly grateful to my supervisor, HD Dr. Martin Klingenspor, not only for his constant support, encouragement and valuable scientific advice to my professional development but also for his enthusiasm and help during my living in Marburg. I really appreciate the fact that he always had time for me whatever questions I might have had.

I would like to address my cordial thanks to all members and students in our research group, especially to
Dr. Mauricio Berriel Díaz and Carola Meyer for their help and discussions about the technical problem and reading and correction of my thesis.
Dr. Jan Rozman for his working in body fat measurement and other help.
Birgit Samans for her statistical support in the array data analysis.
Reza Khorooshi and Alexander Tups for their teaching me techniques of in situ hybridization.
Timo Müller and Jörn Wessels for their discussion in the real-time RT-PCR experiment.
Tobias Fromme and Kathrin Reichwald (IMB, Jena) for their SNP analysis.
Martin Jastroch for his discussion in my work and translation of the summary into German.
Timo Kanzleiter, Tatjana Schneider, Sigrid Stöhr, Gábor Szerencsi for their help in my work.
Jeanne Eggerstedt, Dr. Cornelia Exner and Regina Löchel for their taking care of my mice.
Mechthild Zissel for her friendly support in all of my administrative matters concerning my status as student of the Philipps-University Marburg.

My deep gratitude goes to my family for their love, understanding and support.

11 Curriculum Vitae

Name	Lianxing YANG
Birthday	06 Oct. 1971
Birthplace	Tangshan, Hebei, P. R. China
Nationality	Chinese

09. 1979 – 07. 1985	Primary School, Tangshan, Hebei, China
09. 1985 – 07. 1988	Middle School, Tangshan, Hebei, China
09. 1988 – 07. 1991	High School, Tangshan, Hebei, China
09. 1991 – 07. 1996	Shandong Medical University, Ji'nan, Shandong, China
07. 1996	B.Sc. in Medicine
08. 1996 – 09. 1999	Shaanxi Provincial Peoples' Hospital, Xi'an, Shaanxi, China
	Resident surgeon
10. 1999 – 06. 2001	Mannheim University of Applied Sciences, Mannheim, Germany
06. 2001	M.Sc. in Biotechnology
07. 2001 – present	Philipps-University Marburg, Marburg, Germany
	Ph.D. student